An investigation of the role of *FAF* (Female Associated Factor) in female gonad development of chickens.

by

Zane Oberholzer

(909187)

Thesis

Submitted in fulfilment of the requirements for the degree

Master of Science

in

Molecular and Cell Biology

in the Faculty of Science, University of the Witwatersrand, Johannesburg, South Africa

Supervisor: Prof. N. Nikitina

April, 2020

Candidate declaration

I, Zane Oberholzer, declare that this thesis is my own, unaided work. It is being submitted for the Degree of Master of Science at the University of the Witwatersrand, Johannesburg. It has not been submitted before for any degree or examination at any other University.

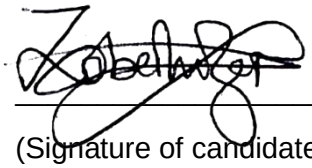

(Signature of candidate)

22nd day of **April** 20**20**

Abstract

Birds use a ZW sex determination system where males are homogametic ZZ and females are heterogametic ZW. Although it has been established that avian sex determination is governed by the inheritance of these sex chromosomes, the underlying molecular mechanism still largely remains a mystery and no gene/s have been identified as the master regulator of sex determination. The W-linked gene *FAF* (Female Associated Factor) is a promising candidate of ovarian development since its expression is restricted to females only and is initiated prior to the start of sex differentiation. This project aimed to determine the functional role of *FAF* in the gonadal development of *Gallus gallus* by investigating the effects of the knockdown of *FAF* in ZW females and the ectopic expression of *FAF* in ZZ males. 5'-RACE was conducted on mRNA extracted from HH24-25 female whole-body and gonad tissue to annotate the 5'-UTR of *FAF*. Using this data, two non-overlapping morpholinos were designed to target *FAF.* The morpholinos and pCI-*FAF*-RFP expression plasmid was delivered to embryos (HH14-16) via *in ovo* electroporation. While male embryos electroporated with the *FAF*-targeting morpholinos (at 1mM and 2mM) developed to HH30-34, female embryos died 24-48 hr post-electroporation. Female embryos electroporated with the control morpholino (at 1mM and 2mM), however, developed normally to HH30-34. This suggests delivery of the construct was not isolated to the gonads alone as the gonads are not essential to survival. Consistent with this, it was identified that the morpholinos were also delivered to the dorsal aorta, suggesting *FAF* may have a role in the formation/functioning of the dorsal aorta. The ectopic expression of *FAF* in ZZ males resulted in the gonads developing a female-like morphology, suggesting a male-to-female sex reversal whereas the overexpression of *FAF* in ZW females had no morphological effect on the gonads. Currently it is unclear if *FAF* acts as a protein or non-coding RNA, however, based on the findings from this project, it is clear that *FAF* is implicated in normal female development and gonad differentiation which warrants further investigation.

Dedication

To my family and friends for their unconditional love and support.

Acknowledgements

I would firstly like to acknowledge my supervisor, Prof. N. Nikitina, for her unwavering support and guidance. Secondly, I would like to acknowledge the University of the Witwatersrand and The National Research Foundation (NRF) for their funding for the duration of my MSc. Lastly, I would like to acknowledge Innocent Kambule for his assistance and allowing me to use his histology facility.

Table of Contents

List of Figures

List of Tables

List of abbreviations

17β-HSD	17β-hydroxysteroid dehydrogenase
AMH/*Amh*	Anti-Müllerian hormone
AROM/*CYP191A1*	Aromatase
BLAST	Basic Local Alignment Search Tool
BLASTn	Nucleotide BLAST
Bp	base pair
BSA	Bovine serum albumin
$CaCl_2$	Calcium chloride
cAMP	Cyclic adenosine monophosphate
CAPN5	Calpain-5
CASI	Cell autonomous sex identity
cDNA	Complimentary DNA
CDS	Coding Sequence
Cdt1	Chromatin licensing and DNA replication factor 1
cGMP	Cyclic guanosine monophosphate
CIP	Calf intestinal phosphatase
CMV	Cytomegalovirus
DA	Dorsal aorta
DD-PCR	Differential display PCR
dH_2O	Distilled water
Dmr	*Dmrt1*-related gene
DMRT1/*Dmrt1*	Doublesex and mab-3 related transcription factor 1
DNA	Deoxyribonucleic acid
E	Embryonic day

E. coli	*Escherichia coli*
EDTA	Ethylenediaminetetraacetic acid
ER-α	Oestrogen receptor alpha
FAF	Female associated factor
FET-1	Female expressed transcript #1
FITC	Fluorescein isothiocyanate
FOXL2/*Foxl2*	Forkhead Box L2
GAF	c**G**MP-specific phosphodiesterases, **a**denylyl cyclases and **F**hlA
gDNA	Genomic DNA
GFP	Green fluorescent protein
GPR56	G-protein coupled receptor 56
HCl	Hydrochloric acid
H&E	Hematoxylin and eosin
HEMGN	Hemogen
HH	Hamburger Hamilton Stage
HINTW	Histidine triad nucleotide binding protein W
HINTZ	Histidine triad nucleotide binding protein Z
HMGA1a	High mobility group AT-hook 1a
IHC	Immunohistochemistry
KCl	Potassium chloride
LB	Lysogeny broth
LHX9/*Lhx9*	LIM homeobox 9
LincRNA	Long intervening/intergenic noncoding RNA
MD	Müllerian duct

MHM	Male hypermethylation
miRNA	MicroRNA
MO	Morpholino
mRNA	Messenger RNA
MSA	Multiple sequence alignment
Na_2HPO_4	Disodium hydrogen phosphate
NaCl	Sodium chloride
NaH_2PO_4	Sodium dihydrogen phosphate
ncRNA	Non-coding RNA
NEC	No electroporation control
NTC	No template control
ORC	Origin recognition complex
PBS	Phosphate buffered saline
PCR	Polymerase chain reaction
PDB	Protein Data Bank
PFA	Paraformaldehyde
PGCs	Primordial germ cells
PITX2	Paired like homeodomain 2
PPIA	Peptidylprolyl isomerase A
PWWP	Proline-tryptophan-tryptophan-proline
RACE	**R**apid **A**mplification of **c**DNA **E**nds
qPCR	Quantitative polymerase chain reaction
RFP	Red fluorescent protein
RSPO1/*Rspo1*	R-spondin 1
RT	Reverse transcription

SF1/*Sf1*	Steroidogenic factor-1
sORF	Short **o**pen **r**eading **f**rame
SOX9/*Sox9*	SRY-box 9
SPARC	Secreted protein acidic and cysteine rich
SPF	Specific pathogen free
SRY/*Sry*	Sex-determining region Y
TAP	Tobacco acid pyrophosphatase
TBS	Tris buffered saline
TBST	Tris buffered saline with Tween 20
TD-PCR	Touchdown PCR
Tm	Melting temperature
UTR	Untranslated region
VIM	Vimentin
WNT4/*Wnt4*	Wnt family member 4
WT1/*Wt1*	Wilms tumor 1
XX/XY	Mammalian sex determining system
ZW	Genotypic female
ZZ	Genotypic male
ZZ/ZW	Avian sex determining system

1. Chapter 1 - Introduction

1. Literature review

1.1. Sex determination vs sex differentiation

For the purposes of this thesis, it is important to distinguish between sex determination and sex differentiation. Sex determination refers to the mechanism by which an organism's sex is determined. Two main mechanisms exist, namely chromosomal systems and environmental systems (Coriat *et al.*, 1994). Sex differentiation however refers to the process by which sex-dichotomous differences arise. This includes gonadal sex differentiation, which entails how the genital organs (testis, ovaries, sex ducts & uterus) are established by the actions of genes and hormones and secondary sexual characteristics which involves the development of sex-dichotomous characteristics of the rest of the body, excluding the genital organs (Hirst, Major and Smith, 2018). This chapter will explore these two concepts in more detail, focusing on *Gallus gallus*.

1.2. Chromosomal sex determination systems

Chromosomal systems are centred on the inheritance of sex-specific chromosomes. While several types of chromosomal sex determination systems exist, the most well studied one would be the XX/XY sex determining system and is used as a model to extrapolate information for all other sex determining systems (Bull, 1985). Considering this, an overview of the XX/XY sex determining system will be provided. Birds, including chickens (*Gallus gallus*), use a ZW sex determining system, which is less well understood and forms the focus of this work.

1.2.1. The XX/XY sex determining system

In mammals, males are the heterogametic sex (XY) whereas females are homogametic (XX). The analysis of sex-aneuploids revealed that the Y chromosome is required for maleness however it was unclear which gene/s on the Y chromosome was responsible for male development (Ford *et al.*, 1959; Jacobs and Strong, 1959). While it was believed that *Sry* (sex determining region Y), found on the Y chromosome, was the master sex regulator it was only experimentally confirmed by Koopman et al., (1991). The work done by Koopman et al., (1991) entailed the ectopic expression of *Sry* in XX female mice which resulted in complete female-to-male sex reversal (Koopman *et al.*, 1991). Evidently, *SRY* acts as the 'master switch' triggering male development.

1.2.2. The ZZ/ZW sex determining system

The ZW sex determining system is used by birds and some fish, crustaceans, insects and reptiles. In the case of birds, males are the homogametic sex (ZZ) and females are the heterogametic sex (ZW) (Clinton, 1998). The Z chromosome in birds is equivalent to the mammalian X chromosome in the sense that it is large (82 Mb) and gene rich, harbouring over 1000 genes and 348 non-coding RNAs (Ayers *et al.*, 2013; Bellott *et al.*, 2017). Most of these genes however serve a regulatory function and do not contribute to sex determination (Schmid *et al.*, 2015). Conversely, the W chromosome, equivalent to the mammalian Y chromosome in terms of gene density, has undergone genetic decay. The W chromosome is approximately 7 Mb in length and is comprised mostly of repetitive elements (*Xho*I, *Eco*RI, and *Ssp*I classes) which makes sequencing and annotation difficult. However, current annotations (galGal5) predict there to be ~28 putative protein coding genes and 116 non-coding RNAs (Itoh and Mizuno, 2002; Ayers *et al.*, 2013; Bellott *et al.*, 2017).

1.3. Gonadal sex differentiation in *Gallus gallus*

1.3.1. Formation of the genital ridge

The gonads are derived from intermediate mesoderm and gonadal development, in both male and females, commences at about HH18, where the coelomic epithelium (outermost layer of the male and female gonads) ventral to the mesonephros (primitive kidney) starts to thicken (Merchant-larios, Popova and Reyss-Brion, 1984). Concurrently, the primordial germ cells (PGCs) which are found in the area pellucida segregate and migrate to and from the germinal crescent to the circulatory system and then to the gonads (Ginsburg and Eyal-giladi, 1987). The transcription factors *SF1* (Steroidogenic Factor-1), *GATA4*, *WT-1* (Wilm's Tumour associated protein) and *LHX9* (LIM homeobox protein) are essential for the initial stages of gonadal differentiation and establishing the genital ridge (Oréal *et al.*, 2002). While functional work involving the knockdown of these transcription factors have not been done in chickens, knockouts of *Gata4* or *Sf1* in mice resulted in the gonads not forming as the coelomic epithelium did not thicken, suggesting a role in genital ridge formation (Luo, Ikeda and Parker, 1994; Hu, Okumura and Page, 2013). Interestingly, in chickens, *DAX1* (a nuclear receptor protein) is expressed from HH18 in both sexes at low levels and peaks during the period of gonad differentiation. In mice, it was found that *Dax1* functions in regulating spermatogenesis and folliculogenesis. The increased expression during

gonad differentiation suggests *DAX1* may function similarly in chickens to aid in testis/ovary development, particularly that of spermatogenesis/folliculogenesis (Smith, Smith and Sinclair, 1999; Smith *et al.*, 2000; Meeks *et al.*, 2003; Yamamoto *et al.*, 2003; Caetano *et al.*, 2014). **Figure 1.1** below illustrates the transcription factors essential for establishing the genital ridge.

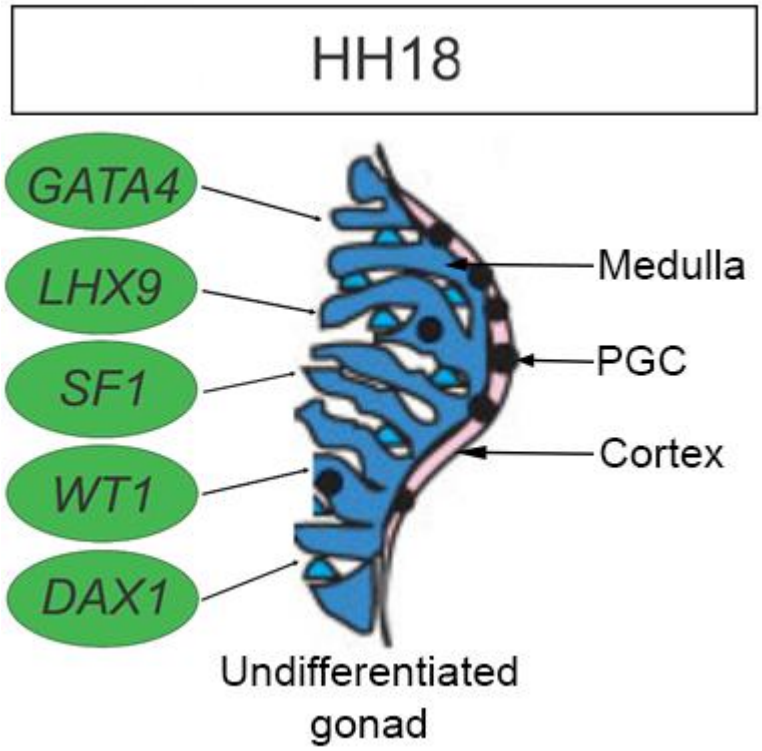

Figure 1.1. *Formation of the genital ridge*. The coelomic epithelium ventral to the mesonephros starts to thicken from HH18 onwards, initiated by the expression of the transcription factors *SF1*, *GATA4*, *WT-1*, *LHX9* and *DAX1.* The green circles indicate the expression of these factors in both males and females. Concurrently, the primordial germ cells migrate to the genital ridge, predominantly being found in the cortex, represented by the black circles.

1.3.2. Genes expressed in males and females, prior to gonadal differentiation

By HH24, the genital ridge has been established and comprises of an outer epithelial layer (derived from the thickened coelomic epithelium) and is referred to as the cortex. Beneath the cortex are cords (derived from proliferating coelomic epithelial cells) of somatic cells separated by loose mesenchyme. This region is referred to as the medulla (Merchant-larios, Popova and Reyss-Brion, 1984;

Rodemer-lenz, 1989). The PGCs are found within the medulla and cortex however they are localized primarily to the cortex. The process of gonad differentiation essentially refers to how the cortex and medulla develop and which region claims the PGCs. Gonadal differentiation starts at HH24-25, but male and female gonads are morphologically indistinguishable at this point and only become morphologically different at HH29-30 (Merchant-larios, Popova and Reyss-Brion, 1984; Ginsburg and Eyal-giladi, 1987; Ebensperger *et al.*, 1988).

DMRT1

The first gene expressed that is essential to gonad differentiation is *DMRT1* (doublesex and mab-3-related transcription factor 1) which encodes for a transcription factor, essential to testis development in many species including birds. While *DMRT1* is expressed in both male and female birds, it is expressed approximately 2-fold higher in males than females (likely because it is Z-linked and therefore there are two copies in males). *DMRT1* expression is present from as early as HH22 however it is unclear what activates its expression (Raymond *et al.*, 1999; Smith *et al.*, 1999, 2009; Omotehara *et al.*, 2014). The importance of *DMRT1* as a testis determinant is discussed in Chapter 1.4.3.

AMH

AMH (Anti-Müllerian hormone) is detectable at HH24 and, interestingly, is expressed in the medullary cells of both males and females (Oreal *et al.*, 1998). *AMH* is an essential hormone that directs the regression of the Müllerian ducts in males. The female left gonad is believed to be protected from *AMH* by the local action of oestrogens found there whereas the right gonad lacks these oestrogens and it is therefore believed that *AMH* may play a role in the degradation of the right Müllerian duct in females (Hutson, Ikawa and Donahoe, 1982). In mammals, the expression of *AMH* is initiated by *SOX9* however in chickens, *AMH* mRNA and protein is detected prior to *SOX9* (first detected at HH28) (Smith, Smith and Sinclair, 1999; Nishikimi *et al.*, 2000). *SOX9* therefore cannot initiate AMH expression in chickens. It is believed that since *AMH* is detected in both male and female chickens, a general transcription factor such as *SF1* may activate *AMH* expression, while a male-specific factor such as *SOX9* may cause male-specific upregulation of *AMH*. Functional work involving the knockdown of *AMH* by RNA interference showed that the knockdown of *AMH* did not alter the expression of the

male-specific markers *DMRT1* or *SOX9* however the gonads and mesonephros were much smaller than the male controls and there was a significant decrease in the number of germ cells. Furthermore, no changes in steroidogenic activity were observed in *AMH*-deficient males. In *AMH*-deficient females, the gonads and mesonephros were smaller however there was no change in female-specific marker expression (*Aromatase*). Interestingly, *AMH* knockdown of the right female gonad did not result in a more female-like organisation nor was there a change in the expression of *Aromatase* (Lambeth *et al.*, 2015). Taken together, this suggests that *AMH* in the chicken is not directly implicated in testis development but rather has a sex-independent role in the growth and proliferation of the gonads.

1.3.3. Genes essential for testis development

HEMGN & SOX9

SOX9 (SRY-box 9) is one of the few genes involved in gonad development that is conserved across multiple vertebrate species and is expressed in a sexually dimorphic manner (Cutting, Chue and Smith, 2013). *SOX9* is one of the downstream targets of *DMRT1* and it is expressed exclusively in males. SOX9 protein is first detected at HH28 whereas *DMRT1* is expressed from HH24 (Caetano *et al.*, 2014; Ayers *et al.*, 2015). Due to this time lag, other chicken-specific factor/s are likely to be expressed between HH24 and HH28 (Chue and Smith, 2011). *HEMGN* (Hemogen) is a transcription factor expressed only in the male gonad from HH27 in the nucleus of Sertoli cells. Based on the temporal and spatial expression of *HEMGN*, it is proposed that *HEMGN* acts between *DMRT1* and *SOX9*, initiating *SOX9* expression. Functional work involving the ectopic expression of *HEMGN* in ZW female gonads resulted in a male-like morphology developing with the activation of *SOX9* and the loss of female markers (*AROM* and *FOXL2*) (Nakata *et al.*, 2013). This confirms that *HEMGN* is able to activate *SOX9* expression; however, it is still unclear whether *HEMGN* activates *SOX9* directly or indirectly.

The SOX9 protein is localised to the nuclei of Sertoli cells and is essential to normal testis development and Sertoli cell differentiation. Its expression remains high throughout gonad development and in adult ZZ males (Lambeth *et al.*, 2014). While no functional work of *SOX9* has been done in chickens, female-to-male sex reversal induced by aromatase inhibitors (Fadrozole) results in the activation of

SOX9 in sex reversed females, illustrating a clear role in testis development (Hirst *et al.*, 2017). An overview of the male sex determination pathway is shown below in **Figure 1.2** below.

During the differentiation of male gonads, the left and right gonads develop symmetrically, to form two elongated structures. The cortex remains a single monolayer of epithelial cells whereas the medulla thickens and gives rise to the seminiferous cords. The thickening of the medulla is attributed to the proliferation and differentiation of the Sertoli cells, within the cords. The PGCs are enclosed within the seminiferous cords and enter mitotic arrest, only entering meiosis after hatching (Smith and Sinclair, 2004).

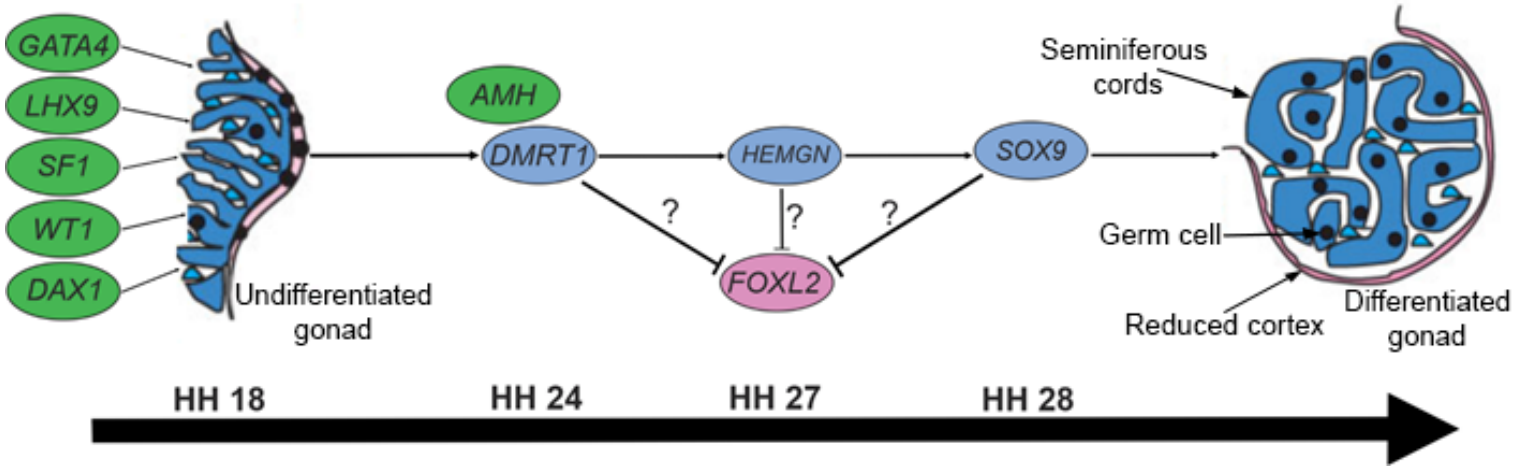

Figure 1.2. *Overview of the male sex differentiation pathway.* The circles denote the onset of gene expression. Green circles represent genes expressed in both sexes. Blue circles represent male-specific expression. Pink circles represent female-specific expression. Testis development is initiated by the expression of *DMRT1. HEMGN* is activated by *DMRT1* which in turn activates *SOX9*. It is unclear whether the activation of these genes suppresses the female pathway, for example by suppressing the expression of *FOXL2.* The differentiated male gonad consists of a thin cortex (pink) and a medulla comprised of seminiferous cords (blue), where the primordial germ cells are found (black circles).

1.3.4. Genes essential for ovarian development

Two pathways act in parallel in female gonad development, namely the *FOXL2*/*CYP19A1* pathway and the *WNT4*/*RSPO1*/*β-catenin* pathway. While both of these pathways act to promote ovarian development, it remains unclear how they interact with each other or whether there is a direct link between them (Hirst, Major and Smith, 2018). Based on the spatial expression of the two pathways – *FOXL2*/*CYP19A1* pathway being expressed in the medulla whereas the

WNT4/*RSPO1*/*β-catenin* pathway being expressed in the cortex, they may not interact with each other directly, but rather through an as yet unidentified diffusible intermediate (Govoroun *et al.*, 2004; Smith *et al.*, 2008).

FOXL2/*CYP19A1*

FOXL2 (Forkhead box L2) is a transcription factor essential to the development of the ovarian pathway in many species, including mammals, fish and birds (Hirst, Major and Smith, 2018). In birds, *FOXL2* is expressed exclusively in the medulla of female gonads from HH28 (Govoroun *et al.*, 2004). Currently, it is unknown what activates *FOXL2* expression in chickens. Soon after *FOXL2* is expressed however *CYP19A1* (Aromatase) expression is detected at HH29 in the medulla of female gonads (Smith, Andrews and Sinclair, 1997). Based on the expression pattern of the two genes and the fact that expression is localised to the medullary cells, it is thought that *FOXL2* activates *CYP19A1*. In line with this, *in vitro* studies have confirmed that *FOXL2* can bind to a forkhead element in the promoter of *CYP19A1* (Fleming *et al.*, 2010). While it has not been experimentally validated that *FOXL2* can directly regulate *CYP19A1*, the inhibition of *CYP19A1* (by compounds such as Fadrozole) also decreases the expression of *FOXL2*, suggesting that a feedback loop between the two genes exists (Hudson, Smith and Sinclair, 2005).

FOXL2, *CYP19A1* and *17β–HSD* (17β-hydroxysteroid dehydrogenase) function together to convert androgen substrates into oestrogen. These three genes are only expressed in the female medulla and as such oestrogen is only detected in female gonads (Smith, Andrews and Sinclair, 1997; Nakabayashi *et al.*, 1998; Nishikimi *et al.*, 2000). Oestrogens, such as estradiol, are first detected in the female gonad at HH35-36 and are essential to ovarian development by interacting with the oestrogen receptor (ER-α) to signal cortical thickening (Ayers *et al.*, 2013). The significance of oestrogens is further highlighted by the female-to-male sex reversal observed when Fadrozole is administered, blocking the conversion of androgens into oestrogen (Imataka *et al.*, 1989). Interestingly, exogenous addition of oestrogen to these females treated with Fadrozole rescues their phenotype, highlighting the importance of oestrogen in ovarian development (Elbrecht and Smith, 1992).

WNT4/*RSPO1*/*β-catenin*

WNT4 (mRNA and protein) is expressed in both male and female gonads at HH24 however its expression is lost in ZZ male gonads at the onset of sexual differentiation (HH28) and becomes confined to the cortex of the left female gonad. *RSPO1* (R-spondin-1) is expressed in a dimorphic manner at HH24, being expressed at higher levels in females. At the onset of sexual differentiation, *RPSO1* expression decreases (in both males and females) however from HH35 its expression increases and becomes strongly enriched in the cortex of the left female gonad. While it has not been experimentally validated in chickens, it is believed that *WNT4* and *RSPO1* interact with each other to activate the expression of *β-catenin* (Smith *et al.*, 2008; Ayers, Sinclair and Smith, 2013). The *WNT4*/*RSPO1*/*β-catenin* interaction is observed in mice and the loss of any one of these three factors in mice results in masculinisation of the female gonad. The amino acid sequence of β-catenin between mice and chickens is highly conserved (99% similarity) and *β-catenin* therefore likely has a conserved role in ovarian development across vertebrates (Lu, Chuong and Widelitz, 1997). Experimental validation of the role of the *WNT4*/*RSPO1*/*β-catenin* pathway in chickens is needed however. An overview of the female sex determination pathway is shown below in **Figure 1.3**.

In the differentiated female gonad, the cortex thickens as a result of the proliferation of the coelomic epithelial cells. The PGCs accumulate within the cortex and also proliferate here. It is only after HH34 that the PGCs start folliculogenesis. The cords within the medulla of females become vacuolated, forming hole-like structures called lacunae. Interestingly, the left and right gonad develop asymmetrically, forming a functional left gonad that is considerably larger than the non-functional right gonad (Smith and Sinclair, 2004; Ayers, Smith and Lambeth, 2013; Hirst, Major and Smith, 2018). This asymmetrical development of the gonads is attributed to the transcription factor, *PITX2* (paired like homeodomain 2), being expressed in the left gonad but not the right gonad. Ectopic expression of *PITX2* in the right gonad was enough to prevent it from regressing and induce the thickening of the cortex. *PITX2* functions by regulating the expression of oestrogen receptor-α and in conjunction with *CyclinD1* is essential to cell proliferation and differentiation of both somatic cells and PGCs thus regulating the size of the left gonad (Guioli and Lovell-Badge, 2007; Ishimaru *et al.*, 2008; Rodriguez-Leon J *et al.*, 2008).

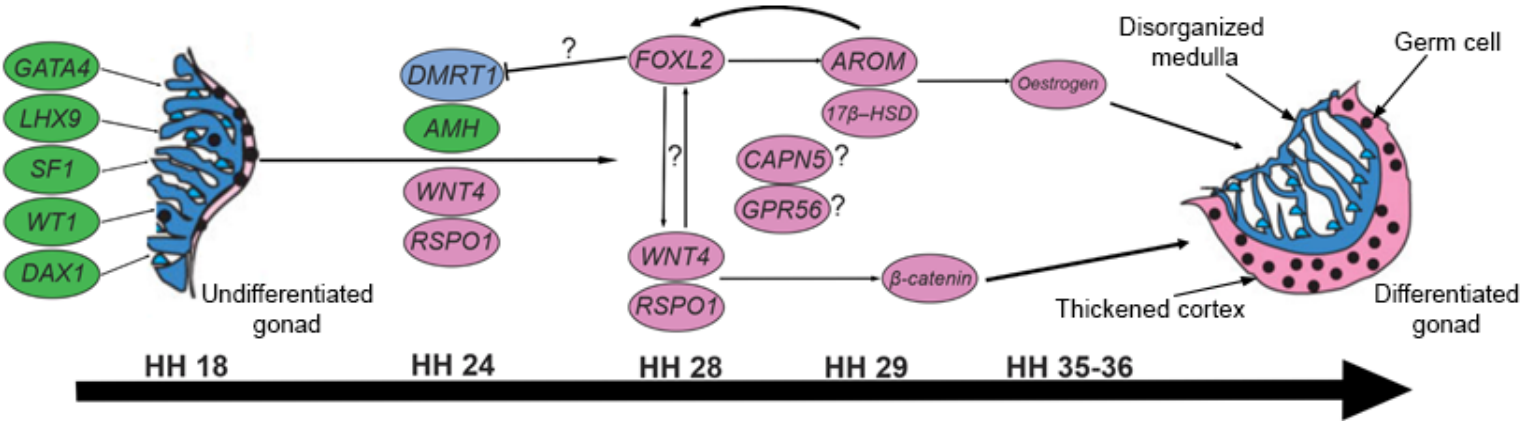

Figure 1.3. *Overview of the female sex differentiation pathway.* The circles denote the onset of gene expression. Green circles represent genes expressed in both sexes. Blue circles represent male-specific expression. Pink circles represent female-specific expression. Ovarian development is regulated by two parallel acting pathways – the *FOXL2/CYP19A1 pathway* and the *WNT4/RSPO1/β-catenin* pathway. It remains unclear whether there is a direct interaction between the two pathways or whether they are able to suppress the male pathway. *FOXL2* activates *Aromatase*, creating a positive feedback loop. The *FOXL2/CYP19A1* together with *17β–HSD* is responsible for the synthesis of Oestrogen, essential to ovarian development. The *WNT4/RSPO1* pathway activates the expression of *β-catenin*. The female-enriched genes *CAPN5* and *GPR56* may also contribute to ovarian development. The differentiated female gonad consists of a thick cortex (pink) with primordial germ cells (black circles) and a disorganised medulla consisting of lacunae (blue).

1.3.5. Other genes potentially involved in ovarian development

Two other genes, namely *CAPN5* (Calpain-5) and *GPR56* (G-protein coupled receptor 56) show a female-biased increase in expression at HH28-29. *CAPN5* is expressed in the juxta-cortical medulla whereas *GPR56* is expressed within the cortex. Interestingly, while low levels of *CAPN5* expression are detected in male gonads, *GPR56* expression is not detected in male gonads. Based on when these genes are upregulated (the onset of sex differentiation), they are unlikely to be female sex determinants, but may rather play a role in ovarian development and warrant further investigation (Ayers *et al.*, 2015).

1.4 Sex chromosomes and their role in sex determination

According to chromosomal evolutionary theories, sex chromosomes arise to carry sex-specific genes. In the case of mammals, the Y chromosome segregated to carry the male-determining-gene, *SRY* as well as other genes essential to spermatogenesis. These genes are isolated to the Y chromosome since the Y chromosome and X chromosome, under normal circumstances, are unable to recombine (Ohno, 1971). Extending this postulate to the ZW sex determining

system, the W chromosome would therefore have segregated from the Z chromosome to isolate female-sex-determining gene/s and other genes essential to folliculogenesis. Sex chromosome aneuploids provide useful insight with respect to the role of sex chromosomes in sex determination (Ayers, Sinclair and Smith, 2013). The aneuploids are mostly derived from diploid ova produced by chromosomal non-disjunction during oogenesis however there have been reports of aneuploids as a result of dispermy or fertilization by diploid sperm (Bitgood and Shoffner, 1990). ZWW chickens have not been reported and are therefore likely embryo lethal (Graves, 2003). ZZW chickens, after hatching, had a normal right testis however the left gonad developed as ovotestis, lacking a male type Wolffian duct. At adulthood however there are mixed reports – where some ZZW chickens develop to be phenotypically female, have both testicular and ovarian tissue or develop to be more male-like (Lin *et al.*, 1995; Thome *et al.*, 1997; Arit *et al.*, 2004; Kupper *et al.*, 2012). Taken together, this suggests the requirement of a W-linked input for female development.

1.4.1. Dosage compensation of the Z chromosome?

Unlike the mammalian X chromosome, the avian Z chromosome lacks any global dosage compensation (Itoh *et al.*, 2007; Melamed and Arnold, 2007; Arnold, Itoh and Melamed, 2008; Ellegren, 2011; Naurin *et al.*, 2012; Wang *et al.*, 2017). The first functional work in support of this was fluorescent *in situ* hybridisation of five Z-linked genes which showed that these five genes were transcribed from both Z chromosomes (Kuroda *et al.*, 2001). While it should not be generalized that all Z-linked genes escape dosage compensation from this study, it showed that there is no global inactivation of one of the Z chromosomes, like there is in mammals. It was confirmed by a microarray experiment (using tissue from the heart, left gonad and diencephalon) that Z-linked genes are expressed 1.4-1.6 times higher in males than females which is consistent with the absence of dosage compensation (Ellegren *et al.*, 2007). While this confirms the lack of global dosage compensation, it does not mean that there is no dosage compensation. It was postulated that genes may be compensated locally, on a gene-by-gene basis or by a tissue-by-tissue basis. Alternatively, compensation of the Z chromosome may occur at critical developmental time points. Global gene expression profiling conducted on male and female somatic tissue (at different time points) revealed that the Z chromosome exhibits a local gene-by-gene basis of dosage compensation. This suggests that birds are able to tolerate a slight male bias for many Z-linked genes

and that the expression of only certain Z-linked genes are compensated for (Mank and Ellegren, 2009). The mechanism by which these genes are compensated for is not fully understood but it has been suggested that compensation occurs as a result of the interaction with other genes, protein complexes or may be regulated at a protein level (Arnold, Itoh and Melamed, 2008). Consequently, the higher expression of Z-linked genes in ZZ males may drive gonad differentiation by promoting testis development.

1.4.2. Criteria of being a sex determinant

For a gene to be considered as a sex determinant, it would need to meet the following criteria: 1) the gene would need to be found on one of the sex chromosomes, likely lacking a gametologue, 2) the onset of its expression would need to be prior to gonad differentiation (i.e. prior to HH24) and upregulated in one of the sexes and 3) the gene would need to be expressed in the gonads and in the case of chickens, it would likely also be expressed in somatic tissue since there is genetic component to the male vs female identity of the sexually dimorphic somatic tissues in birds.

1.4.3. Z-linked genes as potential male determinants

DMRT1 and MHM

DMRT1 is one of the Z-linked genes that escapes dosage compensation and is expressed approximately two-fold higher in males than females. As discussed in Chapter 1.3.2 it is expressed prior to gonad differentiation (HH24) (Raymond *et al.*, 1999; Smith *et al.*, 1999, 2009; Omotehara *et al.*, 2014). Female-to-male sex reversal induced by Fadrozole resulted in the upregulation of *DMRT1* in the female gonads (Smith, Katz and Sinclair, 2003). Knockdown of *DMRT1* in ZZ male gonads using RNA interference resulted in the loss of *SOX9* expression and the activation of *FOXL2* and *Aromatase*. Interestingly, the *DMRT1* deficient gonads developed female like morphology (Smith *et al.*, 2009). Furthermore, overexpression of *DMRT1* in ZW female gonads resulted in the development of male-like gonads, characterized by seminiferous tubes, the expression of *SOX9* and the loss of *FOXL2* (Lambeth *et al.*, 2014). Taken together, this clearly illustrates the requirement of *DMRT1* for testis development. However, due to a phenomenon known as CASI (Cell Autonomous Sex Identity) (discussed in Chapter 1.5), *DMRT1* cannot be a master sex determinant due to its expression being restricted to the urogenital system.

Interestingly, a region that comprises of over 200 copies of a 2.2 kb tandem repeat sequence (rich in CpG islands) found on the short arm of the Z chromosome is found to be hypermethylated (and therefore transcriptionally inactive) on both male Z chromosomes, but hypomethylated on the female Z chromosome (Teranishi *et al.*, 2001). This region, dubbed as the MHM (male hypermethylated) region, does not encode for a protein but a high molecular weight non-coding RNA is transcribed in females which coats the female Z chromosome, adjacent to the *DMRT1* locus and suppresses its expression. This suggests that a W-linked factor may be involved in altering the methylation status/activating transcription of the MHM region in females (see **Figure 1.4** below). In support of this, analysis of sex aneuploids showed that the MHM region remains hypermethylated in ZZZ chickens but is hypomethylated in ZZW chickens. While the MHM region is likely to contribute to gonad differentiation in females, it is not the main driving force behind ovarian development since the MHM region is unable to completely repress *DMRT1* (Teranishi *et al.*, 2001; Zheng, Chen and Xu, 2011; Roeszler *et al.*, 2012; Caetano *et al.*, 2014; Yang *et al.*, 2016).

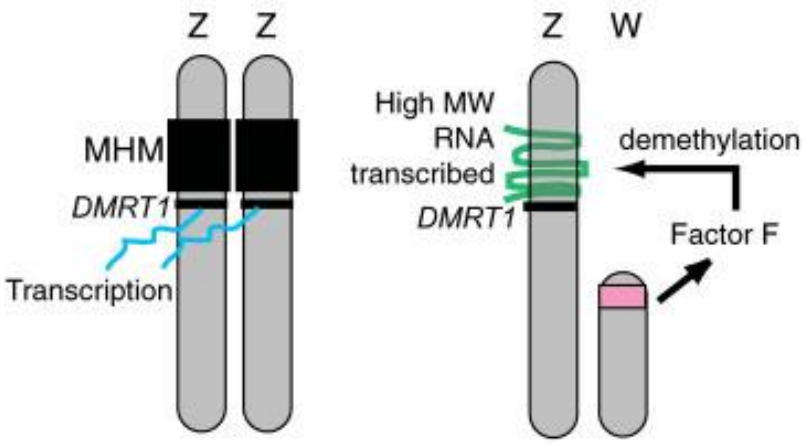

Figure 1.4. *Overview of how the MHM region regulates DMRT1.* In ZZ males, the MHM is hypermethylated and therefore transcriptionally silent. As such, neighbouring genes, including *DMRT1* are freely transcribed. In ZW females, an unknown factor (denoted as Factor F) on the W chromosome induces the demethylation of the MHM which results in the transcription of a high molecular weight RNA that 'coats' the Z-chromosome, adjacent to *DMRT1*, repressing its expression. (Figure adapted from Smith and Sinclair, 2004).

1.4.4. W-linked genes as potential female determinants

HINTW/*HINTZ*

HINTW (histidine triad nucleotide binding protein W) is a W-linked gene with approximately 40 copies on the W chromosome (Bellott *et al.*, 2017). Interestingly, this gene is conserved across several other volant (flying) bird species (such as the zebra finch) and it is expressed widely in female embryos (including the gonads) - suggesting a conserved role in ovarian development (Hori *et al.*, 2000; O'Neill *et al.*, 2000). *HINTW* is a member of the HINT family of nucleotide hydrolases but it lacks the HIT (histidine triad) motif which is needed for it to function, making it aberrant (Brenner, 2002; Parks *et al.*, 2004; Moriyama *et al.*, 2006). While a Z-gametologue of *HINTW* exists, and referred to as *HINTZ*, the two genes share only 65% amino acid homology (Hori *et al.*, 2000). HINTZ has the catalytic domain that is absent in HINTW and it is therefore predicted that HINTZ encodes a *bona fide* HINT enzyme. An important characteristic of HINT proteins is that they require dimerization to function. It is therefore postulated that *HINTW*/*HINTZ* may contribute to gonad development in a dominant negative fashion. In ZZ males, *HINTZ* undergoes homodimerization with itself, stimulating the production of a testis factor. In ZW females however *HINTW* and *HINTZ* forms a heterodimer and this either suppresses the production of a testis factor or promotes the production of an ovarian factor (see **Figure 1.5**) (Brenner *et al.*, 1999; ace and Brenner, 2003; Moghadam *et al.*, 2012; Ayers *et al.*, 2013; Bellott *et al.*, 2017). While this seems plausible, it was shown that the overexpression of *HINTW* in ZZ males did not induce feminisation (Smith, Roeszler and Sinclair, 2009). Furthermore, recent findings have shown that an antibody raised against HINTW, did not detect any HINTW protein, suggesting that *HINTW* does not encode for a protein. While *HINTW* may act as a non-coding RNA, experimental female-to-male sex reversal induced by Fadrozole did not change the levels of *HINTW* RNA present in female gonads (Hirst *et al.*, 2017). Taken together, this suggests that *HINTW* either does not act downstream of *AROM* or it does not act as a female sex determinant.

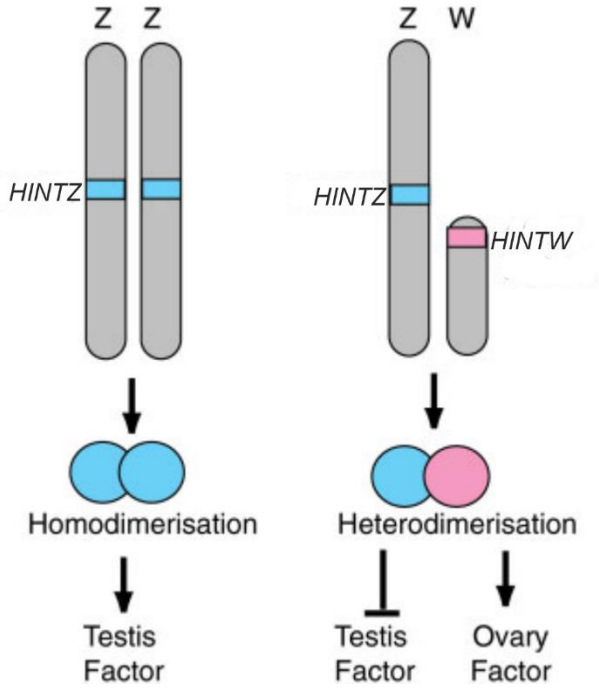

Figure 1.5. *HINTW/HINTZ dimerization hypothesis.* In ZZ males, the *HINTZ* gene product undergoes homodimerization to stimulate the production of a testis factor. In ZW females, the *HINTZ* and *HINTW* gene products undergo heterodimerization and in doing so either suppresses the production of a testis factor or promotes the production of an ovarian factor. (Figure adapted from Smith and Sinclair, 2004).

FET-1

FET-1 (Female-Expressed Transcript #1) is a gene found on the short arm of the W chromosome, identified by Reed and Sinclair. Reed and Sinclair reported the expression of *FET-1* mRNA to be exclusive to the female gonads, caudal somites, neural tube and waste collection ducts (Reed and Sinclair, 2002). A second study conducted by Hirst et al., however showed that *FET-1* mRNA is present in both males and females. While *FET-1* mRNA is detected in both gonads at E4.5 of males and females, the expression of *FET-1* becomes restricted to the left gonad of males at E6.5 but is present in both gonads of females. While functional work on *FET-1* is yet to be conducted, female-to-male sex reversal induced by Fadrozole did not result in changes in *FET-1* expression, suggesting that either *FET-1* acts upstream of *Aromatase*, acts in the *WNT4*/*RSPO1*/*β-catenin* pathway or is not essential to ovarian development (Hirst *et al.*, 2017).

1.5. Cell Autonomous Sex Identity

Cell Autonomous Sex Identity (CASI) refers to the phenomenon whereby somatic cells differentiate as male or female according to their genotype instead of the actions of the circulating sex hormones - physically illustrated by gynandromorphs. Bilateral gynandromorphs are animals in which one side appears to be male and the other side female. Gynandromorphy and therefore an effective CASI system has been documented in insects, crustaceans and birds (Spencer, 1927; Fenner and Moore, 1959; Bowen and Hanson, 1962; Johnson and Otto, 1981). It would suggest then, that gynandromorphy would be a good criterion to determine whether a species demonstrates CASI. However, this criterion would be very superficial seeing as this relies on male and females being distinctly different in appearance or size, which may not always be true. Therefore, it may be more accurate to look at the molecular level and determine the molecular basis of CASI.

1.5.1. Evidence of CASI in chickens

Analysis of chicken gynandromorphs by Zhao *et al.*, (2010) and Morris *et al.*, (2018) showed that the bilateral gynandromorphy observed reflected the relative contributions of ZZ male cells and ZW female cells. Said otherwise, the side that was phenotypically male was predominantly comprised of ZZ male cells and the side that was phenotypically female was predominantly comprised of ZW female cells. The significance hereof is that a gynandromorph exhibits the same hormone profile throughout its entire body, demonstrating that the sex-specific structures (such as comb size and muscle mass) did not respond to the circulating hormones, but instead the genotype of the individual cells that make them up (Zhao *et al.*, 2010; Morris *et al.*, 2018). This is in direct contrast with the standard model of vertebrate sex determination (based on research conducted in mammals) whereby sex-specific structures differentiate according to the hormones they are exposed to, regardless of their genotype (Clinton, *et al.*, 2012).

A transplantation experiment conducted by Zhao *et al.*, (2010) whereby male/female chimeric gonads were created clearly illustrated CASI at the molecular level. In this experiment, the presumptive mesoderm of GFP-expressing embryos (HH12-13) (donor) replaced the equivalent tissue of non-GFP expressing embryos at the same stage (recipient). The donor tissue was only transplanted to the left side of the recipient embryo and the embryos were left to develop to HH31 so that the donor cells had time to integrate. In doing so, same sex chimeras (male donor/male recipient and female donor/female recipient) and mixed sex chimeras

(male donor/female recipient and female donor/male recipient) were created. Same sex chimeras showed that donor cells integrated normally into the recipient embryo and these donor cells showed normal functioning. For example, in male same sex chimeras, male donor cells integrated into the sex cords and showed normal *AMH* expression. The donor cells in the mixed sex chimeras, however, did not integrate into the functional gonad of the recipient embryo and retained their sexual identity. For example, in female donor/male recipient chimeras, the female donor cells were restricted to the interstitial space, evident by the lack of co-localisation. Interestingly, the donor cells in mixed sex chimeras showed normal gene expression reflective of their genotype. For example, in female donor/male recipient chimeras, the female donor cells showed normal *AROM* expression (Zhao *et al.*, 2010). Evidently, it is apparent that somatic cells retain their "sexual identity" conferred by their genotype.

1.5.2. Molecular basis of CASI and implications in avian gonad differentiation

With respect to birds, and more specifically *Gallus gallus*, the most striking difference between male and female somatic cells is the sex chromosomes. As such, CASI must be a function of the genes on the sex chromosomes and how these genes are expressed in a dimorphic manner between males and females. It is likely that CASI genes would be expressed in a sexually dimorphic manner in all cells and tissues, at all stages of development (Clinton *et al.*, 2012). Studies conducted on tissues prior to the formation of the gonads, show there are over 200 transcripts expressed in a sexually dimorphic manner in HH4 male and female embryos (Lee *et al.*, 2006; Scholz *et al.*, 2006; S. O. Zhang *et al.*, 2010). Other similar studies conducted show there may be as many as 300 CASI genes (Itoh *et al.*, 2007; Melamed and Arnold, 2007; Mank and Ellegren, 2009; Mcqueen and Clinton, 2009). It is unclear, however, whether the same CASI genes are involved in establishing a male/female sexual identity in all tissues or whether groups of CASI genes establish the sexual identity in a single tissue. Furthermore, it is unclear whether individual CASI genes exert a significant effect or whether it is the action of several CASI genes, having a cumulative effect or possibly even both (Clinton *et al.*, 2012).

With respect to gonad differentiation, it is possible that CASI directly interacts with key testis (*DMRT1*) or ovary determinants (*FOXL2*) that drive the male/female pathway. Alternatively, it is the expression of these CASI genes in the genital ridge,

prior to the initiation of gonad differentiation that triggers the activation of these testis/ovary determinants (Clinton *et al.*, 2012; Hirst, Major and Smith, 2018). While CASIs role in activating gonad differentiation remains unclear, CASI is definitely involved in establishing and maintaining the gonad phenotype and can override the effects of circulating hormones (Zhao *et al.*, 2010; Morris *et al.*, 2018).

1.6. *FAF* (Female Associated Factor) as a plausible female sex determinant

1.6.1. The identification of *FAF*

FAF was first identified by Zhao, et al (2010) by differential display polymerase chain reaction (DD-PCR) – a technique that identifies differential expression between tissue types based on the intensity of the bands when cDNA products are electrophoresed. DD-PCR of male and female tissue (prior to gonad formation) led to the identification of *FAF* and its female-exclusive expression. Whole mount *in situ* hybridisation of *FAF* at stages HH4, HH14 and HH20 confirmed the DD-PCR results and confirmed that *FAF* is expressed ubiquitously and exclusively in females, illustrated in **Figure 1.6** below (Zhao *et al.*, 2010). RNA-Seq on male and female gonads at HH24-25 conducted by Ayers et al., (2013), supports Zhao et al., (2010) findings that *FAF* is a W-linked gene, lacking any Z-gametologue and is expressed from HH1 and at the onset of gonad differentiation (E4.5) (Ayers *et al.*, 2013). Additionally, **Figure 1.6** confirms the expression of *FAF* mRNA in the gonads of females-only at HH24, HH29 and HH35. In tissue sections, *FAF* mRNA is seen throughout the gonads but concentrated to the cortex (**Figure 1.7**) (Hirst *et al.*, 2017).

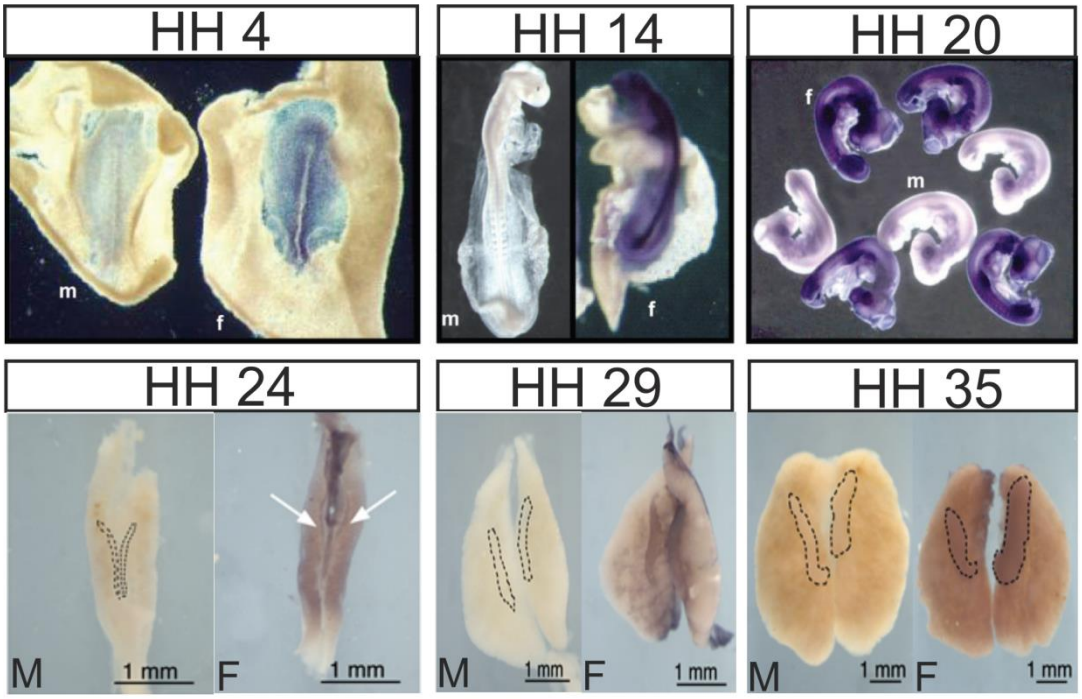

Figure 1.6. *In situ hybridisation showing the expression of FAF mRNA (purple).* It is evident that *FAF* is expressed ubiquitously in female embryos at HH4, 14, 20, 24, 29 and 35, but *FAF* mRNA is not detected in males. M – Males. F – Females. (Figure adapted from Zhao et al., 2010; Hirst et al., 2017).

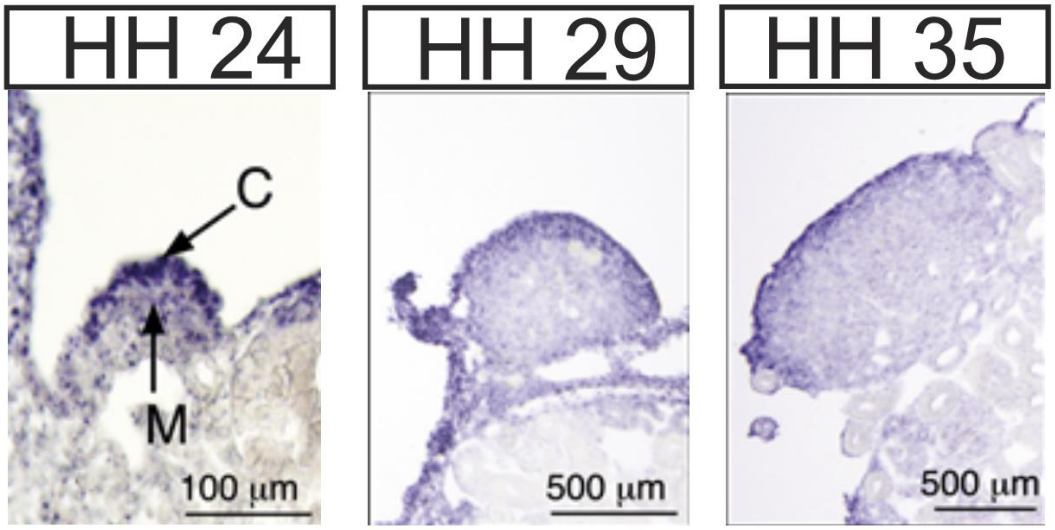

Figure 1.7. *In situ hybridisation of tissue sections showing spatial expression of FAF mRNA (purple) in females gonads. FAF* is expressed throughout the female gonad but concentrated in the cortex. C – Cortex. M – Medulla. (Figure adapted from Hirst *et al.*, 2017).

The gene tree generated using Ensembl (Gallus_gallus-5.0 assembly) shows 16 *FAF* genes and is shown below in **Figure 1.8**. Based on the distribution of the tree and the duplication nodes (red), the *FAF* genes can be 'grouped' into 5 groups. Interestingly, if *FAF* has undergone gene duplication events, it would certainly suggest that *FAF* is essential to female development since it has been conserved on the W chromosome undergoing genetic decay. Alternatively, there may be a single *FAF* gene but since it is split across non-contiguous or gapped regions of the W chromosome, it has been represented by several transcripts (Ayers *et al.*, 2013).

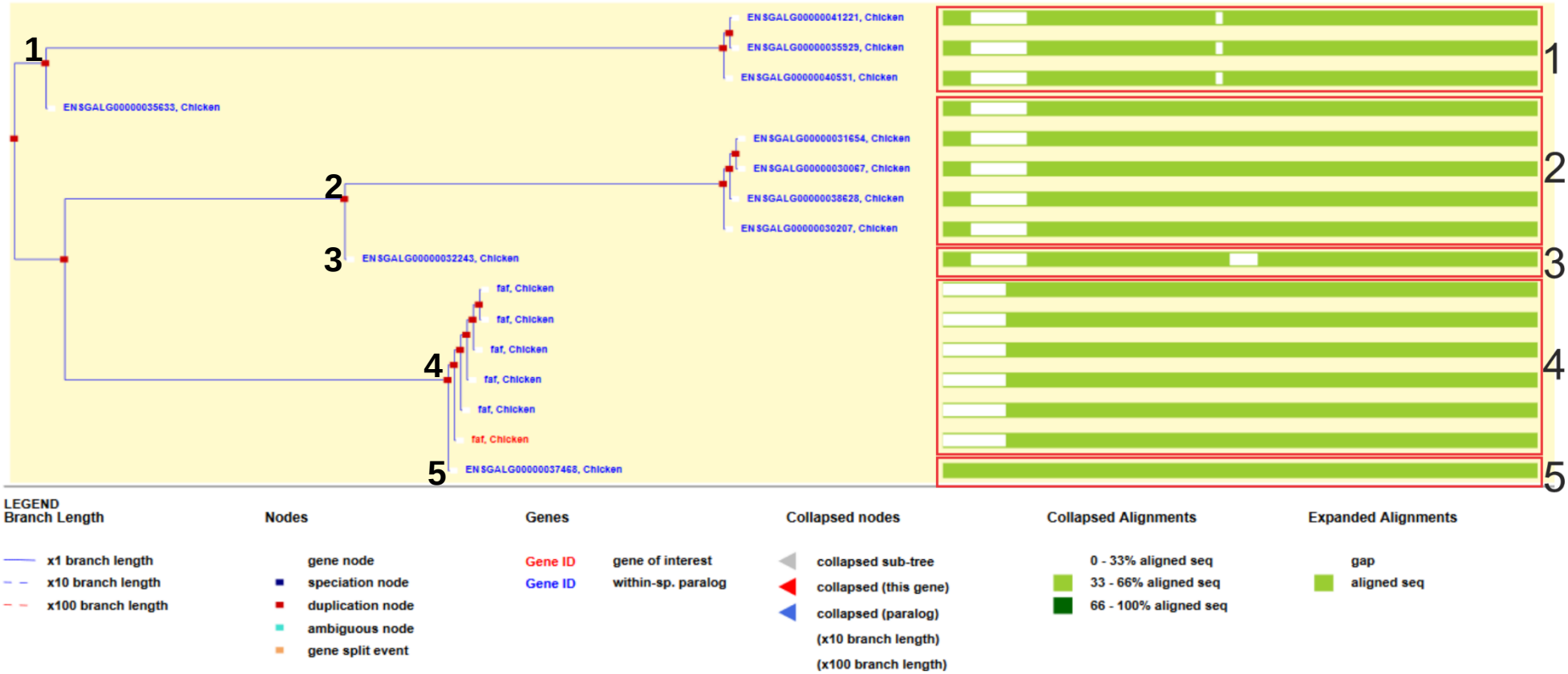

Figure 1.8. *Gene tree generated by Ensembl depicting the alignment of the 16 FAF genes*. The red nodes represent gene duplication events, such that *FAF* can be grouped into 5 groups. Consistent with this, each *FAF* gene within a group shares 33-66% alignment to each other and has gaps in the same regions, shown by the white boxes. *FAF* genes across the different groups also share 33-66% alignment. (Figure adapted from Ensembl).

1.6.2. Temporal and spatial expression of *FAF* suggests a possible role as a CASI gene and female sex determinant

Seeing as *FAF* is expressed in somatic tissue under CASI control, from early stages of development (HH4), in a female exclusive manner, it presents the possibility of being a CASI gene. Furthermore, seeing as *FAF* is a W-linked gene that is expressed prior to HH24-25 in the differentiating gonads of females, it meets the criteria of being a female sex determinant.

1.7. Rationale and motivation for project

Selective breeding in the poultry industry has led to the creation of distinct chicken breeds: egg-laying breeds, optimized to produce high quality eggs and broilers, optimized to have a fast growth rate and increased meat production. Consequently, male chicks of egg-laying breeds are unprofitable as they do not produce eggs and they produce little meat in comparison to broilers. Currently, these male chicks are culled immediately after being hatched and sexed, by methods such as maceration, cervical dislocation or asphyxiation by carbon dioxide (Buhl, 2013; Bruijnis *et al.*, 2015; Degeling, Chris, Lederman and Rock, 2016). It was estimated that, in 2018, 7 billion day-old male layer chicks were culled worldwide, and it is no surprise that this practice has raised many ethical concerns and presents the financial burden of not only hatching the chicks but also having to cull them (Poultry, 2015).

Promising alternative methods have been developed to sex chickens *in ovo.* An example of such a technology is using Raman Spectroscopy whereby eggs are windowed and the blood is spectroscopically analysed for sex-specific differences in the fluorescence spectrum at E3.5 (Embryonic day). The sex of the embryos can be identified, with 93% accuracy (Galli *et al.*, 2017). This technique, however, requires the eggs to be windowed which can be invasive and increase embryo mortality. A second alternative that employs a less invasive strategy is an endocrinological gender test, developed by SELEGGT GmbH which tests the allantois fluid of E9.0 old embryos for a male and female specific marker, with 98% accuracy (Seleggt). Although these techniques provide an alternative to the culling of day old male chicks, both techniques require expensive equipment and the necessary skillset to operate these machines, which many farmers in South Africa are unwilling to invest in. The second major drawback of both these techniques is that they do not eliminate the fact that male chicks are still being produced. Indeed these methods enable male chicks to be disposed of prior to hatching, however, their production still reduces the hatching capacity and still poses the financial burden involved in disposing of them.

Manipulating the molecular mechanism/s that governs sex determination in chickens may therefore be a fruitful approach. If the molecular mechanism that drives sex determination is manipulated to ensure that only female chicks are hatched, it would address both the ethical issue of male chick culling and it would not require any invasive *in ovo* sex screening methods which relies on the use of

expensive machinery and a specialized skillset. The spatiotemporal expression profile of the W-linked gene, *FAF*, makes it an interesting candidate for female sex determinant which warrants investigation. This project therefore aimed at elucidating the functional role of *FAF* in the gonad development of female ZW chickens. If *FAF* does function as a female sex determinant, this knowledge may be used to create a transgenic breed of all-female chickens. This in turn would address both the ethical issue of male chick culling and the financial implications hereof by abolishing the culling process entirely. To put this in perspective, one of the three largest chicken farms in South Africa reportedly cull an estimated 70 000 male chicks per week, which equates to 3.64 million male chicks per year (Tempelhoff, 2009). Should a transgenic breed of all-females be used, an extra 964.6 million eggs (3640000 x 265) could be produced.

Eggs are referred to as being a “functional food” since they are inexpensive to produce, easy to handle and easy to store (Herron and Fernandez, 2004). Furthermore, they are highly nutritious with a moderate calorie source (~150 kcal/100 g), providing 18 vitamins and minerals and 12-13 g of high-quality protein per 100 g (approximately 2 eggs) which is equivalent to ~26% of the daily protein requirement of an average person (Herron and Fernandez, 2004; Natoli *et al.*, 2007; Samman *et al.*, 2009; Fraeye *et al.*, 2012; Miranda *et al.*, 2015). Given this, it is critical that an adequate and affordable supply of eggs is provided.

1.8. Hypothesis, aim and objectives

1.8.1. Hypothesis

It is hypothesized that *FAF* plays a role in avian sex determination and has an instructive role in the formation of the female gonads. Therefore, if the hypothesis is correct, loss of *FAF* expression in ZW female gonads should result in a decreased expression of female specific markers and an upregulation of male specific markers, while loss of *FAF* from ZZ gonads should have no effect on the expression of male specific markers.

1.8.2. Aim

To determine the role of *FAF* in the gonadal development of *Gallus gallus*.

1.8.3. Objectives

Objective 1: Experimentally validate the predicted 5'-UTR of *FAF* by 5'-RACE.

Objective 2: Investigating the effect of morpholino-mediated *FAF* knockdown on the gonadal phenotype of ZZ and ZW chicken embryos.

Objective 3: Investigating the effect of ectopic *FAF* expression on the gonadal phenotype of ZZ chicken embryos.

2. Chapter 2 – Materials and Methods

2.1. *In silico* FAF protein prediction

The amino acid sequence of FAF (ENSGALG00000041221) (Gallus_gallus-5.0 assembly) was used for the *in silico* protein prediction. RaptorX (Källberg, *et al.*, 2012) (using the default parameters) was used to predict the secondary and tertiary structure of FAF. RaptorX was used because it does not use close homologs found in the Protein Data Bank to predict the secondary and tertiary structures which was advantageous because not many structures of chicken proteins have been solved. The amino acid sequence of FAF (ENSGALG00000041221) (Gallus_gallus-5.0 assembly) was also submitted to $(PS)^2$-v2: Protein Structure Prediction Server (Chen, *et al.*, 2009), which used homology modelling to detect homologous proteins based on the submitted sequence and secondary structure information. This was done to determine whether any proteins homologous to FAF exists. The ScanProsite tool (Castro *et al.*, 2006) was used to identify sequence motifs as these are predicted to have a biological function. The default parameters were used for all abovementioned tools.

2.2. Egg incubation

Gallus gallus (domestic chicken) embryos were used in this project since they are model organisms for developmental studies, offering advantages such as an annotated genome, and the ease of genetic manipulation. All eggs used in this project were White Leghorn - SPF (specific pathogen-free) eggs and were obtained from Avi-farms. Ethical clearance to experiment on chick embryos was granted (Wits permit number issued by the Wits animal ethics committee - **2017-01-01-O**) (**Appendix 12**).

2.3. 5'-RACE (Rapid Amplification of cDNA Ends)

RACE (Rapid Amplification of cDNA Ends) is a molecular technique that enables the complete acquisition of mRNA sequences where only a partial sequence is known (Yeku & Frohman, 2011). 5'-RACE was therefore performed to experimentally validate the computationally annotated 5'-UTR of *FAF*. This data was required to design the morpholino constructs. 5'-RACE was conducted twice and henceforth referred to as RACE 1 and RACE 2. 5'-RACE was conducted as per the manufacturer's protocol (Thermo Fisher Scientific). This entails the removal of the 5' phosphate from truncated mRNA and non-mRNA transcripts by CIP (calf intestinal phosphatase), followed by the removal of the 5' cap from intact mRNA

transcripts by TAP (tobacco acid pyrophosphatase). This allowed for the ligation of the GeneRacer RNA Oligo, catalysed by T4 RNA Ligase, which acted as a known priming site for PCR. The modified mRNA transcripts were then reverse transcribed and PCR was conducted on the cDNA using a forward primer complimentary to the GeneRacer RNA Oligo and a reverse primer specific to *FAF*. The workflow of RACE is summarized in **Figure 2.1** below.

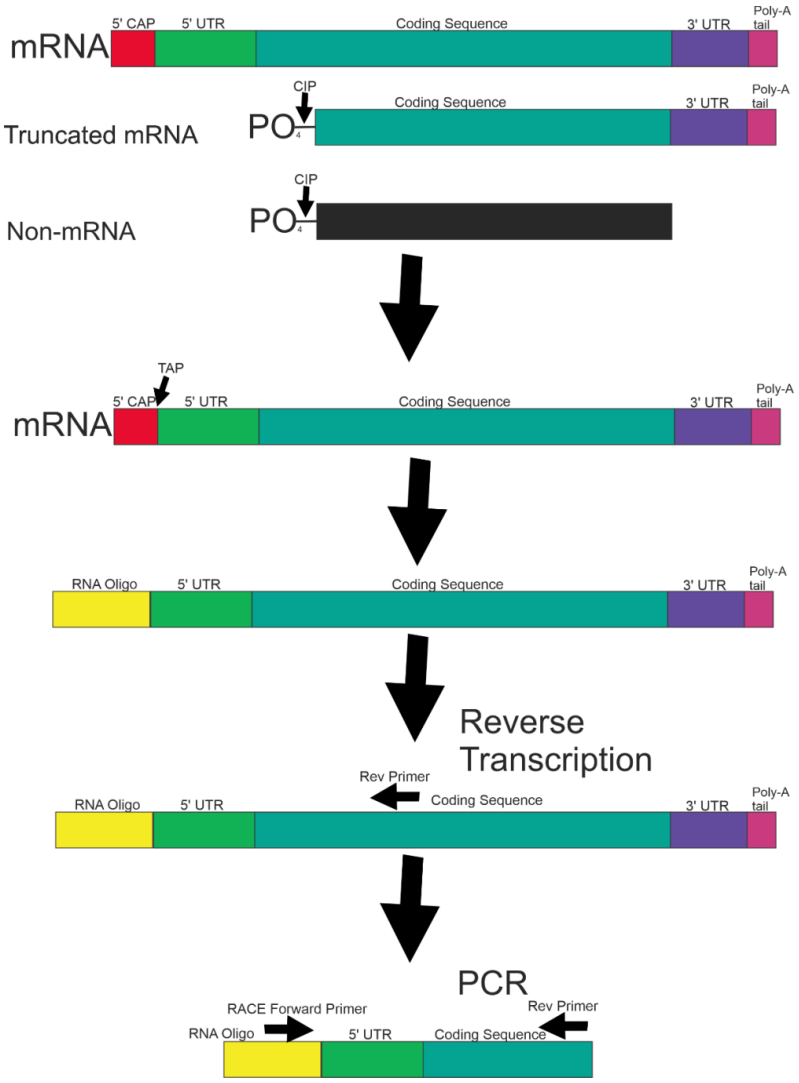

Figure 2.1. *Overview of 5'-RACE*. The isolated total RNA contains full length mRNA transcripts, truncated mRNA transcripts and non-mRNA. The addition of CIP (calf intestinal phosphatase) removes the phosphate (PO_4) group from the truncated mRNAs and non-mRNAs, ensuring the RNA oligo does not ligate to these transcripts. TAP (tobacco acid pyrophosphatase) is added to remove the 5' cap from the full length mRNA transcripts. This is required for the ligation of the GeneRacer RNA Oligo. The GeneRacer RNA Oligo is ligated to the 5' end of the full length mRNA transcripts, using T4 RNA Ligase. The ligated mRNA transcripts are reverse transcribed using a Gene Specific Primer. The cDNA is then amplified using the RACE Forward Primer (complimentary to the GeneRacer RNA Oligo sequence) and the Gene Specific Primer used in the reverse transcription step.

2.3.1. *FAF* gene-specific primer design for 5'-RACE

A reverse primer was designed according to the specifications of the GeneRacer manual. Based on these criteria, a *FAF* reverse primer was designed to bind 48 bp within the *FAF* CDS and had the following parameters, summarized below in **Table 2.1**. The designed primer was aligned to all 16 *FAF* transcripts to ensure it would bind to each of them.

Table 2.1. Parameters of the *FAF* reverse primer, used in 5'-RACE.

Sequence	Length (nt)	GC content (%)	Tm (°C)
5'-CTCGGTCGATCACAGGCGGAAGGA-3'	24	62.5	71

The primer was evaluated for self-dimer formation and heterodimer formation with the RACE forward primer provided (5′-CGACTGGAGCACGAGGACACTGA-3′) using the OligoAnalyzer tool (Integrated DNA Technologies), ensuring that the ΔG values were greater than -9 kcal/mole as this meant that no strong secondary structures were present. The primer was subject to a BLAST search (Altschup *et al.*, 1990) against the chicken genome (Gallus_gallus-5.0 assembly), using the refseq_rna database for potential off-targets (NCBI).

2.3.2 Embryo dissections for RNA collection

Before any dissections were done, the working area and dissecting instruments was sterilized with 70% ethanol and RNaseZap (Sigma). RNaseZap was used to inactivate RNases. The eggs were sterilised by spraying 70% ethanol on their shell to remove any debris and bacteria. A 5 ml syringe (fitted with an 18 gauge needle) was used to make a hole on one side of the horizontally placed egg. The needle was inserted into the holes and 2-5 ml of albumin was removed and discarded. The removal of albumin caused the embryo to drop, ensuring it remained unharmed during subsequent steps. After the removal of the albumin, another hole was made on the top of the horizontally positioned egg. A pair of fine forceps was used to window the egg by chipping off pieces of the eggshell until the embryo was visible. With the aid of a pair of fine scissors, the membranes and blood vessels surrounding the embryo were cut so that the embryo could be transferred to a petri dish containing 1x PBS (0.15 M NaCl, 8.01 mM Na_2HPO_4 and 2 mM NaH_2PO_4). With the aid of a dissecting microscope (CL 6000 LED, Zeiss), the embryos were staged according to the Hamburger and Hamilton staging system (Hamburger and

Hamilton, 1992) and the membranes encasing the embryo were removed. Tissue from the head (3 mm x 3 mm) was collected for PCR based sexing, as described below.

2.3.2.1 Whole body and gonad collection for 5'-RACE

Since *FAF* is expressed ubiquitously, 5'-RACE was performed on the RNA isolated from either the whole body or only the gonads. After tissue from the head was collected for sexing, the remaining body of the embryo or only the gonads were collected and placed in a 1.5 mL RNase-free micro-centrifuge tube containing 30 µL RA1 buffer (Macherey Nagel). The RA1 buffer contained large amounts of chaotropic ions which inactivated any RNases present. Since the gonads at HH24 were still small and transparent (shown by arrow in **Figure 2.2** below), extra precaution was taken to get as little mesonephros tissue as possible.

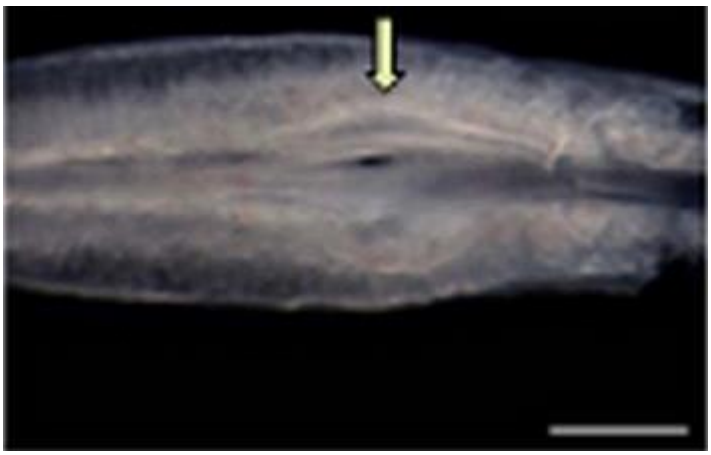

Figure 2.2. *Chick urogenital system at HH24-25*. Image depicting the mesenphros and gonad of chick embryo at HH24-25. Arrow denotes the gonad. (Figure adapted from Caetano *et al.*, 2014).

2.3.3. DNA extraction and PCR sexing

A crude DNA extraction method, described by Li *et al.*, 2011 was performed on the tissue collected. The collected tissue was placed in 100 µL lysis buffer (10 mM Tris-HCl (pH = 8), 2 mM EDTA (pH = 8) and 0.2 M NaCl) and 1 µL Proteinase K (20 mg/ml) was added to the solution to digest contaminating proteins and nucleases. The tissue was vortexed vigorously for 30 sec and then incubated at 55 °C for 15 min. The samples were vortexed again for 30 sec and incubated for another 15 min at 55 °C. A final 5 min incubation at 95 °C was performed to

inactivate the Proteinase K. The samples were vortexed again for 30 sec and were then centrifuged (>10000g) for 1 min to pellet the cellular debris. The DNA present in the supernatant was used for the subsequent PCR reaction.

The protocol outlined by Clinton *et al.* was used to sex the embryos (Clinton *et al.*, 2001). Clinton *et al.* describes a rapid, simple PCR reaction that can be used to sex chicken embryos prior to the evaluation by morphological features which can only be conducted at HH32-33 (Clinton, *et al.*, 2001). Two sets of primers were used: the first set amplified a region of the *18S ribosomal gene* from position 1267 to 1522, present in both male and female embryos (used as an internal control) and the second set amplified an *Xho*I repeat sequence present only on the W chromosome of female embryos. **Table 2.2** below summarizes the primer sequences used and their expected product size.

Table 2.2. Primer sequences used for sexing PCR.

Gene amplified	Primer sequence	Expected product size (bp)
18S ribosomal gene	F: 5'- AGCTCTTTCTCGATTCCGTG -3'	256
	R: 5'- GGGTAGACACAAGCTGAGCC -3'	
*Xho*I repeat sequence	F: 5'- CCCAAATATAACACGCTTCACT -3'	415
	R: 5´- GAAATGAATTATTTTCTGGCGAC -3´	

The PCR reaction comprised of: 12.5 µL Taq DNA Polymerase 2x Master Mix (Ampliqon), 1.25 µL (10 µM) of each *18S ribosomal gene* primer, 2.5 µL (10 µM) of each X*ho*I repeat sequence primer, 4 µL of crude DNA and 1 µL dH_2O. A no template control was also prepared and consisted of the same components, except the crude DNA was replaced by dH_2O. The PCR conditions were optimised by Clinton, *et al.*, 2001 and were: 94°C for 2 min followed by 25 cycles of 94°C for 5 sec, 56°C for 5 sec and 72°C for 5 sec. A final extension step of 72°C for 5 min was performed.

The PCR products were electrophoresed on a 1% agarose gel (see **Appendix A1.1** for gel preparation). The gel was run for 45 min at 120V to allow for the migration of the DNA. Male embryos were identified by the presence of a single

band (256 bp) and female embryos were identified by the presence of two bands (256 bp and 415 bp).

2.3.4. RNA isolation for RACE

Based on the sexing PCR results, multiple female embryo or female gonad samples were pooled. Male embryos were discarded since it has been confirmed that *FAF* is only expressed in females (Zhao *et al*., 2010). Embryos were pooled to increase the final RNA concentration. RNA isolation was performed using the NucleoSpin RNA kit (Macherey Nagel), as per the manufacturer's instructions. The NucleoSpin RNA kit uses silica membrane technology to selectively bind RNA and DNA. Bound DNA was subsequently removed by the addition of rDNase (supplied in the kit). RNA was eluted in 50 µL RNase-free water and stored at -80 ◦C until use. The purity and concentration of the eluted RNA was assessed using the NanoDrop ND-1000 Spectrophotometer (ISOGEN) and the concentrations are shown below in **Table 2.3**.

Table 2.3. RNA concentrations obtained from HH24-25 female whole body and gonad tissue.

Experiment		RNA concentration (ng/µL)
RACE 1	Female whole body	386.0
	Female gonads	177.0
RACE 2	Female gonads	404.7

The GeneRacer kit (Invitrogen) recommends that 1-5 µg total RNA be used for each RACE reaction. **Table 2.4** below illustrates the amount of total RNA used in each RACE reaction.

Table 2.4. The amount of total RNA used in each RACE reaction.

Experiment		Volume of RNA used (µL)	Quantity of RNA used (µg)
RACE 1	Female whole body	6	2.32
	Female gonads	6	1.06
RACE 2	Female gonads	3	2.43

2.3.5. Reverse Transcription of the RNA oligo-ligated mRNA

The SuperScript Ⅲ RT Reaction Kit (Invitrogen) supplied in the GeneRacer kit was used for the reverse transcription (RT) step. This kit was used specifically since it

has improved efficiency in dealing with GC rich target RNAs, such as in the 5'-UTR of many transcripts (Invitrogen).

The RT reaction comprised of: 10 µL of ligated RNA, 1 µL of the *FAF* gene specific reverse primer, 1 µL dNTP mix and 1 µL dH_2O. The reaction was incubated at 65 °C for 5 min (RACE 1) or at 72 °C for 10 min (RACE 2) to remove any RNA secondary structures. After this incubation step, 4 µL of the 5X First Strand Buffer, 1 µL 0.1 M DTT, 1 µL RNaseOut (40 U/µL) and 1 µL SuperScript Ⅲ RT (200 U/µL) was added to the RNA/primer mixture and gently mixed by pipetting. The reaction mix was incubated at 55 °C for 60 min and then inactivated at 70 °C for 15 min. To remove any RNA that was not reverse transcribed, 1 µL of RNase H (2 U) was added to the reaction mix and incubated at 37 °C for 20 min. A RT minus control (contained all components except 1 µL SuperScript Ⅲ RT (200 U/µL) was set up for the second RACE reaction. The reverse transcribed product was used in subsequent PCR reactions.

2.3.6. PCR on RT-product

Touchdown PCR (TD-PCR) is a variation of conventional PCR where the initial annealing temperature is higher (~10 °C higher) than the optimal annealing temperature of the primers and is progressively reduced over subsequent cycles until the optimal annealing temperature is reached. This improves PCR amplification specificity by having cycles at a range of different temperatures so that the optimal temperature for the correct primer/template combination can be found. The progressive transition to a lower temperature ensures that the desired amplicon in the reaction out-competes any non-specific amplicons and/or primer dimers (Korbie and Mattick, 2008). Since the RNA oligo that is ligated to the mRNA during RACE is able to ligate to any available mRNA, increased amounts of off-targets were expected. TD-PCR in combination with a high fidelity DNA polymerase was therefore used to improve PCR amplification specificity.

The PCR reaction comprised of 5 µL 5x MyFi Reaction Buffer (Bioline), 1 µL MyFi DNA Polymerase (Bioline) 1.5 µL RACE forward primer (10 µM), 1.5 µL *FAF* gene specific reverse primer (see **Table 2.1**) (10 µM), 2 µL RT product and 14 µL dH_2O. A no template control (NTC) was also set up and contained the same components, except that the RT product was substituted with dH_2O. **Table 2.5** below shows the optimized TD-PCR conditions that were used. The MyFi DNA Polymerase was used since it was compatible with TA cloning, required for the successful ligation

into the pCR™4-TOPO® plasmid (See **Chapter 2.3.7**). The thermocycling conditions used were decided based on the suggested conditions described in the MyFi DNA Polymerase protocol, the TD-PCR protocol outlined by Korbie and Mattick, 2008 and the annealing temperature of the primers. Additionally, a second set of PCR conditions (used by a previous student) were also tested. This was done to mitigate any PCR bias that may exist. **Table 2.6** shows the PCR conditions used by the previous student.

Table 2.5. Optimized TD-PCR conditions used for 5'-RACE PCR.

Phase I			
	Step	**Temperature (°C)**	**Length (sec)**
10X cycles	Initial denaturation	98	30
	Denaturation	95	30
	Anneal	72*	30
	Elongate	72	60
Phase II			
	Step	**Temperature (°C)**	**Length (sec)**
30X cycles	Denaturation	98	30
	Anneal	62	30
	Elongate	72	60
Phase III			
	Step	**Temperature (°C)**	**Length (sec)**
	Final elongation	72	120
	Terminate	4	120
	Hold	4	∞

[*] Annealing temperature decreased by 1 °C after each cycle.

Table 2.6. Optimized PCR conditions used by previous student for 5'-RACE PCR.

Phase I			
	Step	**Temperature (°C)**	**Length (sec)**
10 cycles	Initial denaturation	95	120
	Denaturation	94	15
	Anneal	60	30
	Elongate	72	60

Phase II			
	Step	**Temperature (°C)**	**Length (sec)**
20 cycles	Denaturation	94	15
	Anneal	60	30
	Elongate	72	60*

Phase III			
	Step	**Temperature (°C)**	**Length (sec)**
	Final elongation	72	420
	Terminate	4	120
	Hold	4	∞

[*] Elongation time increased by 5 sec after each cycle.

The PCR products were electrophoresed on a 1% agarose gel as described in **Appendix A1.1**. The gel was run for 90 min at 100V to allow for the migration of the DNA.

2.3.7. PCR product cloning: Ligation and transformation

The RACE-PCR products were ligated directly into the pCR™4-TOPO® plasmid as per the manufacturer's instructions (Invitrogen). A gel extraction of the two largest bands (750 bp and 500 bp) was first performed on the RACE2-PCR products as described in **Appendix A1.3** before these isolated bands were ligated into the pCR™4-TOPO® plasmid.

The pCR™4-TOPO® plasmid offers a quick one-step ligation step without the need of DNA ligase. Additionally, this system does not require any screening method (such as blue/white screening) as successful ligation of an insert disrupts the expression of a lethal gene (*ccd*B) which kills cells that do not contain the recombinant plasmid upon plating (Bernard and Couturier, 1992; Bernard *et al.*, 1993; Bernard *et al.*, 1994).

A ligation reaction comprised of 3 µL of fresh PCR product, 1 µL salt solution (1.2 M NaCl; 0.06 M $MgCl_2$ to improve transformation efficiency), 1 µL pCR™4-TOPO® plasmid and 1 µL of dH_2O. The ligation mixture was incubated at 22 °C for 30 min. A separate ligation reaction was set up for each PCR product.

The rapid chemical transformation protocol outlined in the TOPO TA Cloning Kit (Invitrogen) was followed to transform the recombinant pCR™4-TOPO® plasmid into One Shot chemically competent *E. coli* cells. 2 µL of the recombinant plasmid was added to a vial of competent cells. 50 µL of the transformed cells was plated on each LB Agar plate (pH 7.4), supplemented with 100 µg/mL ampicillin. The plates were incubated overnight at 37 °C.

2.3.8. Colony PCR

Colony PCR was performed as described in **Appendix A1.2**. The T3 Forward primer (5'-ATTAACCCTCACTAAAGGGA-3') and T7 Reverse primer (5'-TAATACGACTCACTATAGGG-3') were used. **Table 2.7** below shows the PCR conditions that were used.

Table 2.7. PCR conditions used for colony PCR.

	Step	*Temperature (°C)*	*Length (sec)*
	Initial denaturation	98	600
30X cycles	Denaturation	95	25
	Anneal	55	35
	Elongation	72	60
	Final extension	72	120

The PCR products were electrophoresed on a 1% agarose gel as described in **Appendix A1.1**. The gel was run for 60 min at 100V to allow for the migration of the DNA. Lanes with a single band indicated the presence of an insert and were used in subsequent steps.

2.3.9. Plasmid extraction and sequencing

A plasmid extraction was performed on the colonies that were successful in colony PCR by using the remaining liquid culture. The Zyppy Plasmid Miniprep Kit (Zymo Research) was used. It was ensured that fresh liquid culture was used as this affects the extracted plasmid concentration. Following the protocol, 6 mL of the liquid culture was pelleted and re-suspended in 600 µL dH_2O. The extracted plasmid was eluted in 30 µL pre-warmed elution buffer (50 °C). Prior to elution, the

elution buffer was incubated on the column matrix for 10 min. 1 µL of the isolated plasmid was used to assess the purity and concentration of each sample using the NanoDrop ND-1000 Spectrophotometer (ISOGEN). Only samples that had a concentration greater than 30 ng/µL were sent for sequencing.

The isolated plasmids were sent to Inqaba Biotech for Sanger sequencing. The M13F forward primer (5'-GTAAAACGACGGCCAGT-3') and M13R reverse primer (5'-CAGGAAACAGCTATGAC-3') were used for sequencing.

2.3.10. Sequencing analysis

BLASTn (NCBI) (Altschup *et al.*, 1990) was used to conduct a pairwise alignment of the sequenced insert and the pCR™4-TOPO® plasmid. This showed which regions of the sequence coincided with the plasmid backbone and these bases were trimmed out. Next, sequences containing both the full RNA Oligo sequence (5'-CGACTGGAGCACGAGGACACTGACATGGACTGAAGGAGTAGAAA-3') and the reverse complement of the *FAF* gene specific primer (5'-TCCTTCCGCCTGTGATCGACCGAG-3') were identified and only these sequences were analysed further. The RNA Oligo sequence was trimmed out and Jalview 2 (Waterhouse *et al.*, 2009) was used to generate a multiple sequence alignment (MSA) using the 16 *FAF* cDNA sequences and the RACE clones as input sequences.

2.3.11. mRNA secondary structure analysis of *FAF*

The secondary structures of *FAF* cDNA was analysed by Mfold (Zuker, 2003). *FAF* transcript ENSGALG00000041221 (Gallus_gallus-5.0 assembly) was used as the input sequence and the default parameters of Mfold was used. The advantage of using Mfold was that it depicts a graphical representation of how the mRNA will fold, which was used to confirm whether strong base interactions (such as G-C pairs) were present.

The melting temperature/s required to linearize the secondary structures of *FAF* mRNA (ENSGALG00000041221) (Gallus_gallus-5.0 assembly) was analysed using the UNAFold tool (IDT Technologies) and the Oligo Calc tool (Kibbe, 2007). The default parameters of both programs were used. Only the region from where the *FAF* gene specific primer (see **Table 2.1**) binds to 500 bp upstream of the start codon was analysed. The advantage of using the Oligo Calc tool was that it is not restricted to only being able to analyse 255 bases whereas the UNAFold tool (IDT

Technologies) was. This was done to determine the temperature required to linearize the secondary structures found in this region.

2.4. Morpholino-mediated knockdown of FAF

Morpholinos (MO) are anti-sense oligo molecules that bind to complementary sequences of mRNA, thereby blocking access to other molecules. This RNA-blocking property has several applications, including gene knockdowns (Moulton, 2016). The MO-mediated knockdown of FAF was achieved by designing two non-overlapping FITC-tagged-MOs that target the 5' untranslated region of *FAF*. This steric blocking interferes with the formation/progression of the ribosomal initiation complex and hence prevents the translation of the mRNA into protein. The absence of the FAF protein will demonstrate whether it is essential to the development of the female gonads.

2.4.1. Morpholino design

Using a combination of the RACE results obtained and the *FAF* sequences found on Ensembl (Gallus_gallus-5.0 assembly), a comprehensive multiple sequence alignment was generated using the DNASTAR computer software (Lasergene). The alignment illustrated regions of the 5'- UTR that were identical between all the *FAF* genes and hence potential regions to target. The alignment was sent to Gene Tools and several MO sequences were provided. Two non-overlapping FITC-tagged-MOs were chosen (their alignment to *FAF* is shown in **Appendix 5**) and were evaluated for potential off-targets using BLAST (NCBI) (Altschup *et al.*, 1990). The reverse complement of each *FAF* MO sequence (i.e. the oligo's target sequence) was subject to a BLAST search (Altschup *et al.*, 1990) against the chicken genome (Gallus_gallus-5.0 assembly), using the refseq_rna database (NCBI). Matches with less than 80% homology were considered acceptable. The number of consecutive homologous bases between the *FAF* MO and an off-target was also considered. It was confirmed that neither of the *FAF* MOs shared more than 15 consecutive homologous bases to a potential off-target, as this would be enough to efficiently block translation. Next, it was confirmed that neither of the *FAF* MOs bound to the 5'-UTR or the first 25 bases of the coding sequence of any off-target - further mitigating the possibility of an unintended knock down. Lastly, it was confirmed that neither of the *FAF* MOs bound across intron-exon boundaries of any off-target as this could affect the splicing of that gene (Moulton, 2016). A detailed summary of the potential off targets is provided in **Appendix 5**. A standard

control MO was also used. This control MO targets a human beta-globin intron mutation and the target sequence is not found within the chicken genome (GeneTools). As such, this control MO was used as a negative control. The sequences of all the MOs are shown in **Table 2.8** below.

Table 2.8. The sequences of all the Morpholinos used and their target.

Morpholino	Sequence	Target
FAF MO1	5'-ACAGACAGAAGTAAAGAAGGCACTG-3'	5'-UTR (77 bp upstream of start codon)
FAF MO2	5'-GTTCTCCTTGGGTTGCTCATAGTAA-3'	5'-UTR (22 bp upstream of start codon)
Control MO	5'-CCTCTTACCTCAGTTACAATTTATA-3'	Negative control

The use of two MOs targeting the same gene at two different places is a type of specificity control. If the two MOs are administered in separate experiments and produced a similar phenotype, it indicates that the resultant phenotype was due to the interactions between the MO and the target mRNA and not an off-target.

2.5. pCI-*FAF*-RFP expression plasmid

The ectopic expression of *FAF* in ZZ males was investigated to determine whether *FAF* could repress the male sex determining pathway. The pCI-RFP expression plasmid (Williams *et al.*, 2018) was used since it has successfully been used to drive high levels of gene expression in a wide range of cell types in chickens. The high levels of gene expression is attributed to the 'CAG' promoter which comprises of the cytomegalovirus (CMV) early enhancer element, the chicken beta-actin promoter and the 3' splice acceptor of the rabbit beta-globin gene (Miyazaki *et al.*, 1989; Niwa, Yamamura and Miyazaki, 1991). The map of pCI-RFP is shown below in **Figure 2.3**. The red boxes indicate the restriction sites that were selected, namely *Xba*I and *Sma*I. Both restriction enzymes are unique cutters. The 197 bp region between these two restriction sites was replaced by the complete *FAF* coding sequence (CDS).

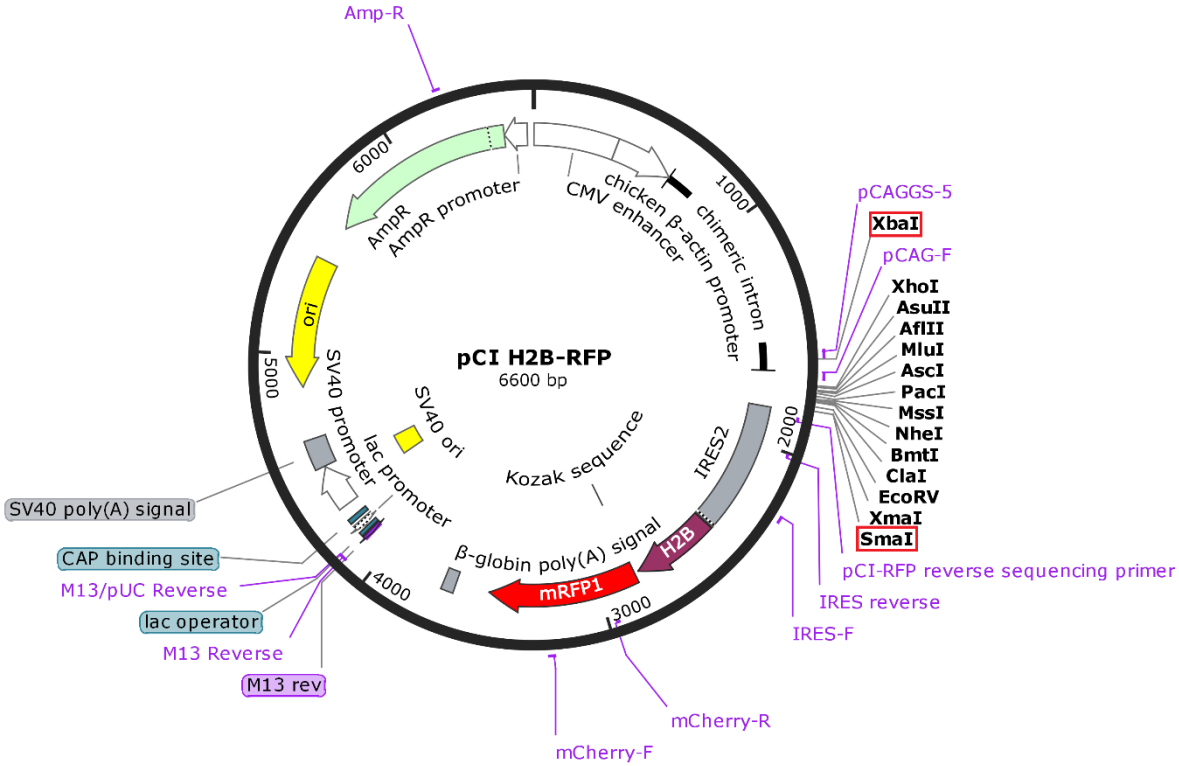

Figure 2.3. *Map of pCI-RFP.* The important regulatory elements required for gene expression (CMV enhancer and chicken β-actin promoter) are shown. The restriction sites (*Xba*I and *Sma*I) used are shown with red boxes.

2.5.1. *FAF* primer design

In order to insert the full coding sequence (CDS) of *FAF*, a forward and a reverse primer were designed. Since it was unclear whether the pCI-RFP expression plasmid or the *FAF* CDS contained a Kozak sequence, a Kozak sequence was also added. The Kozak sequence acts as a protein translation initiation site. The forward and reverse primer sequences are shown below in **Table 2.9**. Two different restriction enzymes were used to ensure that the *FAF* CDS would be ligated in the correct orientation. This was possible since *Xba*I creates sticky ends whereas *Sma*I creates blunt ends after digestion. Importantly, it was confirmed that neither restriction enzyme cuts within the *FAF* CDS. The self-dimerization and hetero-dimerization of the forward and reverse primers were evaluated with the OligoAnalyzer tool (Integrated DNA Technologies), ensuring that the ΔG values were greater than -9 kcal/mole as this meant that no strong secondary structures were present. The primer pair was subject to a BLAST search (Altschup *et al.*,

1990) against the chicken genome (Gallus_gallus-5.0 assembly), using the nucleotide collection database for potential off-targets (NCBI).

Table 2.9. Primer sequences used for cloning *FAF* into pCI-RFP and their conditions.

Primer	Sequence	Length (nt)	GC content (%)	Tm (°C)
FAF forward cloning primer	5'-agcatctagagccaccatggactctgcaaaaactttg-3'*	38	44.74	74.4
FAF reverse cloning primer	5'-tgcttacccgggctaggcctggggatggga-3'*	30	66.67	81.6

[*] – Bases in orange were used to facilitate restriction enzyme cutting efficiency. Bases in blue denote the restriction site. Bases in green denote the Kozak sequence. Bases in red denote the bases complimentary to *FAF*.

2.5.2. PCR amplification of *FAF* CDS

Two PCR reactions were set up – one using male template DNA (101 ng/µL) and the other using female template DNA (103 ng/µL). A high fidelity DNA polymerase was used to minimize errors during amplification. Each 50 µL PCR reaction comprised of: 25 µL Q5 High-Fidelity 2X Master Mix (NEB), 2.5 µL *FAF* forward cloning primer (10 µM), 2.5 µL *FAF* reverse cloning primer (10 µM), 5 µL template DNA and 15 µL nuclease free dH_2O. Additionally, a no template control was also added and contained the same components, except that the template DNA was replaced with nuclease free dH_2O. **Table 2.10** shows the PCR conditions that were used.

Table 2.10. PCR conditions used to amplify *FAF* CDS.

	Step	Temperature (°C)	Length (sec)
	Initial denaturation	98	30
28X cycles	Denaturation	98	10
	Anneal	64.4	25
	Elongation	72	30
	Final extension	72	60
	Hold	4	∞

The PCR products were electrophoresed on a 1% agarose gel as described in **Appendix A1.1**. The gel was run for 60 min at 100V to allow for the migration of the DNA. A single band of 259 bp was expected when female template DNA was used.

2.5.3. PCR purification

For the subsequent restriction digest, the PCR product had to be cleaned up as components in the PCR reaction could inhibit restriction enzyme activity. The Monarch PCR & DNA Cleanup Kit (NEB) was used. This kit uses spin column based technology to selectively bind DNA and wash steps to remove all traces of possible contaminants that may hinder the activity of restriction enzymes. 44 µL of the PCR product (that used female template DNA) was used for the PCR clean-up. The PCR product was eluted in 6 µL of the elution buffer and 1 µL was used to assess the purity and concentration using the NanoDrop ND-1000 Spectrophotometer (ISOGEN).

2.5.4. Restriction digest of pCI-RFP plasmid and *FAF* PCR product

Individual restriction digests of the pCI-RFP plasmid and the purified *FAF* PCR product were performed using the Time-Saver *Xba*I restriction enzyme (NEB) and the Time-Saver *Sma*I restriction enzyme (NEB). 1 µg of the pCI-RFP plasmid and 1 µg of the purified PCR product were digested. The restriction digest reactions for the purified PCR product and for the pCI-RFP plasmid were set as shown in **Table 2.11** below.

Table 2.11. Reaction set-up of the restriction digest of *FAF* CDS and pCI-RFP with *Sma*I and *Xba*I.

Component	Volume added (µL)	
	Purified PCR product (358.4 ng/µL)	pCI-RFP plasmid (1.27 µg/µL)
Template	2.8	0.8
10X CutSmart buffer	5	5
*Sma*I restriction enzyme	1	1
*Xba*I restriction enzyme	1	1
Nuclease free dH_2O	40.2	42.2
Final volume	50	50

It should be noted that *Sma*I and *Xba*I required different incubation temperatures. Therefore, the restriction digest reactions were set-up containing all the components except for the *Xba*I restriction enzyme and were incubated at 25 °C for 15 min and then the *Xba*I restriction enzyme was added and incubated at 37 °C for 15 min. The restriction digest was then terminated at 65 °C for 20 min.

The digested products along with undigested controls were electrophoresed on a 1% agarose gel as described in **Appendix A1.1**. 50 µL of the digested PCR product, 3 µL of the undigested PCR product, 20 µL of the digested pCI-RFP plasmid and 3 µL of the undigested pCI-RFP plasmid were loaded with 1 µL loading dye. The gel was run for 120 min at 100V to allow for the migration of the DNA.

2.5.5. Gel extraction of digested products

A gel extraction of the digested PCR product and the pCI-RFP plasmid was performed as described in **Appendix A1.3**.

2.5.6. Ligation of digested PCR product into digested pCI-RFP plasmid

The digested PCR product was ligated into the digested pCI-RFP plasmid using T4 DNA Ligase (Promega). The 10 µL ligation reaction was set up as shown in **Table 2.12** below. The ligation reaction was incubated at 4 °C overnight.

Table 2.12. Reaction set-up of the ligation reaction. The digested *FAF* CDS was ligated into the digested pCI-RFP plasmid.

Component	Initial Concentration	Final Concentration	Volume added (µL)
pCI-RFP plasmid	3.6 µg/µL	100 ng	0.3
PCR product	80.2 ng/µL	12.03 ng	1.5

Ligase buffer	10X	1X	1
T4 DNA Ligase	1 u	1 u	1
Nuclease free dH_2O	N/A	N/A	6.2

2.5.7. Transformation of pCI-*FAF*-RFP

The pCI-*FAF*-RFP recombinant plasmid was transformed into Mix & Go Competent *E. coli* cells (JM109 strain) (Zymo Research) as per the manufacturer's guidelines. 2.2 µL of the ligation product was added to 50 µL of the competent cells and were incubated for 30 min on ice. 50 µL of the transformed cells was plated on a LB Agar plate (pH 7.4), supplemented with 100 µg/mL ampicillin. The plate was incubated overnight at 37 °C.

2.5.8. Colony PCR

Colony PCR was conducted on the transformed colonies to ensure that the *FAF* CDS insert was present. Colony PCR was performed as described in **Appendix A1.2**. The *FAF* primers (from 2.5.1) were used. **Table 2.13** below depicts the PCR conditions that were used.

Table 2.13. The PCR conditions used for colony PCR.

	Step	*Temperature (°C)*	*Length (sec)*
	Initial denaturation	98	600
30X cycles	Denaturation	95	25
	Anneal	64.4	25
	Elongation	72	30
	Final extension	72	60

The PCR products were electrophoresed on a 1% agarose gel as described in **Appendix A1.1**. The gel was run for 90 min at 100V to allow for the migration of the DNA. Only colonies that had the *FAF* CDS insert were used in subsequent steps.

2.5.9. Plasmid extraction and sequencing

A plasmid extraction (of the colonies that had the *FAF* CDS insert) was performed on the remaining liquid culture using the Zyppy Plasmid Miniprep Kit (Zymo Research). 6 mL of the liquid culture was pelleted and re-suspended in 600 µL dH_2O. The extracted plasmid was eluted in 30 µL pre-warmed elution buffer (50

°C). Prior to elution, the elution buffer was incubated on the column matrix for 10 min. The purity and concentration of each sample was determined using the NanoDrop ND-1000 Spectrophotometer (ISOGEN). Only samples that had a concentration greater than 30 ng/µL were sent for sequencing.

The isolated plasmids were sent to Inqaba Biotech for Sanger sequencing. The pCAGGS-5 forward primer (5'-GGTTCGGCTTCTGGCGTGTGACC-3') and the pCI-RFP Reverse Sequencing Primer (5'-CTAACGTTACTGGCCGAAGC-3') were used for sequencing.

2.5.10. Sequencing analysis

BLASTn (Altschup *et al.*, 1990) (NCBI) was used to conduct a pairwise alignment of the sequenced insert and the pCI-RFP plasmid. This showed which regions of the sequence coincided with the plasmid backbone and these bases were trimmed out. The *Xba*I and *Sma*I restriction sites were then identified and trimmed out (as this would affect the multiple sequence alignment). Jalview 2 (Waterhouse *et al.*, 2009) was used to analyse the sequences. A MSA (using the MUSCLE algorithm) was generated using all 16 *FAF* CDS and the sequenced insert as input sequences.

2.5.11. Midiprep

The ZymoPURE II Plasmid Midiprep Kit (Zymo Research) was used to create a stock of the sequenced pCI-*FAF*-RFP plasmid and the empty pCI-RFP plasmid, as per the manufacturer's instructions. The ZymoPURE II Plasmid Midiprep Kit (Zymo Research) uses spin-column technology to obtain transfection grade plasmid DNA. A midiprep was performed so that a high concentration (> 1 µg/µL) of the plasmid was obtained, which was needed for electroporation. 100 mL of fresh liquid culture was used. The plasmid DNA was eluted in 200 µL of pre-warmed elution buffer (50 °C). The EndoZero step was also performed to ensure the isolated plasmids were endotoxin-free. The eluted plasmid DNA was stored at -20 °C until use.

2.6. Electroporation of Morpholino and pCI-*FAF*-RFP construct

2.6.1. Egg incubation

Fertilized White Leghorn chicken (*Gallus gallus*) eggs were incubated at 37.4 °C at 60-70% humidity, in a humidified incubator (Pleysier Incubators) until HH14-16. This stage of development was used since it provided access to the coelomic cavity (area where construct was delivered) and it is ~24hr prior to the formation of the genital ridge and hence would provide a holistic overview of the role of *FAF* in

gonad development. Embryos were placed horizontally, with their long axis oriented horizontally and the top marked to know where the embryo would be situated.

2.6.2. Egg windowing

Before the egg was windowed, it was sprayed with 70% ethanol to remove any debris and bacteria. A small piece of cellotape (0.5 cm x 0.5 cm) was cut and placed on the side of the egg opposite to the air sac. An 18G needle (attached to a 5 mL syringe) (Lasec) was used to pierce the eggshell and 1-2 mL of albumin was removed. This was done so that the embryo would lower in the egg, preventing it from being damaged in subsequent steps. The hole used to remove the albumin was then sealed with another piece of cellotape, to prevent further albumin from leaking out and bacteria from entering the egg. A piece of cellotape (2 cm x 2 cm) was placed on top of the eggshell and a circle (1 cm in diameter) was cut out. The cellotape prevented pieces of eggshell from falling into the egg, which may be detrimental to the survival of the embryo. One to two drops (approximately 100 µL) of Ringer's solution (0.12 M NaCl, 4.96 mM KCl, 1.53 mM $CaCl_2 \cdot H_2O$, pH 7.3-7.5) with Ampicillin (2 mg/mL) was added to the embryo which prevented it from drying out. A 25G needle (attached to a 5 mL syringe) (Lasec) was used to inject India ink (1:24 dilution in Ringer's solution) below the embryo which improved the contrast and made all the embryonic structures visible. It should be noted that minimal amounts of India ink was used as it has been noted that it can be toxic to embryos in large volumes. The vitelline membrane overlying the left coelomic cavity was carefully removed, making the coelomic cavity accessible for microinjection.

2.6.3. Microinjection and electroporation

The protocol outlined by Hirst *et al.*, was used for the microinjection and electroporation of the embryos. The left coelomic cavity was chosen for microinjection because electroporation in a dorsomedial manner (see **Figure 2.4**) resulted in the delivery of the construct into the intermediate mesoderm (derivative of the gonad). Only the left coelomic cavity was electroporated as the right gonad in females regresses and becomes non-functional (Hirst *et al.*, 2017). The right gonad was therefore used as an internal negative control. Both *FAF* MOs and the control MO were delivered at a final concentration of either 2 mM or 1 mM. The

two *FAF* MOs were also co-delivered at 0.5 mM each. The *FAF* MOs were delivered with the pCI-RFP plasmid to aid delivery. 504 ng of the pCI-*FAF*-RFP construct and 500 ng of the empty pCI-RFP plasmid (used as a negative control) was delivered. Each batch of embryos electroporated consisted of the experiment embryos, control embryos (electroporated with either the control MO or the empty pCI-RFP plasmid) and no electroporation controls (NEC). The NECs were processed in the same manner as the experiment embryos, however, they were not microinjected or electroporated. The dilutions for each construct is shown in **Appendix 3**.

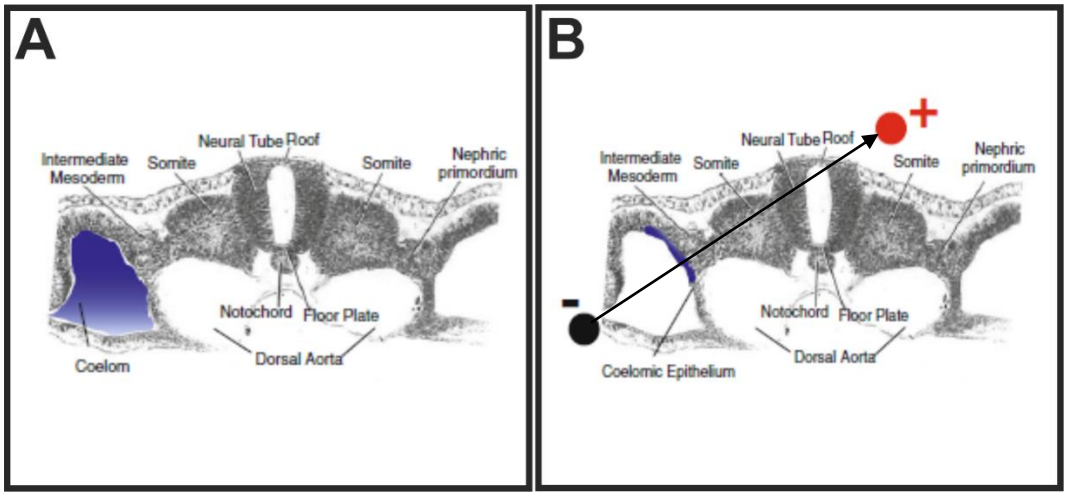

Figure 2.4. *Schematic diagram illustrating how the electroporation procedure was carried out.* **[A]** The construct (blue) was delivered to the coelomic cavity. **[B]** The negative electrode (black circle) was placed slightly beneath the left coelomic cavity and the positive electrode (red circle) was placed on top of the embryo near somite 21. The electric field (shown by the black arrow) created will encourage the negatively charged construct to move towards the positive electrode, into the surrounding coelomic epithelium and intermediate mesoderm. (Figure adapted from Hirst *et al.*, 2017).

Pulled glass capillary needles (see **Appendix 4** for preparation) were filled with 10 µL of the construct and mounted to a mouth pipette (Thomas Scientific). Mouth pipettes are fitted with filters on both ends which allows for the controlled delivery of the construct while remaining sterile. The capillary needle was inserted into the left coelomic cavity posteriorly and the construct mixed with tracking dye (8X dilution, Robertsons green colouring) was delivered by gently blowing into the mouthpiece, until the entire cavity was filled (approximately 0.5 µL) (See **Figure 2.5** below). Two to three drops (approximately 100-150 µL) of Ringer's solution (0.12 M NaCl, 4.96 mM KCl, 1.53 mM $CaCl_2 \cdot H_2O$, pH 7.3-7.5) with Ampicillin (2

mg/mL) was added on top of the embryo. This was done to improve conductivity properties and to ensure the construct was successfully delivered to the cavity (after the addition of Ringers, the construct would diffuse throughout the egg if it is not in the cavity). The negative electrode (gold plated, tip diameter of 0.5 mm) was placed slightly beneath the left coelomic cavity and the positive electrode (gold plated, tip diameter of 0.5 mm) was placed on top of the embryo (near somite 21), parallel to the negative electrode (as seen in **Figure 2.4**). Precaution was taken not to touch the embryo with either electrode as this would harm the embryo. The ECM 830 Electro Square Porator (BTX) was used to deliver the voltage with the following parameters: 2 pulses, of 30 V with a 10 ms width, with 150 ms between pulses. Precaution was taken not to damage the vitelline artery as this would kill the embryo. Immediately after electroporation, the embryo's heartbeat was monitored for 5-10 seconds to ensure it survived the voltage application. Embryos that did not have a clear heart beat were discarded. 1 mL of Ringer's solution (0.12 M NaCl, 4.96 mM KCl, 1.53 mM $CaCl_2 \cdot H_2O$, pH 7.3-7.5) with Ampicillin (2 mg/mL) was added to the embryo and the opening was sealed tightly with cellotape. Embryos were first incubated and collected 24 hr post electroporation to determine the successful electroporation of the genital ridge and then embryos were incubated to HH29-30 or HH31-34 at 37.4 °C at 60-70% humidity, in a humidified incubator (Pleysier Incubators). Embryos were incubated to this stage since the sex markers (*SOX9* and *FOXL2*) are expressed at this stage.

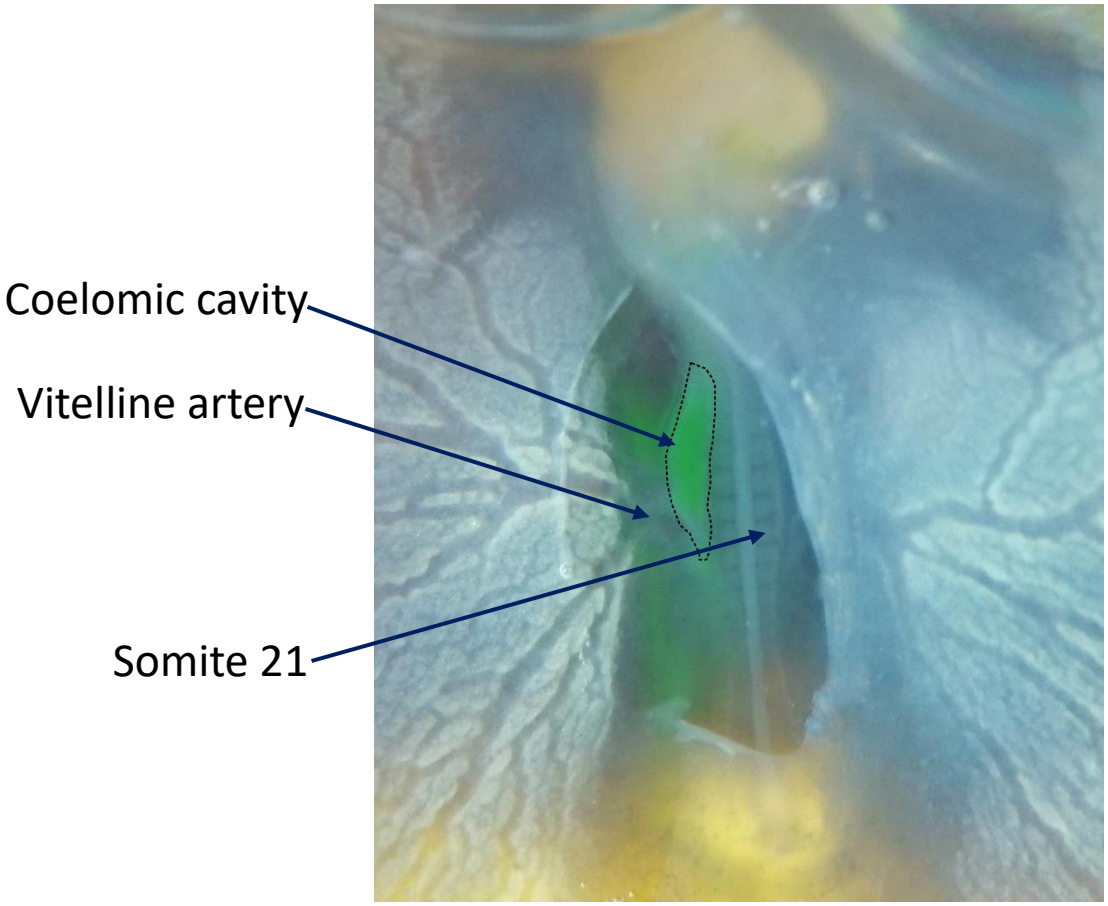

Figure 2.5. Successful microinjection and electroporation of an embryo. The dotted line outlines the left coelomic cavity. The construct (green) was successfully delivered to the left coelomic cavity. The green observed is the tracking dye used. The positions of the vitelline artery and somite 21 are also shown.

2.6.4. Embryo dissection and evaluation of construct delivery to gonads

Embryos were dissected in 1X PBS (0.15 M NaCl, 8.01 mM Na_2HPO_4 and 2 mM NaH_2PO_4) using a dissecting microscope (Zeiss CL 6000 LED) and were staged (Hamburger and Hamilton, 1992). Embryos were dissected such that the urogenital system (kidney, gonad and Müllerian ducts) were exposed and visible. Tissue (3 mm x 3 mm) for each embryo dissected was stored in 100 µL lysis buffer (10 mM Tris-HCl (pH = 8), 2 mM EDTA (pH = 8) and 0.2 M NaCl) for downstream PCR sexing. Embryos were sexed as described in Chapter 2.3.3. Dissected embryos were fixed overnight in 4% PFA (pH = 7.4) at 4 °C and were then washed twice (15 min per wash at 80 rpm) in 1X PBS (0.15 M NaCl, 8.01 mM Na_2HPO_4 and 2 mM NaH_2PO_4). The presence of FITC and mRFP1 was assessed in the fixed embryos using the Axio Zoom.V16 Fluorescence Stereo Zoom Microscope (Zeiss). This

showed whether the construct was successfully delivered to the left gonad. Images were processed using the Zen 2 (Blue edition) (Version 2.5.75.0) package (Zeiss).

2.6.5. Processing electroporated embryos

The fixed embryos that were successfully electroporated were dehydrated through a graded ethanol series (25%, 50%, 70%, 90%) diluted in 1X PBS (0.15 M NaCl, 8.01 mM Na_2HPO_4 and 2 mM NaH_2PO_4). Embryos were washed twice at each ethanol concentration for 1 hr (at 200 rpm) per rinse. Embryos were rinsed in absolute (>99%) ethanol twice (1 hr per rinse at 200 rpm). Embryos were stored in absolute (>99%) ethanol at 4 °C until being processed to wax. Upon processing to wax, the embryos were washed twice (1 hr per rinse at 200 rpm) in HistoChoice (Sigma) (substitute for xylene).

2.6.6. Embedding

To ensure complete infiltration of wax, the dehydrated embryos were incubated at an increasing wax series. Embryos were first incubated at a 1:1 ratio of wax to HistoChoice for 30 min at 60 °C and then embryos were incubated in 100% wax for 20 min at 60 °C. Embryos were placed in metal moulds and were left o/n at room temperature (20-25 °C) in order for the wax to solidify. The embedded embryos were then cut out, re-positioned and re-embedded (by adding more wax) into a cassette so that transverse sections of the urogenital system was obtained. Embedded embryos were stored at 4 °C until being sectioned.

2.6.7. Sectioning

Embedded embryos were sectioned at 4 µM - 9 µM using the Reichert-Jung 820 II Histocut Rotary Microtome (Cambridge Instruments). Sections were floated in a water bath (at 45 °C) before being picked up onto slides. Sections that were used for histological analysis were picked up on uncharged frosted microscope slides (Lasec). Sections that were used for immunofluorescence were picked up on Menzel Superfrost Plus Charged Slides (Thermo). Slides were incubated on a heating block at 40 - 45 °C (kept at 10 °C below melting point of wax) overnight to ensure sections had affixed completely to the slides.

2.6.8. H&E staining

H&E (hematoxylin and eosin) staining is basic staining technique used to improve cellular detail which provides better insight into the morphology of the stained tissue. Hematoxylin has a neutral charge until it is oxidized to hematein which then interacts with a mordant (aluminium alum) resulting in a positive charge. This positively charged product interacts with the negatively charged nucleus of cells, staining them purple. Eosin is negatively charged and interacts with the positively charged cell membrane, staining it pink (Chan, 2014). H&E staining was performed on sections obtained from electroporated and unelectroporated embryos to determine whether the delivery of pCI-*FAF*-RFP resulted in a change in the morphology of the left gonad.

Slides were dewaxed in xylene (ACE chemicals) for 5 min with gentle agitation. Sections were re-hydrated through an ethanol series (100%, 95% and 70%) diluted in dH_2O. Slides were kept at each ethanol concentration for 1 min with gentle agitation to aid penetration. Sections were stained with Mayer's haematoxylin for 10 min, ensuring sections were completely immersed in staining solution. Slides were then submerged in dH_2O for 90 sec with gentle agitation to remove excess stain and were then counterstained in Eosin for 16 min. Sections were then dehydrated through an ethanol series (70%, 95% and 100%) diluted in dH_2O and kept at each ethanol concentration for 30 sec. Slides were passed through xylene twice and mounted with DPX (Sigma). Stained sections were viewed and imaged using the Zeiss Axio Imager 2, using the Zen 2 (Blue edition) (Version 2.5.75.0) package (Zeiss).

2.6.9. Immunohistochemistry

Immunohistochemistry was performed on the sectioned electroporated embryos. This was done to confirm whether the FITC-tagged *FAF* MO was successfully delivered to the left gonad. An antibody that specifically recognizes FITC was therefore used.

Slides were dewaxed in xylene (ACE chemicals), and underwent three xylene changes (each rinse was 5 min, at 55 rpm). Sections were re-hydrated through an ethanol series (100%, 95%, 70% and 50%) diluted in dH_2O. Slides were kept at each ethanol concentration for 15 min, at 55 rpm. Slides were then immersed in dH_2O for 5 min.

Antigen retrieval was performed by boiling the sections at 95°C for 43 min using Sodium Citrate buffer (10mM Tri-sodium Citrate with 0.05% Tween 20, pH = 6.0). Most endogenous alkaline phosphates were inhibited in this step. The slides were immersed in dH_2O for 5 min and were then washed twice in TBST (TBS with 0.05% Tween 20) (5 min per wash) to permeabilize the tissue. The sections were blocked in 1.5% BSA (Glenthan Life Sciences) (prepared in 1x TBS) overnight in a humidity chamber at 4 °C. The slides were then immersed in TBS (two changes for 5 min each) to remove excess BSA and a 5 min rinse in TBST was then performed. Sections were incubated in 1:50 dilution of primary antibody (Anti-FITC-Alkaline Phosphatase antibody produced in rabbit) (Sigma) (diluted in blocking solution) overnight in a humidity chamber at 4 °C. Slides were then washed once in TBS for 5 min to remove unbound antibody. Since high levels of endogenous alkaline phosphatase activity were present in the kidneys, Levamisole (to a final concentration of 0.0002 mol/L) was added to the alkaline phosphatase substrate, BM Purple (Roche). Levamisole is a competitive inhibitor of alkaline phosphatase but it is unable to inhibit the isoenzyme used in alkaline phosphatase conjugates (Belle, 1976). The BM purple/Levamisole mixture was added to the sections and the slides were kept at room temperature until the colour had developed sufficiently (~24 hrs). It was ensured that the sections never dried out and the colour reaction was run until faint colour was seen in the no antibody control. The reaction was stopped by rinsing the slides in dH_2O for 5 min. Slides were mounted with ImmunoHistoMount (Sigma) as per the manufacturer's instructions. Slides were viewed and imaged using the Zeiss Axio Imager 2 (Zeiss).

3. Chapter 3 - Results

3.1. *In silico* FAF protein prediction.

Seeing as the FAF protein is only predicted in Ensembl (Gallus_gallus-5.0 assembly), *in silico* protein prediction of *FAF* was performed. This was pivotal to the MO-mediated knockdown of *FAF* which relies on sterically blocking the translation of *FAF* mRNA transcripts. The predicted FAF protein is shown below in **Figure 3.1**. It was predicted that two α helices (shown in magenta and purple) and three β sheets (shown in blue) are present. Homology modelling of FAF to templates present in the PDB (Protein Data Bank) resulted in a single match to the 2zmfA template with 67.1% alignment (and 69.7% alignment to the chicken GAF domain (template: 3dba_A)). The 2zmfA template is the crystal structure of the C-terminal GAF domain of human phosphodiesterase 10A. The GAF domain is found in cyclic nucleotide phosphodiesterases – proteins that are involved in the degradation cAMP and cGMP (important second messengers in intracellular signal transduction). Consistent with this, analysis of the sequence motifs using the ScanProsite tool (Castro *et al.*, 2006) revealed four distinct motifs, namely: a N-myristoylation site, a Casein kinase II phosphorylation site, a cAMP- and cGMP-dependent protein kinase phosphorylation site and a Protein kinase C phosphorylation site. The motifs are graphically shown below in **Figure 3.2**.

Figure 3.1. *Predicted tertiary structure of FAF*. It was predicted that two α helices (magenta and purple) and three β sheets (blue) are present. The red arrow denotes the first amino acid.

Figure 3.2. *Sequence motif analysis of FAF*. The full 76 amino acid sequence of FAF is shown. The amino acids highlighted denotes the regions of the sequence motif. Green - N- myristoylation site. Blue - Casein kinase II phosphorylation site. Purple - cAMP- and cGMP-dependent protein kinase phosphorylation site. Red - Protein kinase C phosphorylation site.

3.2. 5'-RACE experimentally confirms predicted 5' UTR of *FAF.*

The Ensembl pipeline has annotated a 507 bp 5' UTR for *FAF*, however, this has not been experimentally validated. The 5' UTR is essential for morpholino binding, and as such, 5'-RACE was conducted on total RNA extracted from the gonads of female (HH24) embryos or the whole body with the intention of confirming whether *FAF* has a 5' UTR. **Figure 3.3** below depicts the results obtained from the first 5'-RACE reaction. The two different PCR conditions used show many of the same bands. In each case, a similar banding pattern is evident between the gonads and whole body, suggesting that the same *FAF* transcripts were expressed in the gonads and whole body. The two bands of interest are the 500 bp band and the band at ~600 bp (shown by arrows). The other bands present (250 bp and smaller) may be other *FAF* transcripts with shorter 5' UTRs, however, they are more likely partially amplified transcripts as a result of non-specific binding of the RACE 5' primer or RNA degradation.

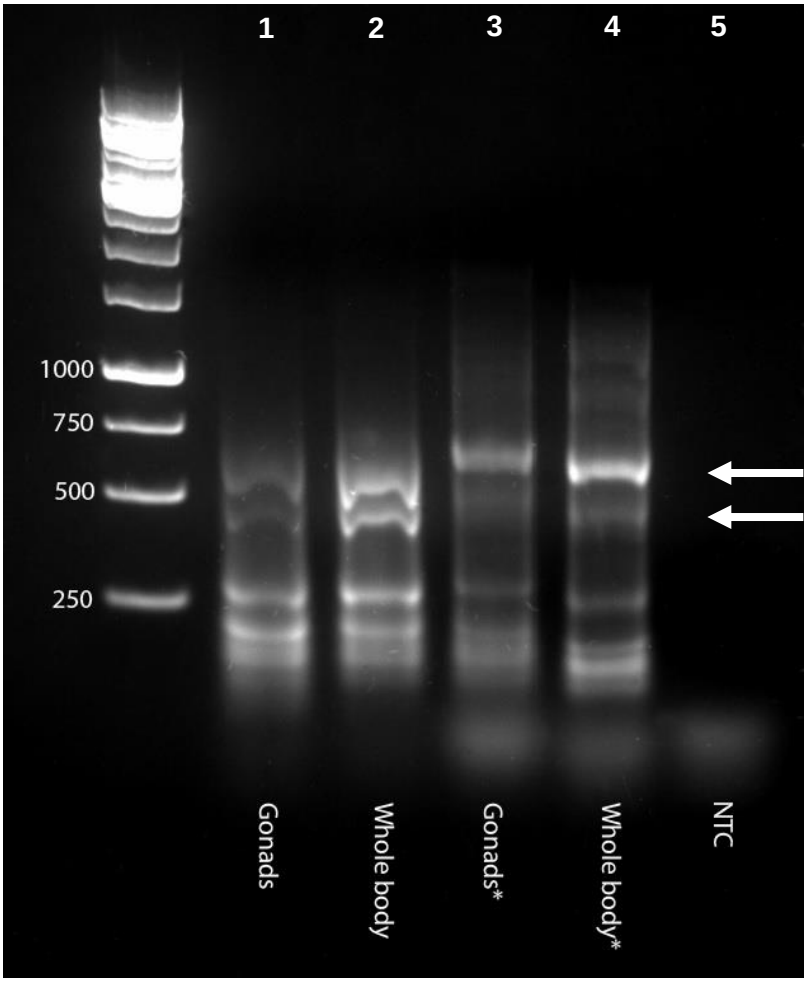

Figure 3.3. *5'-RACE of female HH24 gonad and whole body.* Lanes 1 and 2 depicts the results obtained from the first PCR conditions. Lanes 3 and 4 depicts the results obtained from the second PCR conditions. A similar banding pattern is observed between the gonads and whole body as well as between the two different PCR conditions. The white arrows denotes the two bands of interest that were sequenced. Lane 5 depicts the No Template Control (NTC) illustrating no DNA contamination occurred during the PCR setup.

31 clones were isolated and sent for sequencing using the M13F forward primer and M13R reverse primer. 21 clones contained the full length RNA Oligo sequence and were analysed as this indicated it was a full length mRNA transcript. Sequences that did not contain the full RNA Oligo sequence were discarded as this meant they were non-specific amplicons, amplified because the GeneRacer 5' forward primer was able to bind to them. Of the clones containing the full RNA Oligo sequence, the sequences that also contained the reverse complement of the *FAF* gene specific primer were selected and subject to a BLAST search. While 9 of these clones matched *FAF*, the clones were short and the MSA generated

showed “chunks” of alignment to the 16 *FAF* reference transcripts (see **Figure 3.4**). While this may be attributed to the degradation of the mRNA and as such partial amplification and sequencing, three full, non-specific mRNA transcripts were obtained. These transcripts (*SPARC*, *VIM* and *PPIA*) aligned with 99% homology to the deposited cDNA sequences found in Ensembl (Gallus_gallus-5.0 assembly) and their alignments are shown in **Appendix 6**. Based on the near perfect alignment of these transcripts, it was unlikely that the RNA was degraded and more feasible that either *FAF* transcripts do not contain a 5’-UTR, or that the amplification and/or sequencing of *FAF* was difficult due to the presence of strong secondary structures or stretches of homopolymeric repeats. The GeneRacer protocol that was followed recommended an incubation at 65 °C (for 5 min) and as such, the secondary structures in the *FAF* mRNA were likely not fully removed. Analysis of the secondary structures was performed using the UNAFold tool (IDT Technologies) and confirmed that heating to 65 °C was unable to entirely remove the secondary structures, as seen below in **Figure 3.5**. Consequently, the 5’-RACE experiment was conducted again, except the ligated RNA was heated to 72 °C for 10 min. Due to the propensity of RNA to degrade easily, it was thought best to incubate the ligated RNA for longer, and only slightly increasing the temperature.

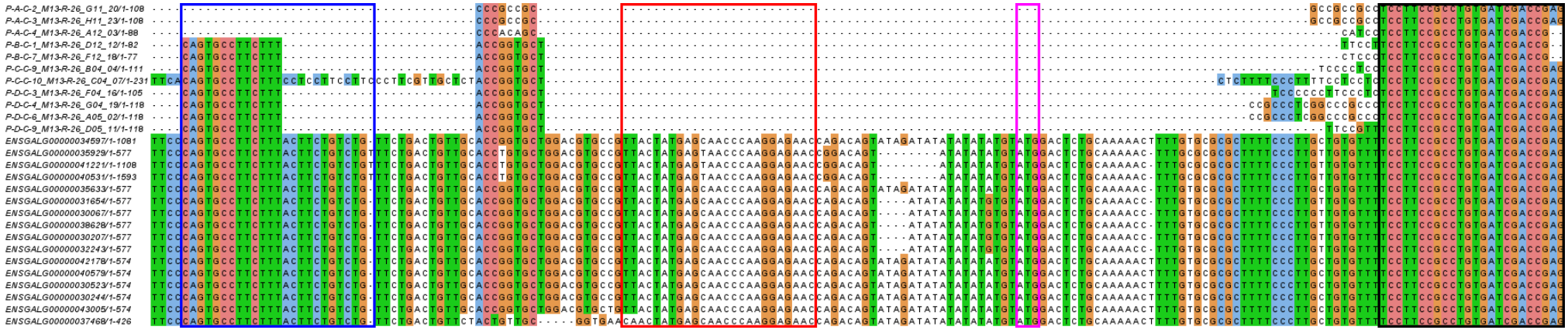

Figure 3.4. *Multiple sequence alignment of RACE clones to 16 FAF cDNA sequences.* The first eleven sequences are the 5'-RACE clones while the remaining sequences are the *FAF* cDNA sequences. Evidently there are small "chunks" of alignment between the 5'-RACE clones and the *FAF* cDNA sequences. The pink box depicts the presumptive start codon (ATG). The red box depicts where *FAF* MO2 will bind. The blue box depicts where *FAF* MO1 will bind. The black box depicts where the *FAF* reverse primer bound. This 5'-RACE experiment suggests that the *FAF* transcripts have very strong secondary structures

A

5'|ACCAGCUAUUCUCAGGGUACUCAGCCCCCUGAGCUGGAAGACGGGGCCGG
GGAGCAGAAUAAACGCCCCUCAAUUCCCAGUGCCUUCUUUACUUCUGUCUGU
UCUGACUGUUGCACCGGUGCUGGACGUGCCGUUACUAUGAGCAACCCAAGG
AGAACCAGACAGUAUAGAUAUAUAUAUAUGUAUGGACUCUGCAAAAACUUUUG
UGCGCGCUUUUCCCUUGCUGUGUUUUCCUUCCGCCUGUGAUCGACCGAG|3'

B

Structure Name	Image	ΔG (kcal.mole^{-1})	T_M (°C)	ΔH (kcal.mole^{-1})	ΔS (cal.K^{-1}mole^{-1})
1		-85.41	69	-664.6	-1942.61
2		-83.24	64.9	-705.3	-2086.41
3		-82.73	67.2	-667.3	-1960.66
4		-81.65	64.9	-691.5	-2045.46

Figure 3.5. *Predicted temperature requirement to linearize the secondary structures of FAF mRNA*. **[A]** The sequence that was analysed. The green bases depict the coding sequence of *FAF*, where the bases underlined shows where the reverse primer binds. The red bases depict the start codon of *FAF*. The blue bases depict the predicted 5'-UTR of *FAF*. Due to the input restraint of UNAFold, a maximum of 255 bases can be analysed at once. **[B]** The predicted temperature required to remove the secondary structure of the input sequence. Evidently, a minimum of 64.9 °C is required, however, this is not sufficient to fully remove the secondary structures.

Figure 3.6 below depicts the results obtained for the second 5'-RACE reaction. The 5'-RACE experiment was only conducted on the total RNA isolated from the female gonads and the same PCR conditions used in the first 5'-RACE experiment were used here. A similar banding pattern is observed between the two 5'-RACE experiments – with two bands of interest: the 500 bp band and the band at ~600bp (shown by arrows). Lane 3 (RT minus control) confirmed that no gDNA contamination was present in the RNA sample during the reverse transcription step. Lane 4 (NTC) confirmed that no gDNA contamination was present in the PCR reagents (buffer, primers and dH_2O).

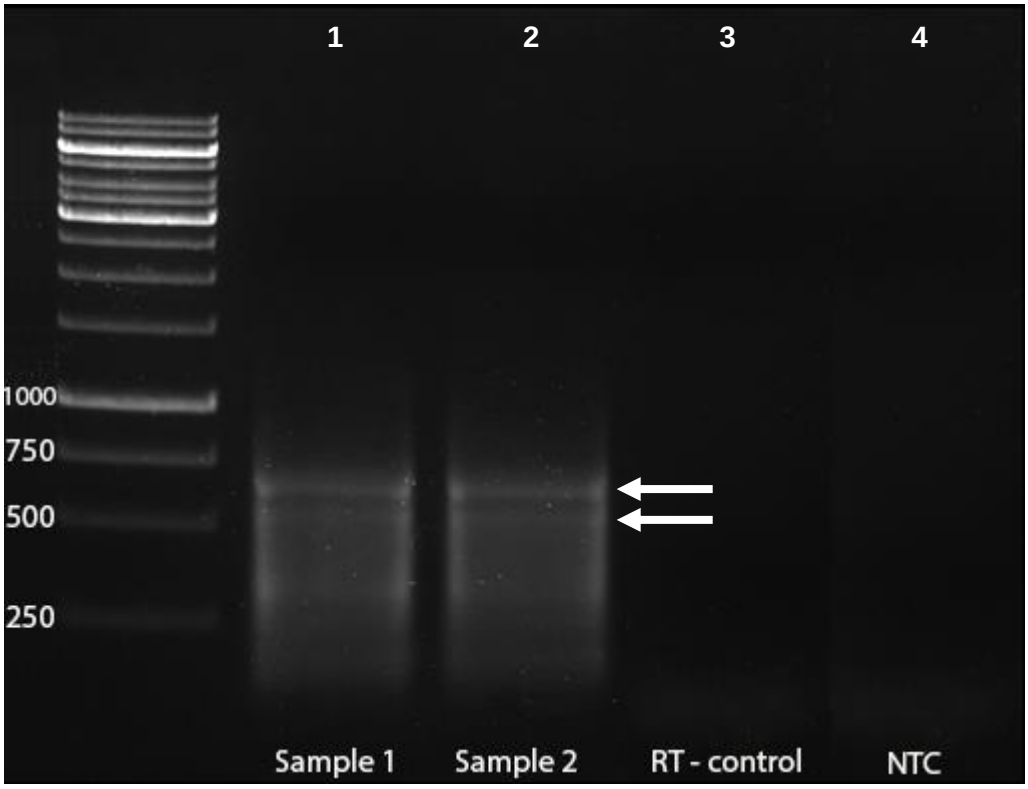

Figure 3.6. *5'-RACE of female HH24 gonad.* Lane 1 depicts the results obtained from the first PCR conditions. Lane 2 depicts the results obtained from the second PCR conditions. A similar banding pattern is observed between the two different PCR conditions. The white arrows denotes the two bands of interest that were sequenced. Lane 3 depicts the result of using the RT – control as a template for PCR, illustrating no DNA was present during reverse transcription. Lane 4 depicts the No Template Control (NTC) illustrating no DNA contamination occurred during the PCR setup.

A gel extraction of these two bands was conducted and the isolated clones were sequenced using the M13F forward primer and M13R reverse primer. The sequences were analysed in the same manner as the sequences from the first 5'-RACE experiment. A MSA (of the 16 *FAF* cDNA sequences and the sequenced clones) was generated using Clustal in JalView and is shown below in **Figure 3.7**. The increased temperature of the ligated RNA drastically improved the sequencing quality, noted by smaller gaps in the alignment (compare **Figure 3.4** and **Figure 3.7**). Evidently, there are still gaps in the alignment which was unexpected. A second evaluation of the secondary structures of the *FAF* cDNA was therefore conducted using the Oligo Calc tool (Kibbe, 2007). The advantage of using this tool was that it is not restricted to only being able to analyse 255 bases whereas the UNAFold tool (IDT Technologies) is. **Figure 3.8** below shows that a Tm of 84.6

°C is required to remove the secondary structures when the entire predicted 5' UTR of *FAF* is analysed, suggesting the gaps in the alignment are due to remaining secondary structures. Irrespectively, the second 5'-RACE experiment confirmed that *FAF* does contain a 5' UTR and the morpholinos designed to target *FAF* fall within the sequenced regions (shown by the blue and red box).

Analysis of the secondary structure by Mfold (Zuker, 2003) was conducted to confirm whether strong base interactions (such as G-C pairs) were present in the poorly sequenced regions. The advantage of using Mfold was that it depicts a graphical representation of how the mRNA will fold. **Figure 3.9** below shows the secondary structure of the cDNA of *FAF*. The regions where the *FAF* MOs would bind are shown in blue and red and the start codon is highlighted in yellow. Evidently, both *FAF* MOs bind to loop structures. The blue shaded regions seen in **Figure 3.9B** and **C**, correlate to the gaps in the alignments of where the *FAF* MOs would bind (**Figure 3.7**).It is clear that these regions contain G-C pairs, A-U pairs and G-U pairs. The G-C pairs and A-U pairs are very strong base interactions, which would require more energy (i.e. heat) to break.

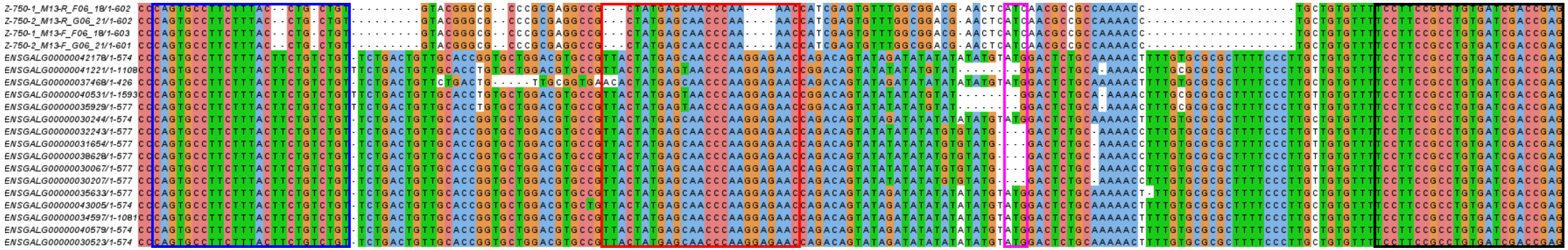

Figure 3.7. *Multiple sequence alignment of RACE clones to 16 FAF cDNA sequences.* The first four sequences are the 5'-RACE clones while the remaining sequences are the *FAF* cDNA sequences. Evidently there are gaps in the alignment between the 5'-RACE clones and the *FAF* cDNA sequences. The pink box depicts the presumptive start codon (ATG). The red box depicts where *FAF* MO2 will bind. The blue box depicts where *FAF* MO1 will bind. The black box depicts where the *FAF* reverse primer bound. The 5'-RACE confirmed that *FAF* contains a 5'-UTR and the *FAF* MOs will bind sufficiently to knockdown *FAF*.

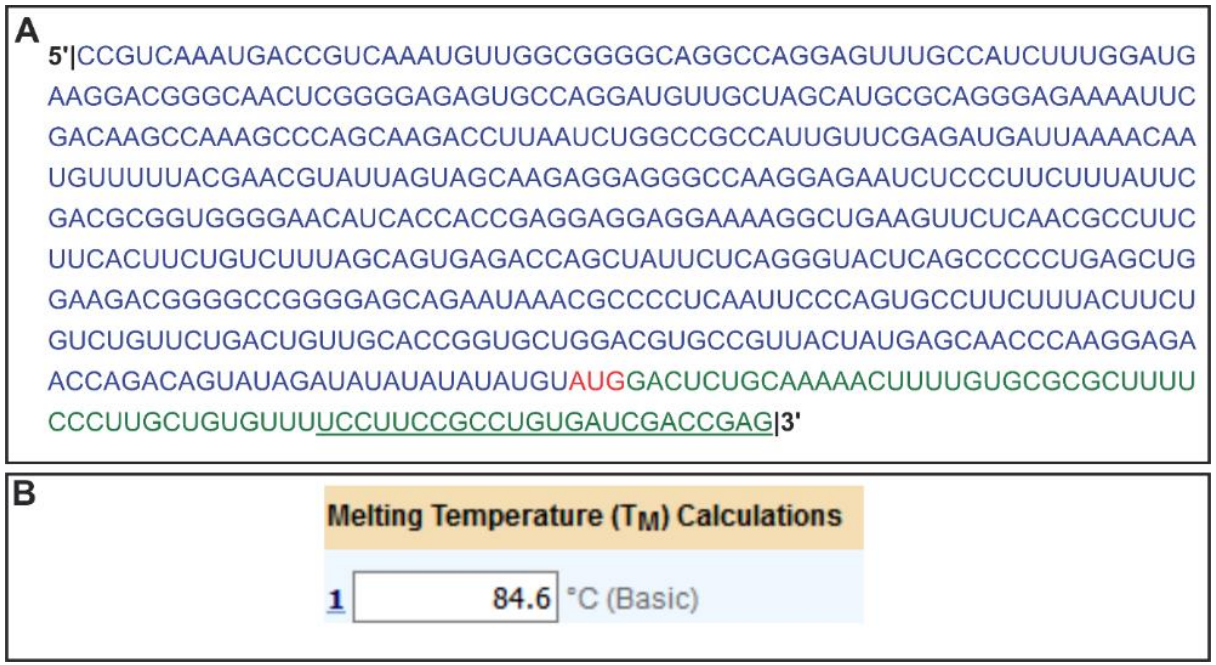

Figure 3.8. *The predicted temperature requirement to linearize the secondary structures of FAF mRNA.* **[A]** The sequence that was analysed. The green bases depict the coding sequence of *FAF*, where the bases underlined shows where the reverse primer binds. The red bases depict the start codon of *FAF*. The blue bases depict the predicted 5'-UTR of *FAF*. The Oligo Calc tool allowed the full presumptive 5'-UTR to be analysed at once. **[B]** The predicted temperature (84.6 °C) required to remove the secondary structure of the input sequence.

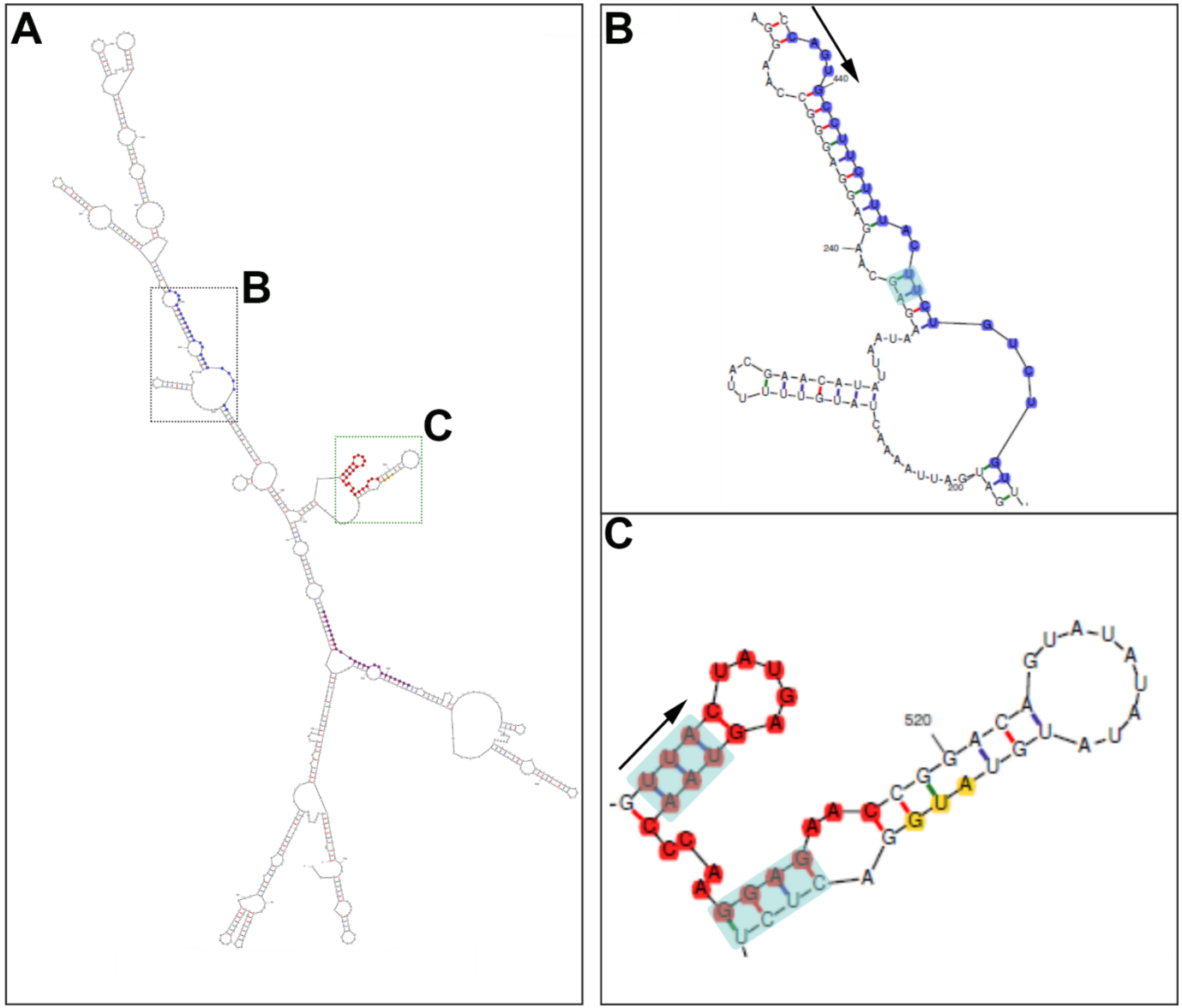

Figure 3.9. *Visual representation of FAFs secondary structure.* **[A]** Mfold's prediction of the secondary structure of *FAF*s full cDNA sequence. The dotted boxes are the regions magnified, denoted as B and C. **[B]** Magnified region of where *FAF* MO1 would bind. **[C]** Magnified region of where *FAF* MO2 would bind. The blue shaded regions seen in **[B]** and **[C]** correlate to the gaps seen in **Figure 3.7**. Evidently, strong bonds such as G-C pairs and A-U pairs are found here. The black arrows show the direction in the bases are to be read. The bases shaded in yellow denotes the start codon.

3.3. Successful *in ovo* electroporation of the neural tube.

The electroporation procedure was first practised on the neural tube. The neural tube was chosen due to its easy access and the ability to get results quickly, since embryos only had to be incubated for 33-40 hr (HH 10-11) and were harvested 24 hr post electroporation. In addition to practising the technique, it also provided an opportunity to ensure the pCI-RFP construct was working. To this end, embryos were electroporated either with just the pCI-RFP construct (250 ng), with only the control MO (0.5 mM) or with a combination of the control MO (0.5 mM) and pCI-RFP (250 ng). Six embryos per condition was analysed. **Figure 3.10** below depicts the successful electroporation of the neural tube. It is evident that only red fluorescence is seen when the pCI-RFP construct was electroporated (top row), indicating it was functional. The middle row of **Figure 3.10** shows the successful delivery of the FITC-tagged control MO to the neural tube, indicated by the green fluorescence. The co-delivery of the pCI-RFP construct and control MO is shown in the bottom row and it demonstrates that both constructs were delivered to the same region. This was an important first step to successfully electroporating the embryonic gonads.

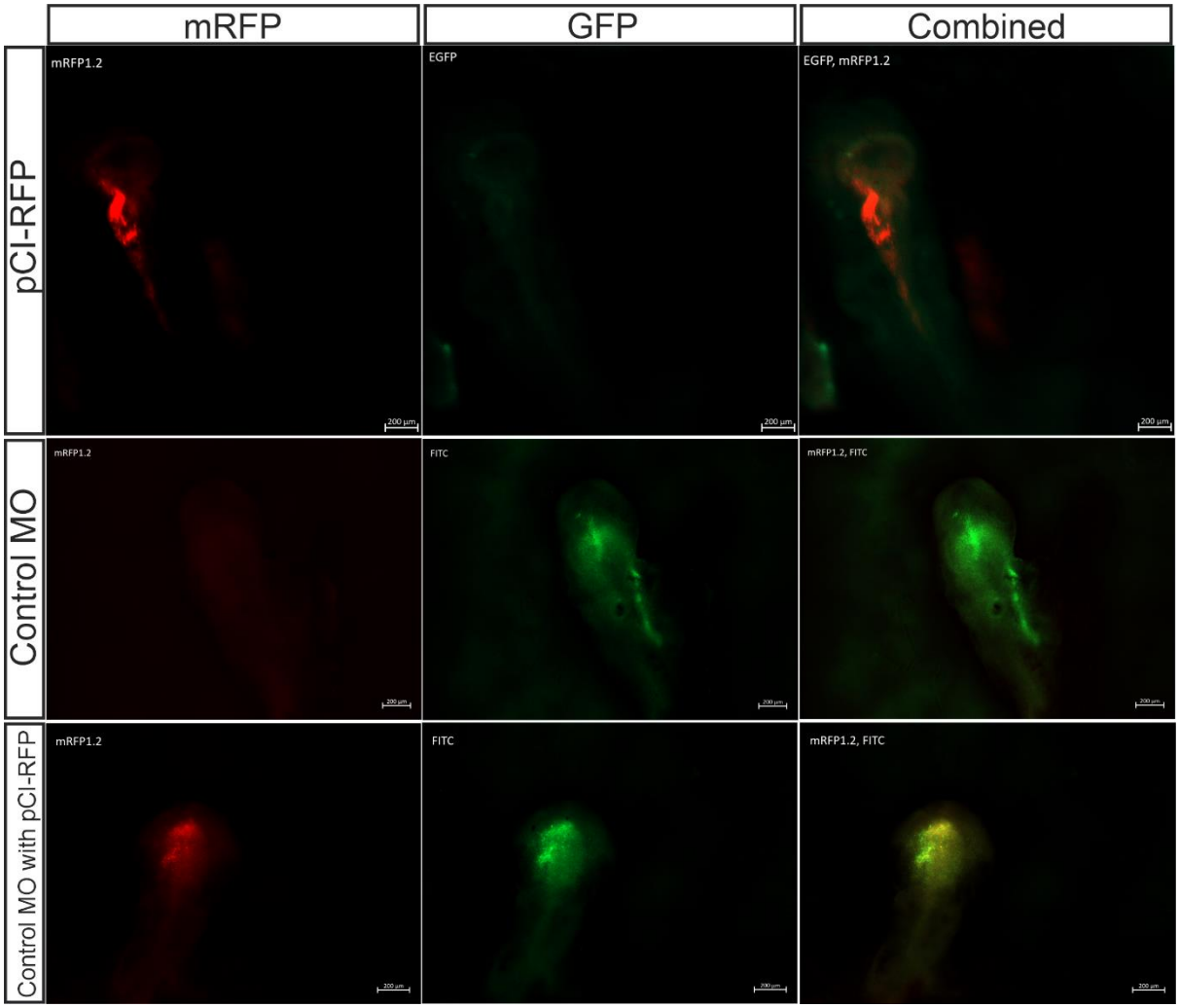

Figure 3.10. *Electroporation of the neural tube (HH10-11).* The empty pCI-RFP plasmid (250 ng) (red), FITC-tagged control morpholino (0.5 mM) (green) or combination of both pCI-RFP (250 ng)/control morpholino (0.5 mM) were electroporated. Embryos were analysed at HH12-13. Evidently, when both constructs are electroporated, they localize to the same region (seen by the yellow colour). Scale bars = 200 µm.

3.4. *In ovo* electroporation of the left genital ridge shows pCI-RFP and FITC-tagged MO localise to the same cells.

Before the knockdown of *FAF* was conducted, it was first necessary to confirm that the construct was being delivered to the left gonad. To this end, the electroporation procedure was followed as described in **Chapter 2.6**, however, instead of letting the embryos develop to >HH29, six embryos were collected 24 hr post electroporation (HH18-20). This provided enough time for the genital ridge to develop and therefore confirm whether the correct region was electroporated. **Figure 3.11** below shows the successful delivery of the FITC-tagged control MO (1 mM) to only the left genital ridge. Since morpholinos carry a neutral charge and it is only the FITC-tag that carries a weak negative charge, a carrier molecule is required to encourage sufficient uptake into the cell. pCI-RFP was used for this purpose – to encourage the migration of the MO into the cell and the red fluorescence seen in **Figure 3.11** is due to the expression of mRFP.

Furthermore, since MOs are unable to replicate in a cell, they become diluted as cell division occurs, making it difficult to detect their expression after 72 hrs. Seeing as the embryos were incubated up to 8 days post electroporation, it was likely that the fluorescence emitted from the MO will be undetectable by direct observation under the fluorescent microscope. pCI-RFP, which is able to drive continuous RFP expression, was therefore also used as a tracer. As seen in **Figure 3.11** below, both mRFP and FITC fluorescence is localised to the same region, indicating that pCI-RFP can successfully be used as a tracer molecule and the presence of mRFP expression would indicate the successful delivery of the MO to the left gonad (see image of the channels merged in **Appendix 7**).

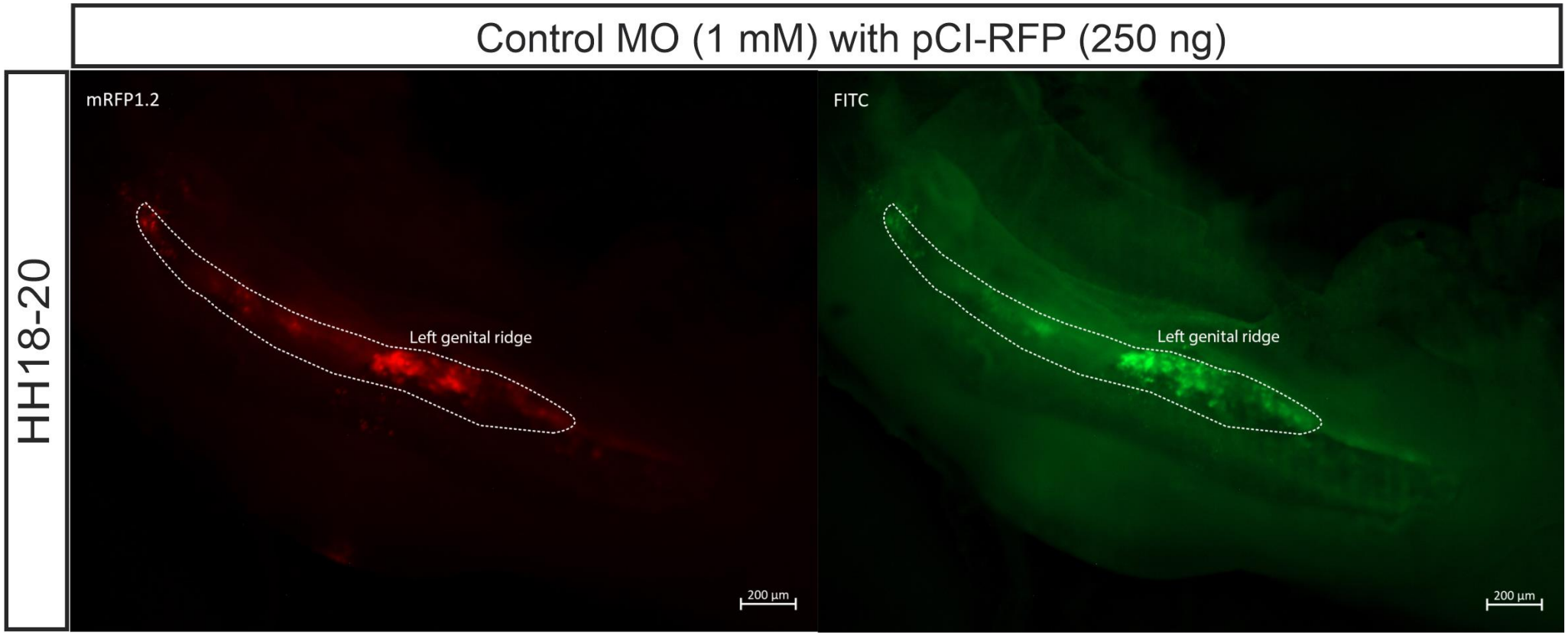

Figure 3.11. *Electroporation of the genital ridge (HH18-20) using the control morpholino (green) and pCI-RFP (red).* Both constructs localize to the left genital ridge (indicated by the dotted line) confirming pCI-RFP can successfully be used as both a tracer and a carrier. Scale bars = 200 µm.

3.5. MO-mediated knockdown of *FAF* results in female exclusive death.

Electroporation of the left gonad was performed in batches, where each batch of embryos consisted of experiment embryos, control embryos (electroporated with the control MO) and no electroporation controls (NEC). The two MO constructs targeting *FAF* (referred to as *FAF* MO1 and *FAF* MO2) and the control MO were electroporated at a final concentration of either 1 mM or 2 mM. *FAF* MO1 and *FAF* MO2 were also co-delivered at 0.5 mM each. The embryos were harvested 5-6 days post electroporation and were then sexed by PCR (see **Appendix 8**), thus ensuring that the male and female specific markers were expressed. The numbers of embryos electroporated with each construct, the number of embryos analysed and the percentage survival are shown below in **Table 3.1**. Of note, no females electroporated with either *FAF* MO construct survived, dying 24-48 hrs post electroporation. Embryos electroporated with the control MO, however, had a survival rate consistent with what was reported by Hirst *et al.*, which reported a 40% survival rate (Hirst *et al.*, 2017).

Table 3.1. Table showing the number of embryos analysed that were electroporated with the *FAF* MO constructs, at different concentrations.

		Construct							
		FAF MO1		FAF MO2		FAF MO combo	Control MO		No Electroporation Control
Concentration of construct delivered		1 mM	2 mM	1 mM	2 mM	0.5 mM each	1 mM	2 mM	
Number of embryos electroporated		15	15	15	15	15	12	12	28
Number of embryos analysed	Male	2	2	2	3	2	3	3	13
	Female	0	0	0	0	0	2	2	12
Percentage survival		13%	13%	13%	20%	13%	42%	42%	89%

Figure 3.12 below illustrates the successful electroporation of the left gonad. As mentioned previously, pCI-RFP was used as both a carrier and a tracer molecule and that pCI-RFP and the FITC-tagged MO localise to the same cells. As such, the red fluorescence seen only in the left gonad (LG) was indicative of both the presence of pCI-RFP and the FITC-tagged MO. The electroporation procedure also resulted in the delivery of both constructs to the left Müllerian duct (MD).

Significant autofluorescence is commonly seen in the kidney, and the red background seen in the kidneys can be attributed to this autofluorescence.

Males electroporated with *FAF* MO1 and/or *FAF* MO2 developed two elongated gonads, with bilateral symmetry. Similar development is seen in the male gonads electroporated with the control MO and the male NECs. Taken together, the delivery of the *FAF* MO (regardless of its concentration) did not produce any noticeable phenotype. Females electroporated with the *FAF* MOs, however, died 24-48 hrs post electroporation. The delivery of the control MO did not kill the females, and the gonads of these females developed asymmetrically, where the right gonad is seen to be regressing, as seen in the female NEC as well. This suggests that the female-exclusive death observed was specifically due to the knockdown of *FAF*.

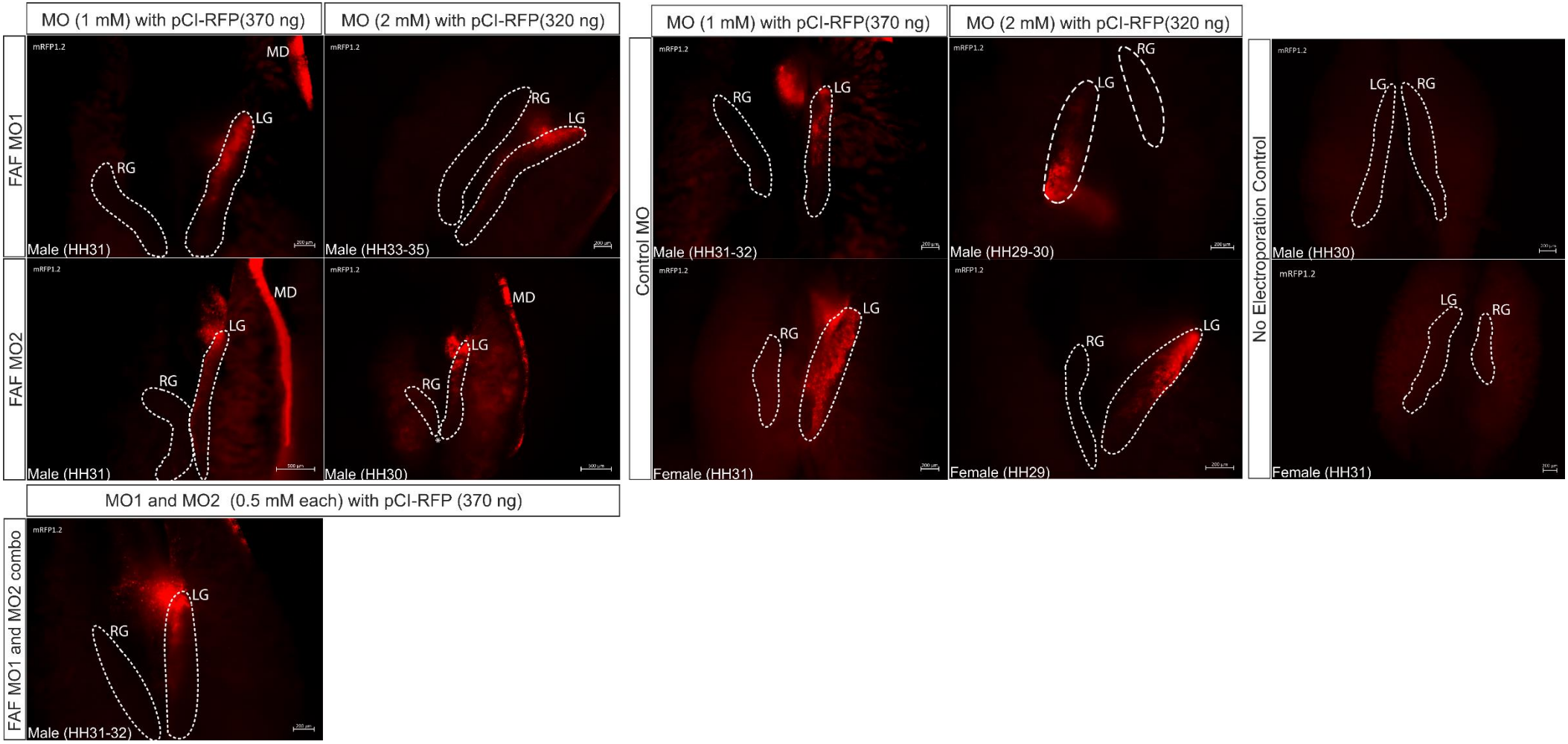

Figure 3.12. *Electroporation of the left gonad with MO constructs*. Only the left gonad was electroporated since in females it develops to be functional whereas the right gonad regresses. Red fluorescence is indicative of successful delivery of the MO construct to the left gonad (outlined by dotted line). *FAF* MO1 and *FAF* MO2 were delivered at a final concentration of 1 mM or 2 mM, with pCI-RFP acting as a carrier and tracer molecule. *FAF* MO1 and *FAF* MO2 were also co-delivered at 0.5 mM each. Males electroporated with the *FAF* MOs developed two elongated gonads, of similar length comparable to the males electroporated with the control MO (1 mM and 2 mM) and male no electroporation control (NEC). Females electroporated with the *FAF* MOs did not survive. Females electroporated with the control MO exhibit a canonical gonadal architecture, similar to the female NEC where the right gonad is seen to be regressing. LG – Left gonad. RG – Right gonad. MD - Müllerian duct. *FAF* MO1, control MO, *FAF* MO combo and NEC scale = 200 µm. *FAF* MO2 scale = 500 µm.

While **Figure 3.11** illustrated that pCI-RFP and the MO localize to the same region, the presence of the MO in the gonad, post electroporation, wanted to be confirmed. To this end, an embryo that was successfully electroporated with the control MO and another embryo that was successfully electroporated with a *FAF* MO were sectioned longitudinally and immunohistochemistry was performed on sections using a rabbit anti-FITC-Alkaline Phosphatase antibody. The antibody would selectively bind to FITC (which is conjugated to the MO), and after incubation with BM Purple (chromogenic substrate of alkaline phosphatase), it would confirm whether the MO was delivered to the gonad as a purple precipitate would develop. **Figure 3.13** below shows the results obtained after immunohistochemistry was performed on the sections. The no antibody control (sections that were not incubated with the antibody) in **Figure 3.13A** showed no colour development in either the left or right gonad. In contrast, a purple precipitate was seen in both the left and right gonad of the sections that were incubated with the antibody (**Figure 3.13B**). Evidently, the MO was delivered to both the medulla and cortex, but staining was concentrated to the cortex (shown by the arrow) and appeared to be cytoplasmic. Since no colour development was seen in the no antibody control sections, overstaining and non-specific staining can be ruled out and this suggests that the MO was delivered to both the left and right gonad.

With respect to the *FAF* MO, a purple precipitate and therefore the *FAF* MO was present in the left gonad and not the right gonad as seen in **Figure 3.14B**. Similar to the control MO, the *FAF* MO was delivered to the cortex and medulla, but was concentrated to the cortex and the staining appeared to be cytoplasmic. No staining was seen in the no antibody control sections (**Figure 3.14A**).

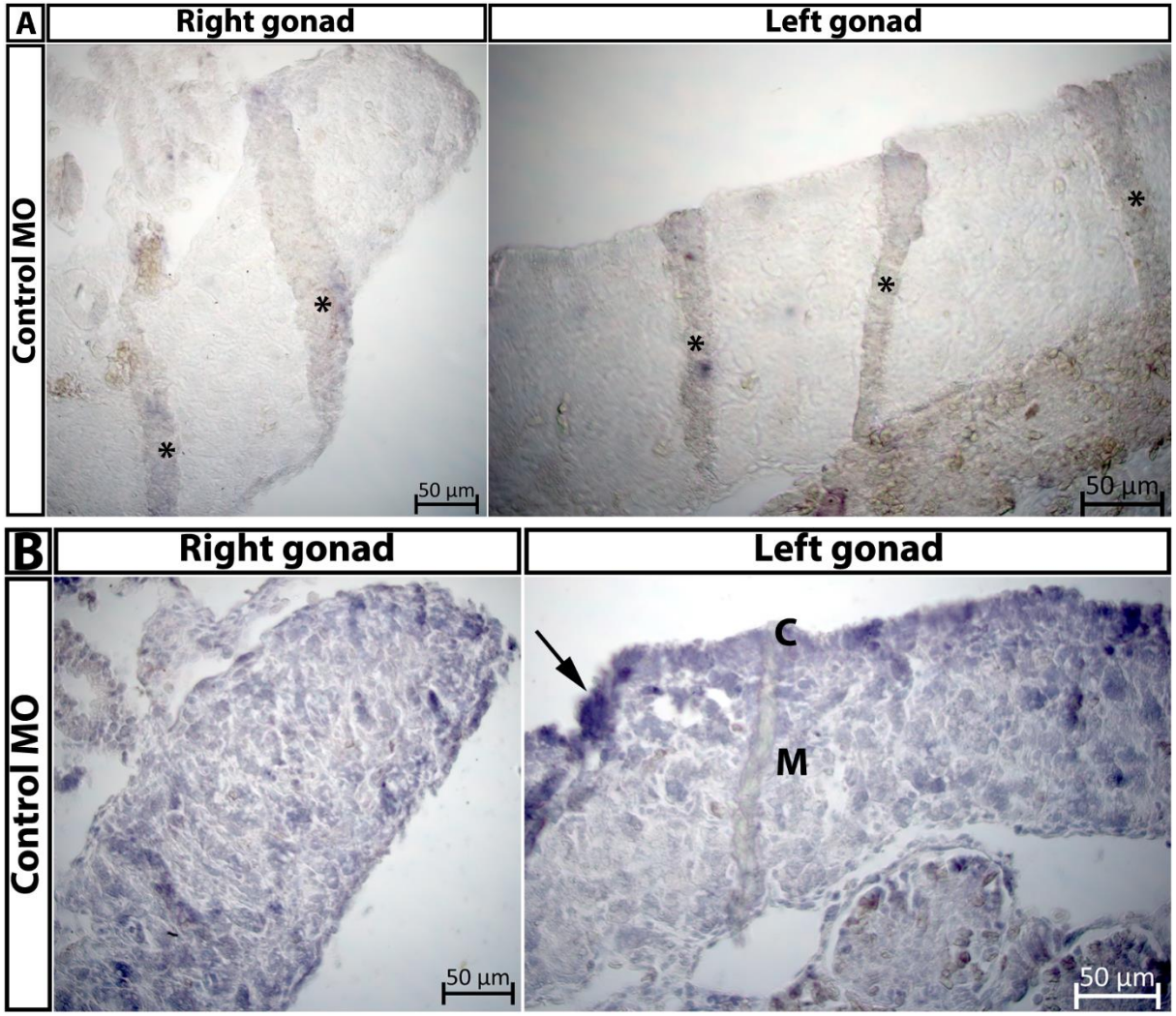

Figure 3.13. *Confirmation of the successful delivery of the control MO into the gonad by immunohistochemistry*. **[A]** No antibody control sections showing no staining in either the left or right gonad, evident by the lack of a purple precipitate. The asterisks (*) depict artifacts. **[B]** Sections incubated with the Rabbit Anti-FITC-Alkaline Phosphatase antibody shows distinct purple precipitate, indicating the presence of the control MO, in both left and right gonad. The control MO is present in both the cortex (C) and medulla (M) but seems to be concentrated in the cortex (arrow). Scale = 50 µm.

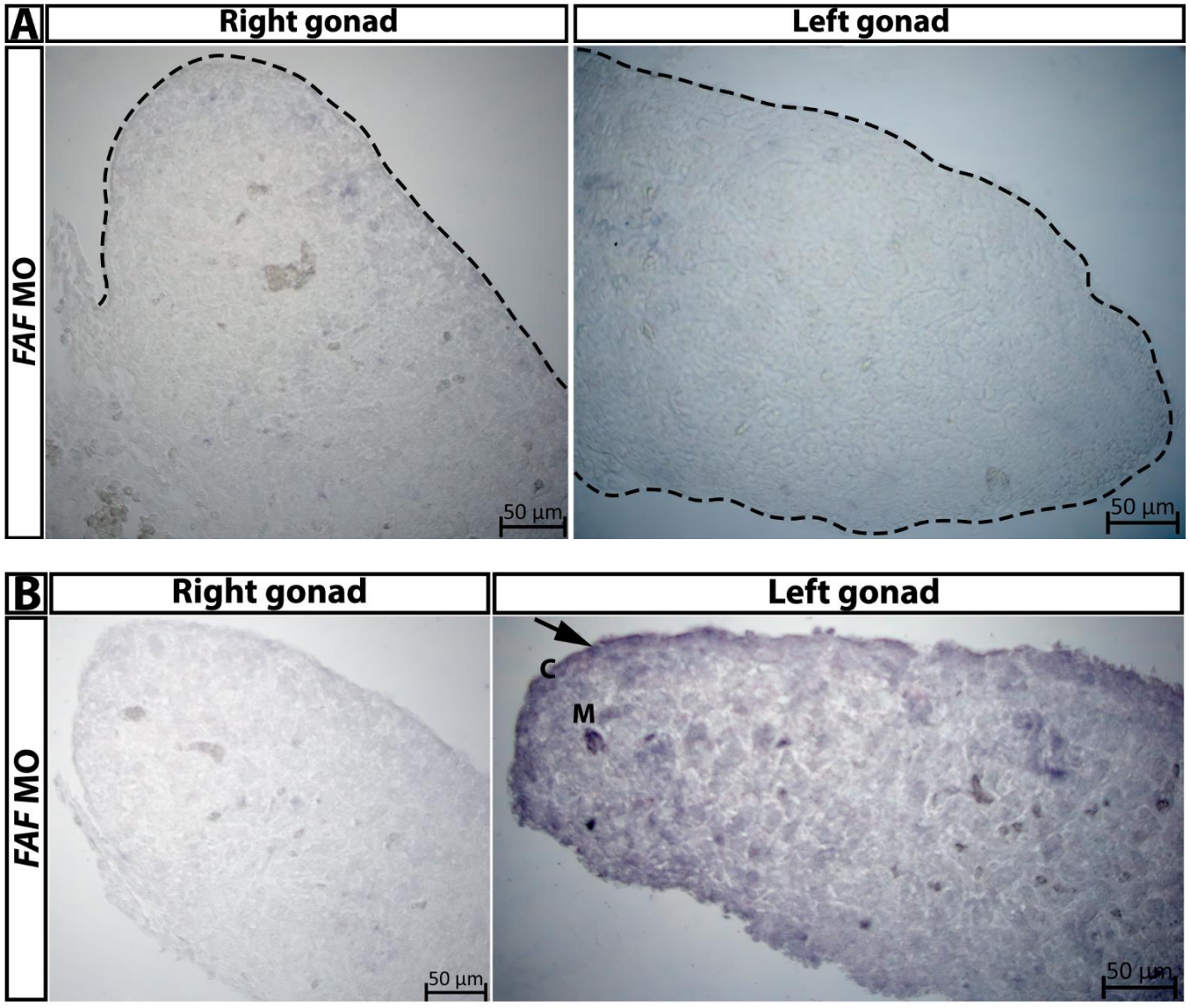

Figure 3.14. *Confirmation of the successful delivery of the FAF MO into the gonad by immunohistochemistry.* **[A]** No antibody control sections showing no staining in either the left or right gonad (outlined by the dotted line), evident by the lack of a purple precipitate. **[B]** Sections incubated with the Rabbit Anti-FITC-Alkaline Phosphatase antibody shows a distinct purple precipitate in the left gonad indicating the presence of the *FAF* MO in only the left gonad. The *FAF* MO is present in both the cortex (C) and medulla (M) but seems to be concentrated in the cortex (arrow). Scale = 50 µm.

3.6. Successful pCI-*FAF*-RFP construct design.

The pCI-*FAF*-RFP construct was created by amplifying the *FAF* CDS and ligating it into the pCI-RFP plasmid as described in Chapter 2.5.1. **Figure 3.15** below illustrates the results obtained from conducting PCR on both male and female template DNA. Male template was used to ensure primer specificity, since *FAF* is not found in males. Evidently, only a single band is seen in Lane 1 (where female template DNA was used) (**Figure 3.15**). The size of this band is approximately 250 bp, coinciding with the expected PCR product size (259 bp).

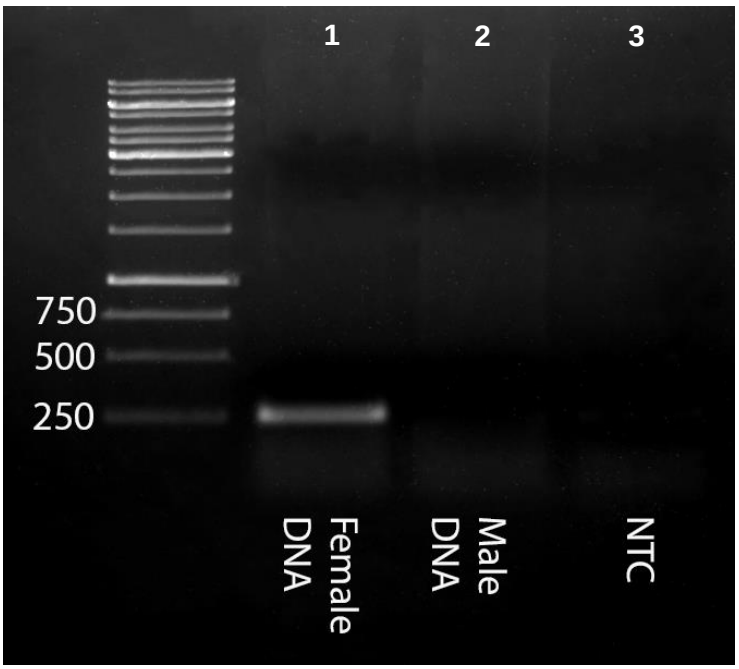

Figure 3.15. *Successful amplification of FAF coding sequence*. A single band (of the expected 259 bp) is seen when female template DNA was used (Lane 1). As expected, no band is seen when male template DNA was used (Lane 2). The no template control (NTC) confirms no gDNA contamination was present while the PCR reaction was set-up (Lane 3).

The successful digestion of the *FAF* CDS and the pCI-RFP plasmid is shown in **Appendix 9**. Several clones were isolated and sent for sequencing using the pCAGGS-5 forward primer and the pCI-RFP Reverse Sequencing Primer (see Chapter 2.5.9 for primer sequences). The bases corresponding to the restriction sites of the sequenced insert were trimmed out and JalView was used to create a MSA using the sequenced insert and the 16 *FAF* CDS as input sequences, shown below in **Figure 3.16**. The complete CDS of *FAF* was successfully cloned into the pCI-RFP plasmid, including the Kozak sequence (bases highlighted in purple).

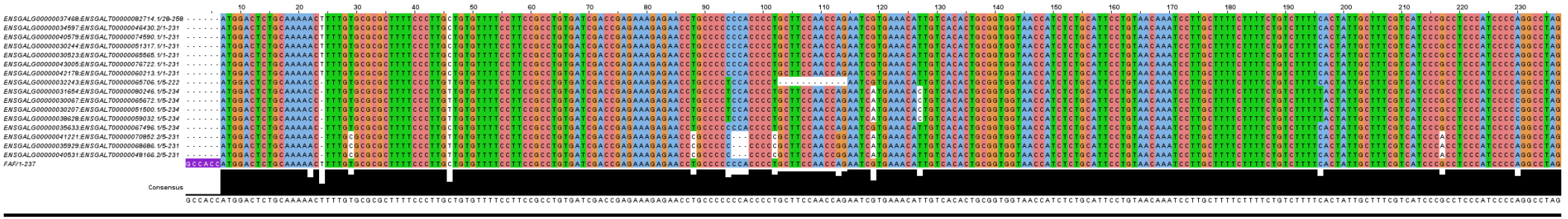

Figure 3.16. *Multiple sequence alignment of FAF coding sequence clone to the 16 FAF reference sequences.* The first 16 sequences are the coding sequences of *FAF* found in Ensembl. The last sequence is the clone. Evidently the clone was sequenced fully. While natural variation exists between the 16 reference sequences, the clone fully matches 7 of the reference sequences. The bases highlighted in purple (of the clone) depicts the Kozak sequence added.

3.7. ZZ males ectopically expressing *FAF* in the left gonad develop *a* female-like morphology.

Electroporation of the left gonad was performed in batches, where each batch of embryos consisted of experiment embryos, control embryos (electroporated with the empty pCI-RFP plasmid) and no electroporation controls (NEC). 504 ng of the pCI-*FAF*-RFP construct and 500 ng of the empty pCI-RFP plasmid was delivered. The embryos were harvested 7-8 days post electroporation (at HH 34-35), ensuring that the male and female specific markers were expressed and a distinct male or female morphology was present. The electroporated embryos were sexed by PCR and is shown in **Appendix 10**. The numbers of embryos electroporated with each construct, the number of embryos analysed and the percentage survival are shown below in **Table 3.2**. Interestingly, both males and females electroporated with the pCI-*FAF*-RFP construct survived. Embryos had a survival rate consistent with what was reported by Hirst *et al.*, which reported a 40% survival rate (Hirst *et al.*, 2017).

Table 3.2. Table showing the number of embryos analysed that were electroporated with the pCI-*FAF*-RFP construct.

		Construct		
		pCI-*FAF*-RFP	pCI-RFP	No Electroporation Control
Amount of construct delivered		504 ng	500 ng	
Number of embryos electroporated		12	2	3
Number of embryos analysed	Male	4	0	1
	Female	1	1	2
Percentage survival		42%	50%	100%

The successful electroporation of only the left gonad with pCI-*FAF*-RFP is shown below in **Figure 3.17**, **Figure 3.18** and **Figure 3.19**, evident by the red fluorescence. The electroporated ZZ males developed two elongated gonads, similar in length. Similar development was seen in the ZZ male NEC. Histologically, however, the electroporated ZZ male gonads displayed asymmetry, in which the left gonad was noticeably larger in overall size than the right gonad; which is in

contrast to the ZZ male NEC. Under high magnification, the ZZ male NEC comprised of a thin cortex and seminiferous tubes were seen in the medulla (marked by asterisks) whereas the electroporated ZZ male had a thickened cortex and a disorganized medulla. No seminiferous tubes were noted in the electroporated ZZ male. These results were consistent with all four males ectopically expressing *FAF* that were analysed. Comparison between the electroporated left gonad and unelectroporated right gonad of ZZ males showed that the right gonad developed similarly to the ZZ male NEC **(Appendix 11)**, attributing the altered phenotype to the ectopic expression of *FAF*.

Overexpressing *FAF* in ZW females had no effect on the left gonad. While only one ZW female overexpressing *FAF* was observed, the gross morphology demonstrated asymmetrical gonad development in both the electroporated and unelectroporated ZW females. Under high magnification, the morphology of the electroporated left gonad was similar to the unelectroporated left gonad, characterized by a thickened cortex and disorganized medulla (**Figure 3.18**) whereas the right gonad showed a male-like morphology, as expected (**Appendix 11**).Consistent with this, the electroporation of the empty pCI-RFP construct did not have any effect on the left gonad either and normal morphology was observed (**Figure 3.19**).

Taken together, the ectopic expression of *FAF* in the left gonad of ZZ males resulted in the development of a female like morphology, suggesting a male-to-female sex reversal. The overexpression of *FAF* in the left gonad of ZW females had no noticeable effects on its morphology.

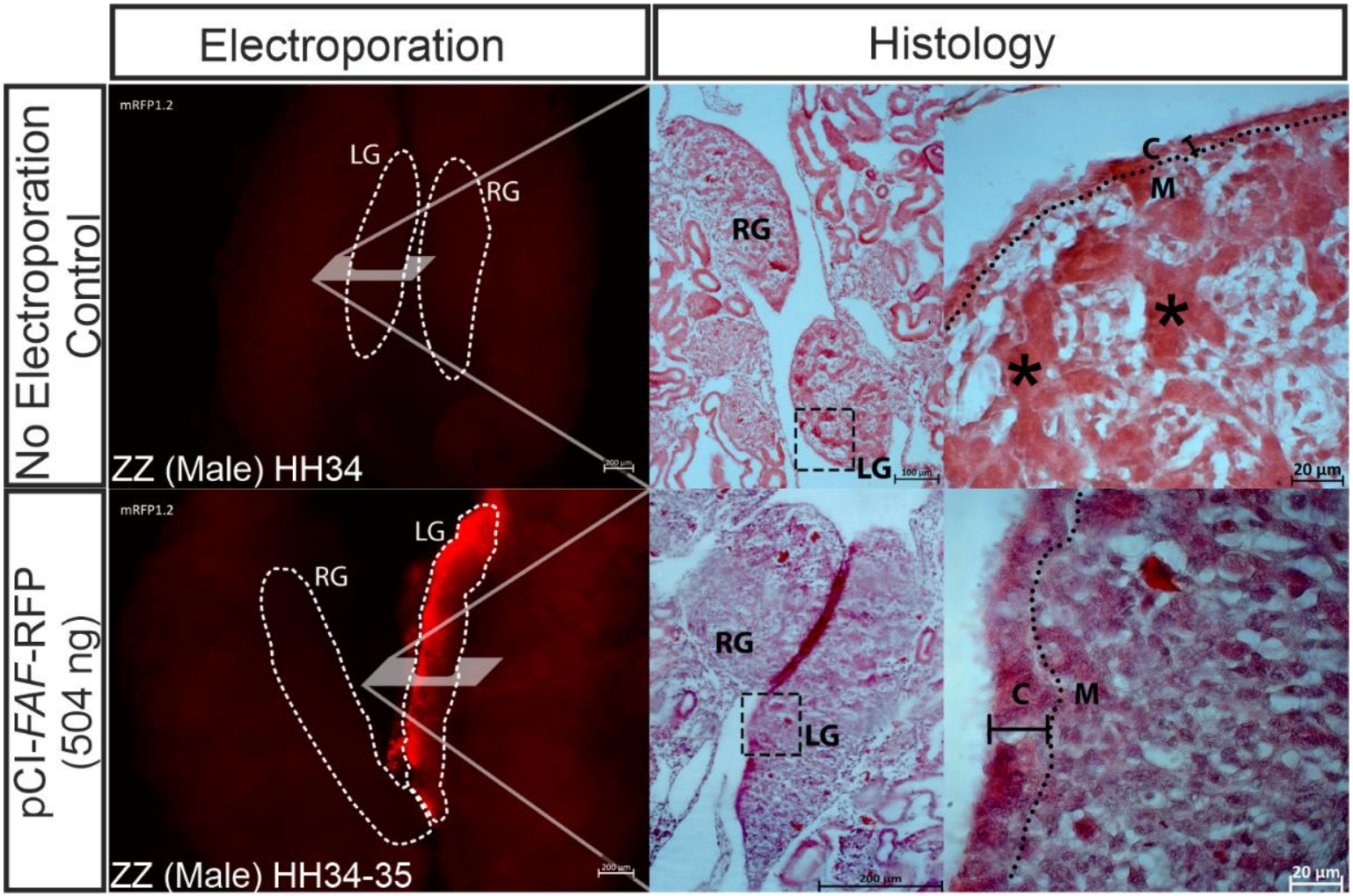

Figure 3.17. *Electroporation of the gonads (Left) with pCI-FAF-RFP and histological analysis (H&E staining) (Right)*. **Top row:** No electroporation ZZ male (HH34) control that has two elongated gonads of equal length. No fluorescence is observed in either of the gonads. Transverse sections under low magnification shows the left and right gonad to be relatively similar in size. High magnification of the left gonad (dotted line shows region magnified) depicts the cortex (C) to be a single layer of cells and the medulla (M) to be organized. Seminiferous tubes are shown by asterisks. **Bottom row:** Electroporated ZZ male (HH34-35) that has two elongated gonads of equal length, similar to male NEC. Red fluorescence is seen only in the left gonad which indicates the successful delivery of the pCI-*FAF*-RFP construct. Transverse sections under low magnification shows the left gonad to be noticeably larger than the right gonad. High magnification of the left gonad shows a thickened cortex (C) and a disorganized medulla (M). Distinct seminiferous tubes cannot be seen. Electroporation scale = 200 µm. Low magnification Histology scale = 100 µm and 200 µm. High magnification Histology scale = 20 µm.

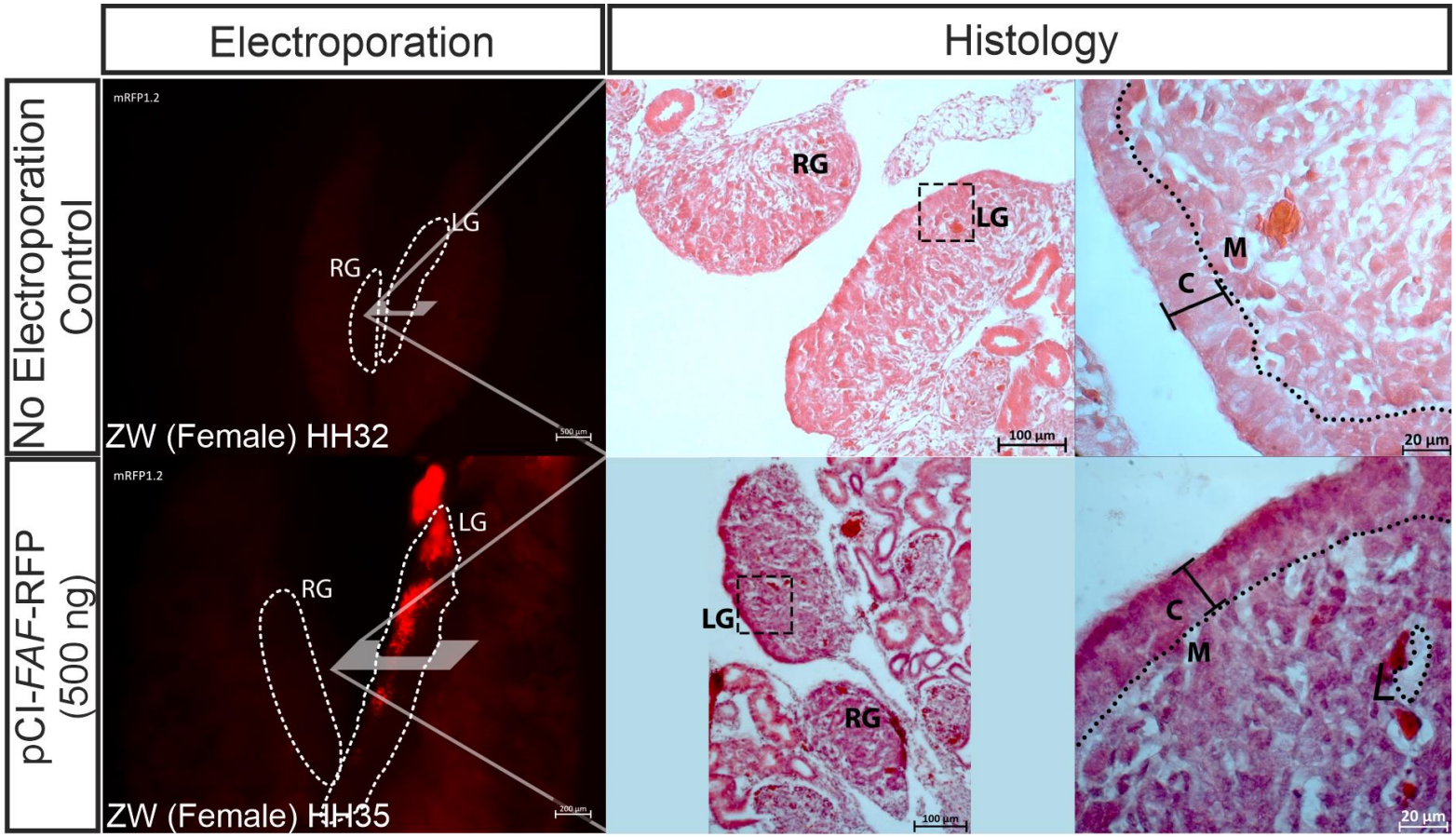

Figure 3.18. *Electroporation of the gonads (Left) with pCI-FAF-RFP and histological analysis (H&E staining) (Right).* **Top row:** No electroporation ZW female (HH32) control is shown, where the right gonad is regressing. No fluorescence is observed in either gonads. Transverse sections under low magnification shows the left gonad to be larger than the right gonad. High magnification of the left gonad (dotted line shows region magnified) depicts a thickened cortex (C) and a disorganized medulla (M). **Bottom row:** Electroporated ZW female (HH35) is shown, where the right gonad is regressing, similar to female NEC. Red fluorescence is seen only in the left gonad which indicates the successful delivery of the pCI-*FAF*-RFP construct. Transverse sections under low magnification shows the left gonad to be noticeably larger than the right gonad. High magnification of the left gonad shows a thickened cortex (C) and a disorganized medulla (M), similar to female NEC. Lacunae (L) are seen to be forming. Electroporation (NEC) scale = 500 µm. Electroporation (pCI-FAF-RFP) scale = 200 µm. Low magnification Histology scale = 100 µm. High magnification Histology scale = 20 µm.

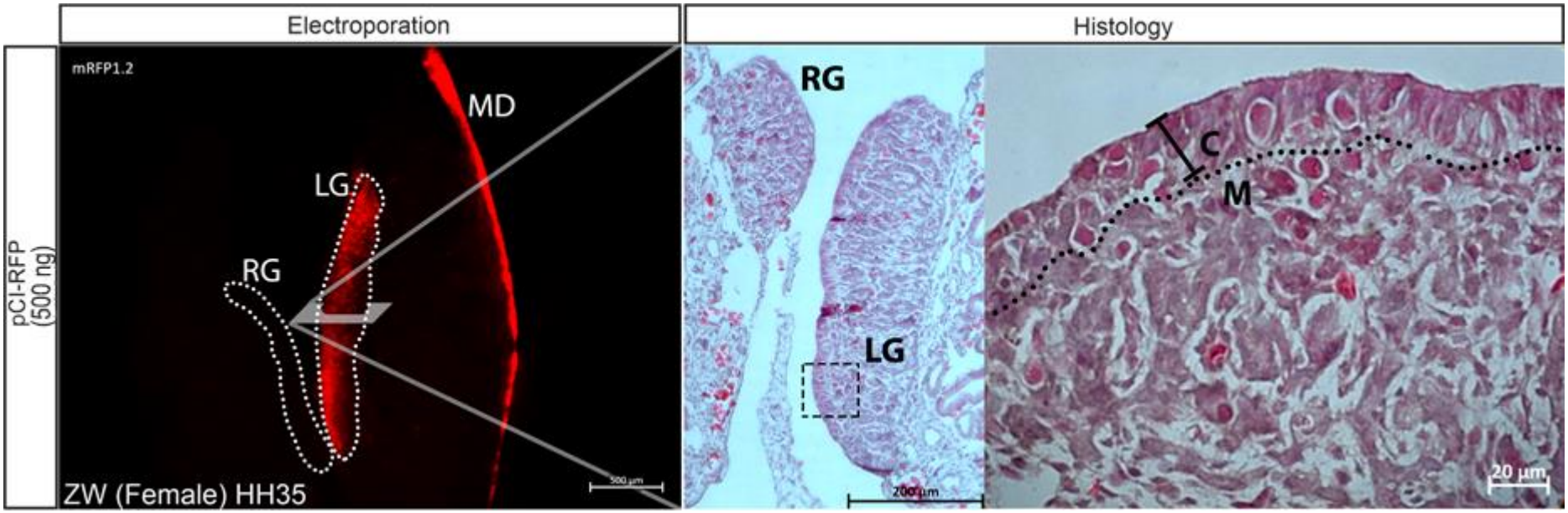

Figure 3.19. *Electroporation of the gonads (Left) with pCI-RFP and histological analysis (H&E staining) (Right).* Electroporated ZW female (HH35) is shown, where the right gonad is regressing. Red fluorescence is seen only in the left gonad (LG) and Müllerian duct (MD) which indicates the successful delivery of the pCI-RFP construct. Transverse sections under low magnification shows the left gonad to be noticeably larger than the right gonad. High magnification of the left gonad shows a thickened cortex (C) and a disorganized medulla (M), similar to female NEC. Electroporation scale = 500 µm. Low magnification Histology scale = 200 µm. High magnification Histology scale = 20 µm.

4. Chapter 4 - Discussion

The 5'-RACE experiment was conducted to verify the predicted 5'-UTR of *FAF*, found in Ensembl. The presence of a 5' UTR is paramount to successful MO-mediated knockdown experiments, seeing as the MO binds to the 5'-UTR of the targeted gene. Based on the results obtained from 5'-RACE on *FAF*, it was confirmed that *FAF* does have a 5' UTR. Due to the strong secondary structures residing in the 5' UTR, however, it cannot be confirmed that all 507 bp (predicted by Ensembl) are part of the 5'-UTR. Nonetheless, the regions that the *FAF* MO bind to fall within the region verified by 5'-RACE. When looking at the two regions where the MOs bind, the alignment between the sequences of inserts obtained from positive colonies in the RACE experiment and the *FAF* cDNA sequences show there to be gaps and mismatches and are presumably due to the secondary structures that were not completely removed. Regardless, both morpholinos have 15 consecutive homologous bases between the 5'-RACE clones and the reference sequences, which has shown to be the minimum requirement for efficient translation blocking (Summerton, 1999; Moulton, 2016).

At present it is unknown whether *FAF* encodes a protein or acts as an ncRNA. Since different technical approaches may be required to successfully to knock down RNA vs protein, *in silico* tools were used to determine whether the predicted FAF peptide contains any conserved/recognizable protein domains, and in this way provide indirect support for the existence of a FAF protein. The amino acid sequence of FAF is 76 aa, and if *FAF* is translated, it would be classified as a microprotein. Microproteins, also referred to as small open reading frame (sORF)-encoded proteins, are proteins smaller than 100 aa (Yang *et al.*, 2011; Su *et al.*, 2013). These proteins often only have a single domain due to their small size and function via protein-protein interactions by fitting into the binding pockets of their target (Eguen *et al.*, 2015). This interaction makes microproteins regulators of protein-protein interactions, cell communication, hormone signalling and enzymatic activity (Su *et al.*, 2013; Cabrera-quio *et al.*, 2016). Consistent with this, the putative FAF protein is predicted to only have a single domain (GAF domain). Homology modelling showed there was only a 67.1% alignment between the human GAF domain of phosphodiesterase 10A, however, homology modelling to the chicken GAF domain (template: 3dba_A) showed a 69.7% alignment. While the alignment to the chicken GAF domain is an improvement, it is not a complete

alignment. This may be due to gene duplication events, degeneration and truncation of FAF which resulted in small changes over time and changes to its functional domain(s), characteristic of microproteins (Floyd *et al.*, 2014). Although plausible, this remains speculation and requires experimental validation. This may be done by generating an antibody against FAF and performing IHC on sections. If successful, it will confirm that *FAF* translates into a protein. Antibody production would likely require artificial synthesis of the antigen and the services of a company such as GenScript will be required.

Seeing as it has not been experimentally verified that *FAF* translates into a protein, the possibility of *FAF* acting as a non-coding RNA cannot be overlooked. Non-coding RNAs (ncRNAs) are functional RNA molecules that are not translated into a protein. These molecules often function in modulating gene expression either at the transcriptional or post-transcriptional level (Mongelli *et al.*, 2019). Based on their length, ncRNAs are classified into two broad groups, namely: long ncRNAs (>200 nt) and short ncRNAs (<200 nt) (Pedersen *et al.*, 2006). ncRNAs have been reported to be expressed in a sexually dimorphic manner and have shown to be implicated in regulating gonad differentiation. In female chickens, *DMRT1* is regulated by the non-coding RNA transcribed from the MHM region. The transcribed non-coding RNA coats the Z chromosome adjacent to the *DMRT1* locus, suppressing its expression (Teranishi *et al.*, 2001; Roeszler *et al.*, 2012; Caetano *et al.*, 2014). In mice, *Dmrt1* is regulated by the lincRNA (long intergenic non coding RNA), *Dmr* (*Dmrt1*-related gene) which is encoded by *Dmrt1*. The *Dmrt1* pre-mRNA and the lincRNA undergo trans-splicing, creating a chimeric isoform of the two molecules. The formation of this chimeric isoform disrupts the coding region of *Dmrt1*, reducing the expression of the DMRT1 protein (L. Zhang *et al.*, 2010).

Short ncRNA may also be implicated in gonad development. In chickens, the miRNA (microRNA), MIR202* shows male biased expression. After the induction of male-to-female sex reversal by *in ovo* injection of estradiol-17β, MIR202* expression decreased to levels observed in control females. The masculinisation of female embryos by Fadrozole resulted in an upregulation in MIR202* expression. Evidently, MIR202* expression correlates to testicular differentiation and functional work involving the knockdown of MIR202* may provide insight into which male-specific gene it interacts with (Bannister *et al.*, 2011; Rastetter, Smith

and Wilhelm, 2015). Taken together, the possibility of *FAF* acting as a non-coding RNA cannot be overlooked. Based on its length, *FAF* would be classified as a long non-coding RNA.

Morpholinos inherently knockdown their target protein by targeting (binding) the 5' UTR or the first 20 bases of the coding sequence. Morpholinos were used in this study to knockdown *FAF* because they offer the advantages of having >80% knockdown efficacy, they are unable to be targeted by nucleases enabling them to maintain their activity for longer (up to seven days in embryos) and they offer the best specificity in comparison to other knockdown constructs (Hudziak *et al.*, 1996; Partridge *et al.*, 1996; Liebert *et al.*, 1997; Stein *et al.*, 1997; Summerton, 1999). Although MO are traditionally used to knockdown protein expression, there have been reports of MO being used to interfere with the function of non-coding RNA. Collart *et al.*, used MOs to target the non-coding Y RNA which is essential in initiating chromosomal DNA replication. In *Xenopus laevis* and zebrafish embryos, MO-mediated knockdown of Y RNA resulted in the inhibition of DNA replication and embryo death before gastrulation. The MOs used in this study were designed to target either the stem or loop structure of the Y RNA that interacts with their target proteins (ORC, Cdt1, and HMGA1a), demonstrating that it is possible to use MO to study the function of non-coding RNA (Collart *et al.*, 2011). Due to the chemical composition of MO, they have a higher binding affinity to their target RNA than DNA, enabling them to invade RNA secondary structures and remaining bound to their target RNA (Stein *et al.*, 1997). Taken together, based on the properties of MOs and the information available on *FAF*, MOs were the most apt knockdown agent to use.

Irrespective of whether *FAF* functions as a microprotein or a non-coding RNA, it does contribute to female development. Morpholino-mediated knockdown of *FAF* in the gonads of female embryos resulted in them dying. This was unexpected seeing as the gonads are not essential to the development or survival of chickens. Several studies have been conducted whereby either a full or partial gonadectomy has been performed and had no negative impact on the survival of the chickens (Domm, 1931; Milićević *et al.*, 1987; Gigli *et al.*, 2005). This would allude to the interaction of the *FAF* MO with some unintended off-target that is crucial to embryonic survival. Although possible, it is unlikely because if true, the male embryos electroporated with the *FAF* MO would also have died. Furthermore, the

delivery of only *FAF* MO1 or *FAF* MO2 and the co-delivery of both MOs produced consistent results – only the male embryos survived and these embryos showed no noticeable phenotype. Another possibility is that the MO was delivered at a concentration that was too high, and as such, it was toxic to the embryo. To address this possibility, the *FAF* MO were delivered at a final concentration of either 2 mM or 1 mM. The decreased concentration did not change the mortality rate of either the male or female embryos and as such, this possibility was eliminated. The most likely scenario therefore is that the *FAF* MO was also delivered to a structure that is important to embryonic development. Consistent with this, the immunohistochemistry done on electroporated sections showed that the control MO (**Figure 3.13B**) was delivered to both gonads, suggesting that electroporation was not always precise. While no exact explanation can be given as to why the MO was detected in the right gonad, but mRFP expression was not observed, it may be because the MO has a lower molecular mass than pCI-RFP and hence migrated further, into the primitive right gonad. This needs to be addressed in future work.

Figure 4.1 below reviews how the electroporation procedure was conducted. The arrow shown in **Figure 4.1A** shows the direction of the electric field and the direction in which the construct will travel. **Figure 4.1B** shows how slightly moving the positive electrode caudally (towards the next somite) will change the direction in which the construct would move. This slight adjustment will result in the migration of the construct into the tip of the primitive gonad as well as into the dorsal aorta. Consistent with this, **Figure 4.2** shows that the construct could have been delivered to the dorsal aorta.

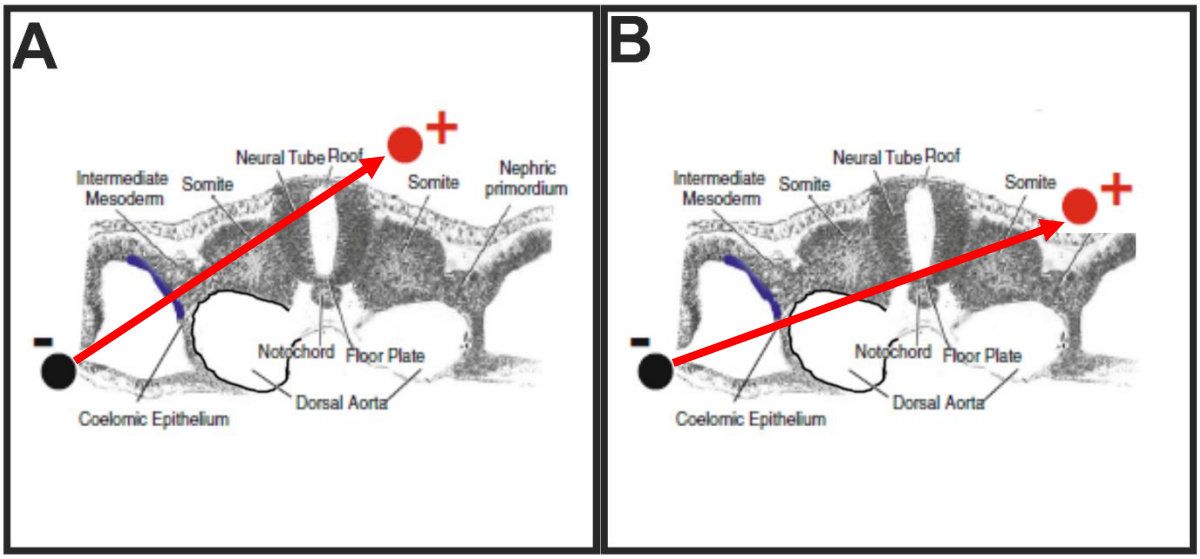

Figure 4.1. *Overview of how the electrodes were positioned during the electroporation procedure.* The construct was delivered to the coelomic cavity. **[A]** By positioning the negative electrode (black) slightly beneath the left coelomic cavity and the positive electrode (red) near somite 21, the electric field generated (shown by the red arrow) encouraged the construct to move dorsomedially into the coelomic epithelium and intermediate mesoderm. **[B]** If the positive electrode is moved caudally, towards somite 22, the electric field generated (shown by the red arrow) will encourage the construct to move into the tip of the coelomic epithelium and dorsal aorta.

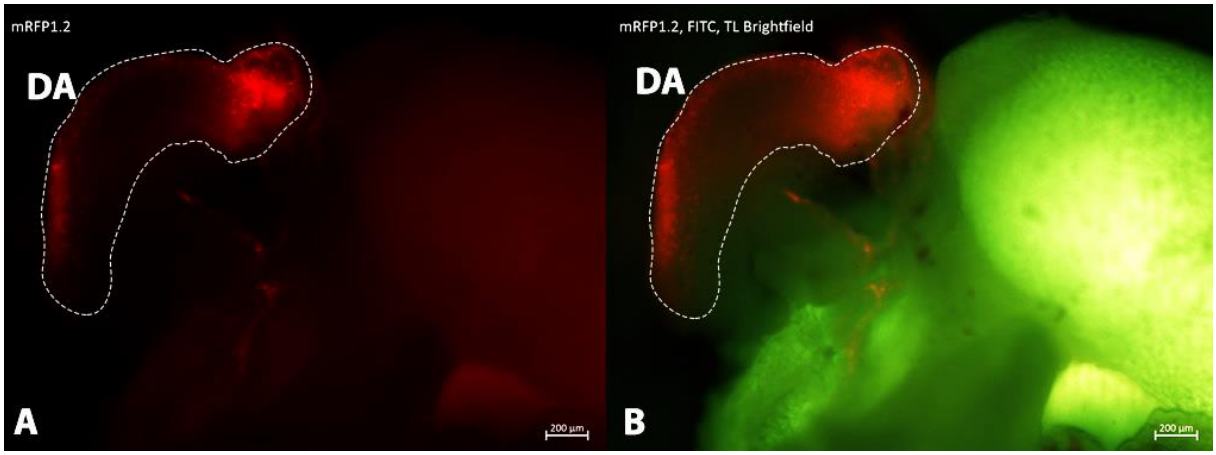

Figure 4.2. *Electroporation of the gonads shows unintended delivery of the construct to the dorsal aorta.* **[A-B]** Red fluorescence is seen in the dorsal aorta (DA) after the electroporation of the gonad with the pCI-RFP/*FAF* MO construct. Scale = 200 µm.

The dorsal aorta functions as the largest blood vessel to circulate blood throughout the developing embryo and a signalling centre indispensable to pancreas differentiation and neural crest cell migration (Lammert *et al.*, 2001; Gammill and Roffers-Agarwal, 2010; Sato, 2013). The dorsal aorta is also a site of hematopoiesis. The knockdown of *FAF* in this tissue presents a plausible explanation to the female exclusive death observed. One of two possibilities exist: either the delivery of the *FAF* MO resulted in the knockdown of an off-target gene

that is essential to normal dorsal aorta formation/function or the knockdown of *FAF* itself negatively affected the dorsal aorta. However, seeing as males developed normally, it would suggest it was the knockdown of *FAF* and not an off-target. Since the formation of the dorsal aorta was out of the scope of this project, the role of *FAF* in dorsal aorta formation was not further investigated. However, this can be investigated by conducting H&E staining on sections (at the wing bud level) obtained from embryos electroporated with *FAF* and unelectroporated embryos. If there is a morphological change between the electroporated and unelectroporated embryos, it would warrant further investigation.

Alternatively, an approach to circumvent the possibility of the MO from entering the dorsal aorta would be to explant the urogenital system of HH14-16 embryos and then deliver the *FAF* MO to the explanted gonads. The explanted gonads will still express male specific and female specific markers and changes in the expression pattern of these markers due to the delivery of the MO can be assessed (Smith and Sinclair, 2004).

While the MO-mediated knockdown of *FAF* was not informative with respect to the role of *FAF* in gonad development, the ectopic expression of *FAF* in males and the overexpression of *FAF* in females was more informative. The ectopic expression of *FAF* in males resulted in the development of a thickened cortex (**Figure 3.17**), which is characteristic of only the female left gonad (**Figure 3.18**). Additionally, the medulla of the males expressing *FAF* is disorganized and no distinct seminiferous tubes can be seen (Smith and Sinclair, 2004). This suggests that at a histological level, a male-to-female sex reversal occurred. The extent of the sex reversal, however, still needs to be determined. To investigate this, the expression patterns of male and female markers should be assessed by immunostaining. If there is a loss of DMRT1 and the ectopic expression of FOXL2 in the left gonad of ZZ males electroporated with pCI-*FAF*-RFP, the possibility that the morphology observed was due to artefacts (such as the sectioning technique) may be ruled out and a more definite conclusion can be made. The overexpression of *FAF* in the left ZW gonad did not have any effect on the morphology of the gonad, seen when comparing the electroporated and unelectroporated female gonad (**Figure 3.18**). This is likely due to transcriptional regulation, post-transcriptional regulation or translational regulation of *FAF*. It should be noted, however, that only one female was analysed and more ZW females overexpressing *FAF* needs to be analysed to

ensure that overexpressing *FAF* does not negatively affect female gonad development.

The results obtained from the ectopic expression of *FAF* in ZZ males, however, is in contradiction to previous work conducted. Hirst *et al*., induced female-to-male sex reversal by using the *Aromatase* inhibitor, Fadrozole. The gonads of ZW embryos treated with Fadrozole were masculinized noted by a reduction in the female markers Aromatase and FOXL2 and the ectopic expression of the male marker AMH. Assessment of the expression of *FAF* in the Fadrozole treated females by qPCR showed no significant change in expression in *FAF* (Hirst *et al.*, 2017). *FAF* mRNA localizes to both the cortex and medulla, where it detected as early as HH24 in the gonads whereas *FOXL2*/*Aromatase* mRNA localizes to the medulla and is only present from HH28. This suggests that *FAF* may either act upstream of *FOXL2*/*Aromatase* or *FAF* does not act in the *FOXL2*/*Aromatase* pathway. Seeing as *FAF* mRNA was also detected in the cortex and its temporal expression coincides with that of *WNT4*/*RSPO1*/*β-catenin*, it may act in this pathway (Smith *et al.*, 2008; Hirst *et al.*, 2017). There has been no studies done to confirm that *FAF* interacts with any of the female or male markers, however.

Furthermore, it has been shown that abolishing the production of oestrogen by the inhibition of *Aromatase*, will also affect genes essential to ovarian development that act upstream of *Aromatase*. Consistent with this, Fadrozole treatment in females resulted in a reduction in the expression of *FOXL2*, *WNT4* and *RSPO1*, all which are expressed prior to *Aromatase* (Hudson, Smith and Sinclair, 2005; Smith *et al.*, 2008). The unaltered expression of *FAF* during female-to-male sex reversal would therefore suggest it either does not respond to oestrogen or it is not essential to ovarian development.

This is not to say that *FAF* does not act in female sex determination. The ectopic expression of *FAF* in ZZ males clearly depicts a morphological change. *FAF* may alternatively act to suppress the male pathway, independently of the female pathway. Since *FAF* is present in females from as early as HH4, it is possible that it is involved in the epigenetic regulation of the MHM region that transcribes a long non-coding RNA which suppresses *DMRT1* (Roeszler *et al.*, 2012).

When ZW females were treated with Fadrozole, the MHM region showed unaltered levels of methylation in the liver but increased levels of methylation in the gonad confirming a role of the MHM in gonad development, attributed to either the loss of

a female factor or the activation of a male one (Zheng, Chen and Xu, 2011). This female factor would act as a demethylase or a methylase inhibitor. If *FAF* is this proposed female factor and it is translated into a protein, it would unlikely act as a demethylase by itself due to its size, and *in silico* experiments did not identify any common domains expected in a demethylase (such as the PWWP domain or a Zinc Finger domain) (Nameki *et al.*, 2005; Mosammaparast and Shi, 2010; Straub and Wenkel, 2017). Instead, it may activate a demethylase via protein-protein interactions or it may inactivate a methylase. Assessing this may be done by conducting *in situ* hybridisation and determining whether the long non-coding RNA product transcribed from the MHM region is present in ZZ embryos ectopically expressing *FAF*. If so and if *FAF* translates into a protein, co-immunoprecipitation can be performed in which FAF will be isolated by a specific antibody and any protein that interacts with FAF will remain bound and can be identified by Western blotting (Iqbal *et al.*, 2018). Alternatively, if *FAF* acts as a non-coding RNA, it would most likely act to suppress the activity of a methylase, either by suppressing its expression or sterically blocking its target site.

Interestingly, it was reported that global mis-expression of the long non-coding RNA product transcribed from the MHM region resulted in defects in both male and female embryos, particularly of the brain and heart (Roeszler *et al.*, 2012). If *FAF* is involved in regulating the methylation status of the MHM region, it provides an alternate explanation as to the female-exclusive death observed when the *FAF* MO was delivered to the dorsal aorta.

Conclusion

It has been experimentally validated in this project that *FAF* has a 5'-UTR, as predicted by Ensembl. Based on the functional work conducted in this project, it is evident that *FAF* may be implicated in embryonic development, and more specifically, female gonad differentiation illustrated by the female-like morphology observed in ZZ males ectopically expressing *FAF*. Further work, however, is required to draw conclusions on how *FAF* is involved in female gonad differentiation.

5. Chapter 5 - Future work

Based on the results obtained in this study, it is clear that *FAF* is important to normal female development and is implicated in sex differentiation. It would therefore be beneficial to determine whether *FAF* acts as a microprotein or a non-coding RNA. This would assist in future functional work studies. The most direct approach to address this would be to generate an antibody against FAF and perform IHC on gonad sections. This would also provide insight as to whether *FAF* is localised to the cytoplasm or nucleus.

Data from the MO-mediated knockdown of FAF would also provide invaluable information. While this data can be obtained from electroporating the MO into a large number of embryos, it may first be worthwhile to explant the urogenital system of HH14-16 embryos and then deliver the *FAF* MO to the explanted gonads. Irrespective of how the results of the knockdown of *FAF* is achieved, an mRNA rescue experiment (in which the altered phenotype is restored) should also be conducted to confirm it is the knockdown of *FAF* that caused the altered phenotype.

With respect to the ZZ males ectopically expressing *FAF*, analysis of more embryos is required to confirm the results obtained here. Measurements from the cortex of the ZZ males ectopically expressing *FAF* and the corresponding (unelectroporated) right gonad should be taken and statistical analysis should be performed using these measurements. This would provide additional evidence to the conclusions that have been made. Additionally, evaluation of the male and female sex markers by immunofluorescence needs to be conducted.

6. Chapter 6 - Reference List

Altschup, S. F., Gish, W., Miller, W., Myers, E. U. and Lipman, D. J. (1990) Basic Local Alignment Search Tool, *J. Mol. Biol.*, 215(3), 403–410.

Arit, D., Bensch, S., Hansson, B., Hasselquist, D. and Westerdahl, H. (2004) Observation of a ZZW female in a natural population: Implications for avian sex determination., *Proc Biol Sci*, 271, S249–S251.

Arnold, A. P., Itoh, Y. and Melamed, E. (2008) A Bird's-Eye View of Sex Chromosome Dosage Compensation, *Annu. Rev. Genomics Hum. Genet.*, 9(1), 109–127.

Ayers, K. L., Davidson, N. M., Demiyah, D., Roeszler, K. N., Grützner, F., Sinclair, A. H., Oshlack, A. and Smith, C. A. (2013) RNA sequencing reveals sexually dimorphic gene expression before gonadal differentiation in chicken and allows comprehensive annotation of the W-chromosome. *Genome Biol*, 14(3), R26.

Ayers, K. L., Lambeth, L. S., Davidson, N. M., Sinclair, A. H., Oshlack, A. and Smith, C. A. (2015) Identification of candidate gonadal sex differentiation genes in the chicken embryo using RNA-seq, *BMC Genomics*. 16, 1–19.

Ayers, K. L., Sinclair, A. H. and Smith, C. A. (2013) The molecular genetics of ovarian differentiation in the avian model, *Sexual Development*, 7, 80–94.

Ayers, K. L., Smith, C. A. and Lambeth, L. S. (2013) The Molecular Genetics of Avian Sex Determination and its Manipulation, *Genesis*, 51, 325–336.

Bannister, S. C., Smith, C. A., Roeszler, K. N., Doran, T. J., Sinclair, A. H., Tizard, M. L. V, Industries, C. L. and Animal, A. (2011) Manipulation of Estrogen Synthesis Alters MIR202* Expression in Embryonic Chicken Gonads, *Biology of Reproduction*, 85, 22–30.

Belle, H. Van (1976) Alkaline Phosphatase. I. Kinetics and Inhibition by Levamisole of Purified lsoenzymes from humans, *Clin. Chem*, 22(7), 972–976.

Bellott, D. W., Skaletsky, H., Cho, T., Brown, L., Locke, D., Chen, N., Galkina, S., Pyntikova, T., Koutseva, N., Graves, T., Kremitzki, C., Warren, W. C., Clark, A. G., Gaginskaya, E., Richard, K. and Page, D. C. (2017) Avian W and mammalian Y chromosomes convergently retained dosage-sensitive regulators, *Nat Genet.*,

49(3), 387–394.

Bernard, P., Kezdy, K. E., Melderen, L. V., Steyaert, J., Wyns, L., Pato, M. L., Higgins, P. N. and Couturier, M. (1993) The F plasmid CcdB protein induces efficient ATP-dependent DNA cleavage by gyrase, *J. Mol. Biol*, 234, 534–541.

Bernard, P., Gabant, P., Bahassi, E. M. and Couturier, M. (1994) Positive Selection Vectors Using the F Plasmid ccdB Killer Gene, *Gene*, 148, 71–74.

Bernard, P. and Couturier, M. (1992) Cell Killing by the F Plasmid CcdB Protein Involves Poisoning of DNA-Topoisomerase II Complexes, *J. Mol. Biol*, 226, 735–745.

Bowen, S. T. and Hanson, J. (1962) A Gynandromorph of the Brine Shrimp, Artemia Salina, *Genetics*, 47, 277–280.

Brenner, C., Bieganowski, P., Pace, H. C. and Huebner, K. (1999) The Histidine Triad Superfamily of Nucleotide-Binding Proteins, *J Cell Physiol*, 181(2), 179–187.

Brenner, C. (2002) Hint, Fhit and GalT: Function, Structure, Evolution and Mechanismof Three Branches of the Histidine Triad Superfamily of Nucleotide Hydrolases and Transferases, *Biochemistry*, 41(29), 9003–9014.

Bruijnis, M. R. N., Blok, V., Stassen, E. N. and Gremmen, H. G. J. (2015) Moral '" Lock-In "' in Responsible Innovation : The Ethical and Social Aspects of Killing Day-Old Chicks and Its Alternatives, *Journal of Agricultural and Environmental Ethics*. Springer Netherlands, 28(5), 939–960. 10.1007/s10806-015-9566-7.

Buhl, A. C. (2013) Legal Aspects of the Prohibition on Chick Shredding in the German State of North Rhine-Westphalia, *Glob. J. Anim. Law*, 2(6), 1–8.

Bull, J. J. (1985) Sex determining mechanisms : An evolutionary perspective, *Experientia*, 41(10), 1285–1296.

Cabrera-quio, L. E., Herberg, S., Pauli, A., Enrique, L., Herberg, S., Decoding, A. P., Cabrera-quio, L. E., Herberg, S. and Pauli, A. (2016) Decoding sORF translation – from small proteins to gene regulation Decoding sORF translation – from small proteins to gene regulation, *RNA Biology*, 13(11), 1051–1059.

Caetano, L. C., Gennaro, F. G. O., Coelho, K., Araújo, F. M., Vila, R. A., Araújo, A., de Melo Bernardo, A., Marcondes, C. R., Chuva de Sousa Lopes, S. M. and

Ramos, E. S. (2014) Differential expression of the MHM region and of sex-determining-related genes during gonadal development in chicken embryos, *Genetics and Molecular Research*, 13(1), 838–849.

Castro, E. De, Sigrist, C. J. A., Gattiker, A., Bulliard, V., Langendijk-genevaux, P. S., Gasteiger, E., Bairoch, A. and Hulo, N. (2006) ScanProsite: detection of PROSITE signature matches and ProRule-associated functional and structural residues in proteins, *Nucleic Acids Research*, 34, W362–W365.

Chan, J. K. C. (2014) The wonderful colors of the hematoxylin-eosin stain in diagnostic surgical pathology., *Int J Surg Pathol.*, 22(1), 12–32.

Chen, C.C. Hwang, J.K. Yang, J.M. (2009). (PS)2-v2: template-based protein structure prediction server. *BMC Bioinformatics*, 10:366

Chue, J. and Smith, C. A. (2011) Sex determination and sexual differentiation in the avian model, *FEBS J*, 278, 1027–1034.

Clinton, M. (1998) Sex Determination and Gonadal Development: A Bird's Eye View, *The Journal of Experimental Zoology*, 281(5), 457–465.

Clinton, M., Haines, L., Belloir, B. and Mcbride, D. (2001) Sexing chick embryos : A rapid and simple protocol, *British Poultry Science*, 42(1), 134–138.

Clinton, M., Zhao, D., Nandi, S. and Mcbride, D. (2012) Evidence for avian cell autonomous sex identity (CASI) and implications for the sex-determination process?, *Chromosome Research*, 20, 177–190.

Collart, C., Christov, C. P., Smith, J. C. and Krude, T. (2011) The Midblastula Transition Defines the Onset of Y RNA-Dependent DNA Replication in Xenopus laevis, *Molecular and Cellular Biology*, 31(18), 3857–3870.

Coriat, A., Valleley, E., Ferguson, M. W. J. and Sharpe, P. T. (1994) Chromosomal and Temperature-Dependent Sex Determination: The Search for a Conserved Mechanism, *The Journal of Experimental Zoology*, 270(1), 112–116.

Cutting, A., Chue, J. and Smith, C. A. (2013) Just how conserved is vertebrate sex determination?, *Developmental Dynamics*, 242(4), 380–387.

Degeling, C., Ã., Lederman, Z. and Rock, M. (2016) Culling and the Common Good : Re-evaluating Harms and Benefits under the One Health Paradigm, *Public Health Ethics*, 9(3), 244–254.

Domm, L. . (1931) A Demonstration of equivalent potencies of right and left testis-like gonads in the ovariotomized fowl, *The anatomical record*, 49(3), 211–249.

Ebensperger, C., Drews, U., Mayerova, A. and Wolf, U. (1988) Serological H-Y antigen in the female chicken occurs during gonadal differentiation, *Differentiation*, 37, 186–191.

Eguen, T., Straub, D., Graeff, M. and Wenkel, S. (2015) MicroProteins: small size – big impact, *Trends in Plant Sci*, 20(8), 477–482.

Elbrecht, A. and Smith, R. G. (1992) Aromatase enzyme activity and sex determination in chickens, *Science*, 255(5043), 467–470.

Ellegren, H., Hultin-rosenberg, L., Brunström, B., Dencker, L., Kultima, K. and Scholz, B. (2007) Faced with inequality : chicken do not have a general dosage compensation of sex-linked genes, *BMC Biol.*, 12, 1–12.

Ellegren, H. (2011) Emergence of male-biased genes on the chicken Z-chromosome: Sex-chromosome contrasts between male and female heterogametic systems, *Genome Res*, 21, 2082–2086.

Fenner, A. C. and Moore, G. M. (1959) A Bicolored Gynandromorph of the Lobster, Homarus americanus, *Biological Bulletin*, 116(2), 226–231.

Fleming, N. I., Knower, K. C., Lazarus, K. A., Fuller, P. J., Simpson, E. R. and Clyne, C. D. (2010) Aromatase is a direct target of FOXL2: C134W in granulosa cell tumors via a single highly conserved binding site in the ovarian specific promoter, *PLoS ONE*, 5(12), e14389.

Floyd, S. K., Ryan, J. G., Conway, S. J., Brenner, E., Burris, K. P., Burris, J. N., Chen, T., Edger, P. P., Graham, S. W., Leebens-mack, J. H., Pires, J. C., Rothfels, C. J., Sigel, E. M., Stevenson, D. W., Stewart, C. N., Wong, G. K. and Bowman, J. L. (2014) Origin of a novel regulatory module by duplication and degeneration of an ancient plant transcription factor, *Mol Phylogenet Evol*., 81, 159–173.

Ford, C. E., Jones, K. W., Polani, P. E., De Almeida, J. C. and Briggs, J. H. (1959) A sex chromosome anomaly in a case of gonadal dysgenesis (Turner's Syndrome), *Lancet*, 1, 711–713.

Fraeye, I., Bruneel, C., Lemahieu, C., Buyse, J., Muylaert, K. and Foubert, I. (2012) Dietary enrichment of eggs with omega-3 fatty acids : A review, *FRIN*, 48(2), 961–969.

Galli, R., Preusse, G., Uckermann, O. and Bartels, T. (2017) In ovo sexing of chicken eggs by fluorescence spectroscopy, *Analytical and Bioanalytical Chemistry*, 1185–1194.

Gammill, L. and Roffers-Agarwal, J. (2010) Division of labor during trunk neural crest development, *Dev Biol*, 344(2), 555–565.

Gigli, I., Cushman, R. A., Wahl, C. M. and Fortune, J. E. (2005) Evidence for a Role for Anti-Mullerian Hormone in the Suppression of Follicle Activation in Mouse Ovaries and Bovine Ovarian Cortex Grafted Beneath the Chick Chorioallantoic Membrane, *Mol Reprod Dev*, 71(4), 480–488.

Ginsburg, M. and Eyal-giladi, H. (1987) Primordial germ cells of the young chick blastoderm originate from the central zone of the area pellucida irrespective of the embryo-forming process, *Development*, 101, 209–219.

Govoroun, M. S., Pannetier, M., Pailhoux, E., Cocquet, J., Brillard, J. P., Couty, I., Batellier, F. and Cotinot, C. (2004) Isolation of chicken homolog of the FOXL2 gene and comparison of its expression patterns with those of aromatase during ovarian development, *Developmental Dynamics*, 231(4), 859–870.

Graves, J. A. M. (2003) Sex and death in birds: A model of dosage compensation that predicts lethality of sex chromosome aneuploids, *Cytogenet Genome Res*, 101, 278–282.

Guioli, S. and Lovell-Badge, R. (2007) PITX2 controls asymmetric gonadal development in both sexes of the chick and can rescue the degeneration of the right ovary, *Development*, 134(23), 4199–4208.

Hamburger, V. and Hamilton, H. L. (1992) A series of normal stages in the development of the chick embryo., *Dev Dyn*, 195(4), 231–272.

Herron, K. L. and Fernandez, M. L. (2004) Issues and Opinions Are the Current Dietary Guidelines Regarding Egg Consumption Appropriate ?, *American Society for Nutritional Sciences. J. Nutr.*, 134, 187–190.

Hirst, C.E, Serralbo, O., Ayers, K. L., Roeszler, K. N. and Smith, C. A. (2017b)

Genetic Manipulation of the Avian Urogenital System Using In Ovo Electroporation, in Sheng, G. (ed.) *Avian and Reptilian Developmental Biology: Methods and Protocols, Methods in Molecular Biology*. 1st edn. Humana Press, 177–190. 10.1007/978-1-4939-7216-6.

Hirst, Claire E., Major, A. T., Ayers, K. L., Brown, R. J., Mariette, M., Sackton, T. B. and Smith, C. A. (2017) Sex reversal and comparative data undermine the W chromosome and support Z-linked DMRT1 as the regulator of gonadal sex differentiation in birds, *Endocrinology*, 158(9), 2970–2987.

Hirst, C. E., Major, A. T. and Smith, C. A. (2018) Sex determination and gonadal sex differentiation in the chicken model, *International Journal of Developmental Biology*, 62(1–3), 149–162.

Hori, T., Asakawa, S., Itoh, Y., Shimizu, N. and Mizuno, S. (2000) Wpkci, Encoding an Altered Form of PKCI, Is Conserved Widely on the Avian W Chromosome and Expressed in Early Female Embryos: Implication of Its Role in Female Sex Determination, *Molecular Biology of the Cell*, 11(10), 3645–3660.

Hu, Y., Okumura, L. M. and Page, D. C. (2013) Gata4 Is Required for Formation of the Genital Ridge in Mice, *PLoS Genet*, 9(7), 1003629.

Hudson, Q. J., Smith, C. A. and Sinclair, A. H. (2005) Aromatase inhibition reduces expression of FOXL2 in the embryonic chicken ovary, *Developmental Dynamics*, 233(3), 1052–1055.

Hudziak, R., Barofsky, E., Barofsky, D. F., Doreen, L., Huang, S. and Weller, D. D. (1996) Resistance of Morpholino Phosphorodiamidate Oligomers Enzymatic Degradation, *Antisense and Nucleic Acid Drug Development*, 6(4), 267–272.

Hutson, J. M., Ikawa, H. and Donahoe, P. K. (1982) Estrogen Inhibition of Mullerian Inhibiting Substance in the Chick Embryo, *Journal of Pediatric Surgery*, 17(6), 953–959.

Imataka, H., Suzuki, K., Inano, H., Kohmoto, K. and Tamaoki, B. (1989) Biosynthetic pathways of testosterone and estradiol-17β in slices of the embryonic ovary and testis of the chicken (Gallus domesticus)., *General and Comparative Endocrinology*, 73(1), 69–79.

Iqbal, H., Akins, D. R., Kenedy, M. R. and City, O. (2018) Co-immunoprecipitation

for Identifying Protein-Protein Interactions in Borrelia burgdorfer, *Methods Mol Biol.*, 1690, 47–55.

Ishimaru, Y., Komatsu, T., Kasahara, M., Katoh-fukui, Y., Ogawa, H., Toyama, Y., Maekawa, M., Toshimori, K., Chandraratna, R. A. S., Morohashi, K. and Yoshioka, H. (2008) Mechanism of asymmetric ovarian development in chick embryos, *Development*, 135(4), 677–685.

Itasaki, N., Bel-Vialar, S. and Krumlauf, R. (1999) 'Shocking' developments in chick embryology: electroporation and in ovo gene expression, *Nature Cell Biology*, 1, E203–E207.

Itoh, Y., Melamed, E., Yang, X., Kampf, K., Wang, S., Yehya, N., Nas, A. Van, Replogle, K., Band, M. R., Clayton, D. F., Schadt, E. E., Lusis, A. J. and Arnold, A. P. (2007) Dosage compensation is less effective in birds than in mammals, *J. Biol*, 6, 1–15.

Itoh, Y. and Mizuno, S. (2002) Molecular and cytological characterization of Ssp I-family repetitive sequence on the chicken W chromosome, *Chromosome Research*, 10(6), 499–511.

Jacobs, P. A. and Strong, J. A. (1959) A case of human intersexuality having a possible XXY sex-determining mechanism., *Nature*, 183, 302–303.

Johnson, P. T. and Otto, S. V. (1981) Histology of a Bilateral Gynandromorph of the Blue Crab, Callinectes sapidus Rathbun (Decapoda: Portunidae), *Biological Bulletin*, 161(2), 236–245.

Källberg, M. Wang, H. Wang, S. Peng, J. Wang, Z. Lu, H. Xu, J.. (2012). Template-based protein structure modeling using the RaptorX web server. *Nature Protocols,* **7**, 1511–1522.

Kibbe, W. A. (2007) OligoCalc: an online oligonucleotide properties calculator, *Nucleic Acids Research*, 35, W43–W46.

Koopman, P., Gubbay, J., Vivian, N., Goodfellow, P. and Lovell-badge, R. (1991) Male development of chromosomally female mice transgenic for Sry, *Nature*, 351, 117–121.

Korbie, D. J. and Mattick, J. S. (2008) Touchdown PCR for increased specificity and sensitivity in PCR amplification, *Nature Protocols*, 3(9), 1452–1456.

Kupper, C., Augustin, J., Edwards, S., Szekely, T., Kosztolanyi, A., Burke, T. and Janes, D. . (2012) Triploid plover female provides support for a role of the W chromosome in avian sex determination, *Biol Lett*, 8, 787–789.

Kuroda, Y., Arai, N., Arita, M., Teranishi, M., Hori, T. and Harata, M. (2001) Absence of Z-chromosome inactivation for five genes in male chickens, *Chromosome Research*, 9, 457-468.

Lambeth, L., Raymond, C. S., Roeszler, K. N., Kuroiwa, A., Nakata, T., Zarkower, D. and Smith, C. A. (2014) Over-expression of DMRT1 induces the male pathway in embryonic chicken gonads, *Dev Biol*, 389(2), 160–172.

Lambeth, L. S., Ayers, K., Cutting, A. D., Doran, T. J., Sinclair, A. H. and Smith, C. A. (2015) Anti-Mullerian Hormone Is Required for Chicken Embryonic Urogenital System Growth but Not Sexual Differentiation, *Biol. Reprod.*, 93(6), 138.

Lammert, E., Lammert, E., Cleaver, O. and Melton, D. (2001) Induction of Pancreatic Differentiation by Signals from Blood Vessels, *Science*, 294, 564–567.

Lee, S., Lee, W. K., Shin, J., Han, B. K., Moon, S., Cho, S., Park, T., Kim, H. and Han, J. (2006) Sexually dimorphic gene expression in the chick brain before gonadal differentiation, *Poult Sci*, 88, 1003–1015.

Li, H., Xu, H., Zhao, C., Sulaiman, Y. and Wu, C. (2011) A PCR amplification method without DNA extraction, *Electrophoresis*, 32(3), 394–397.

Liebert, M. A., Summerton, J., Stein, D., Huang, S. B. E. N., Matthews, P., Weller, D. and Partridge, M. (1997) Morpholino and Phosphorothioate Antisense Oligomers Compared in Cell-Free and In-Cell Systems, *Antisense and Nucleic Acid Drug Development*, 7(2), 63–70.

Lin, M., Thorne, M. H., Martin, I. C. A., Sheldon, B. L. and Jones, R. C. (1995) Development of the gonads in the triploid (ZZW and ZZZ) fowl, Gallus domesticus, and comparison with normal diploid males (ZZ) and females (ZW), *Reprod Fert Dev*, 7, 1185–1197.

Lu, J., Chuong, C. and Widelitz, R. B. (1997) Isolation and characterization of chicken β-catenin., *Gene*, 196(2), 201–207.

Luo, X. R., Ikeda, Y. Y. and Parker, K. L. (1994) A Cell-Specific Nuclear Receptor

Is Essential for Adrenal and Gonadal Development and Sexual-Differentiation, *Cell*, 77(4), 481–490.

Mank, J. E. and Ellegren, H. (2009) All dosage compensation is local: Gene-by-gene regulation of sex-biased expression on the chicken Z chromosome, *Heredity*, 102, 312–320.

Mcqueen, H. A. and Clinton, M. (2009) Avian sex chromosomes: dosage compensation matters, *Chromosome Research*, 17, 687–697.

Meeks, J. J., Crawford, S. E., Russell, T. A., Morohashi, K., Weiss, J. and Jameson, J. L. (2003) Dax1 regulates testis cord organization during gonadal differentiation, *Development*, 130, 1029–1036.

Melamed, E. and Arnold, A. P. (2007) Regional differences in dosage compensation on the chicken Z chromosome, *Genome Biol*, 8, R202.

Merchant-larios, H., Popova, L. and Reyss-Brion, M. (1984) Early Morphogenesis of Chick Gonad in the Absence of Mesonephros, *Develop. Growth and Differ*, 26(5), 403–417.

Milićević, Ži., Isaković, K., Drinka, V., Mićić, M. and Milićević, N. M. (1987) Effects of Neonatal Gonadectomy on Structure of the Bursa of Fabricius in the Chicken, *Anatomia histologia embryologia*, 16(2), 103–113.

Miranda, J. M., Anton, X., Redondo-valbuena, C., Roca-saavedra, P., Rodriguez, J. A., Lamas, A., Franco, C. M. and Cepeda, A. (2015) Egg and Egg-Derived Foods: Effects on Human Health and Use as Functional Foods, *Nutrients*, 7(1), 706–729.

Miyazaki, J., Takaki, S., Araki, K., Tashiroe, F., Tominaga, A., Takatsu, K. and Yamamura, K. (1989) Expression vector system based on the chicken β-actin promoter directs efficient production of interleukin-5, *Gene*, 79, 269–277.

Moghadam, H. K., Pointer, M. A., Wright, A. E. and Mank, J. E. (2012) W chromosome expression responds to female-specific selection, *PNAS*, 109(21), 8207–8211.

Mongelli, A., Martelli, F., Farsetti, A., Gaetano, C. and Carley, A. (2019) The Dark That Matters : Long Non-coding RNAs as Master Regulators of Cellular Metabolism in Non-communicable Diseases, *Front. Physiol.*, 10, 1–13.

Moriyama, S., Ogihara, J., Kato, J., Hori, T. and Mizuno, S. (2006) PKCI-W Forms a Heterodimer with PKCI-Z and Inhibits the Biological Activities of PKCI-Z In Vitro, Supporting the Predicted Role of PKCI-W in Sex Determination in Birds, *J. Biochem*, 139, 91–97.

Morris, K. R., Hirst, C. E., Major, A. T., Ezaz, T., Ford, M., Bibby, S., Doran, T. J. and Smith, C. A. (2018) Gonadal and endocrine analysis of a gynandromorphic chicken, *Endocrinology*, 159(10), 3492–3502.

Mosammaparast, N. and Shi, Y. (2010) Reversal of Histone Methylation: Biochemical and Molecular Mechanisms of Histone Demethylases, *Annu. Rev. Biochem.*, 79, 155–179.

Moulton, J. D. (2016) Guide for Morpholino Users: Toward Therapeutics, *J Drug Discov Develop and Deliv*, 3(2), 1023.

Nakabayashi, O., Kikuchi, H., Kikuchi, T. and Mizuno, S. (1998) Differential expression of genes for aromatase and estrogen receptor during the gonadal development in chicken embryos, *Journal of Molecular Endocrinology*, 20(2), 193–202.

Nakata, T., Ishiguro, M., Aduma, N., Izumi, H. and Kuroiwa, A. (2013) Chicken hemogen homolog is involved in the chicken-specific sex-determining mechanism, *Proceedings of the National Academy of Sciences*, 110(9), 3417–3422.

Nameki, N., Tochio, N., Koshiba, S., Inoue, M., Yabuki, T., Aoki, M., Seki, E., Matsuda, T., Fujikura, Y., Saito, M., Ikari, M., Watanabe, M., Terada, T., Shirouzu, M., Yoshida, M., Hirota, H., Tanaka, A., Hayashizaki, Y. and Güntert, P. (2005) Solution structure of the PWWP domain of the hepatoma-derived growth factor family, *Protein Science*, 14, 756–764.

Natoli, S., Markovic, T., Lim, D., Noakes, M. and Kostner, K. (2007) Unscrambling the research : Eggs , serum cholesterol and coronary heart disease, *Nutrition & Dietetics*, 64, 105–111.

Naurin, S., Hasselquist, D., Bensch, S. and Hansson, B. (2012) Sex-Biased Gene Expression on the Avian Z Chromosome: Highly Expressed Genes Show Higher Male-Biased Expression, *PLoS ONE*, 7(10), e46854.

Nishikimi, H., Kansaku, N., Saito, N., Usami, M., Ohno, Y. and Shimada, K. (2000) Sex Differentiation and mRNA Expression of P450c17, P450arom and AMH in Gonads of the Chicken, *Molecular reproduction and Development*, 55(1), 20–30.

Niwa, H., Yamamura, K. and Miyazaki, J. (1991) Efficient selection for high-expression transfectants with a novel eukaryotic vector, *Gene*, 108, 193–199.

O'Neill, M., Binder, M., Smith, C., Andrews, J., Reed, K., Smith, M., Millar, C., Lambert, D. and Sinclair, A. (2000) ASW: a gene with conserved avian W-linkage and female specific expression in chick embryonic gonad, *Development Genes and Evolution*, 210(5), 243–249.

Ohno, S. (1971) Sex chromosomes and sex-linked traits, *Teratology*, 4(1), 1967.

Omotehara, T., Smith, C. A., Mantani, Y., Kobayashi, Y., Tatsumi, A., Nagahara, D., Hashimoto, R., Hirano, T., Umemura, Y., Yokoyama, T., Kitagawa, H. and Hoshi, N. (2014) Spatiotemporal expression patterns of doublesex and mab-3 related transcription factor 1 in the chicken developing gonads and Müllerian ducts, *Poultry Science*, 93(4), 953–958.

Oreal, E., Pieau, C., Mattei, M. G., Josso, N., Picard, J. Y., Carré-Eusèbe, D. and Magre, S. (1998) Early expression of AMH in chicken embryonic gonads precedes testicular SOX9 expression, *Developmental Dynamics*, 212(4), 522–532.

Oréal, E., Mazaud, S., Picard, J. Y., Magre, S. and Carré-Eusébe, D. (2002) Different patterns of anti-Müllerian hormone expression, as related to DMRT1, SF-1, WT1, GATA-4, Wnt-4, and Lhx9 expression, in the chick differentiating gonads, *Developmental Dynamics*, 225(3), 221–232.

Pace, H. C. and Brenner, C. (2003) Feminizing chicks : a model for avian sex determination based on titration of Hint enzyme activity and the predicted structure of an Asw-Hint heterodimer, *Genome Biol*, 4(3), R18.

Parks, K. P., Seidle, H., Wright, N., Sperry, J. B., Howitz, K., Wright, D. L. and Brenner, C. (2004) Altered specificity of Hint-W123Q supports a role for Hint inhibition by ASW in avian sex determination, *Physiol Genomics*, 20, 12–14.

Partridge, M., Vincent, A., Matthews, P., Puma, J., Stein, D. and Summerton, J.

(1996) A Simple Method for Delivering Morpholino Antisense Oligos into the Cytoplasm of Cells, *Antisense and Nucleic Acid Drug Development*, 6, 169–175.

Pedersen, J. S., Bejerano, G., Siepel, A., Rosenbloom, K., Lindblad-toh, K., Lander, E. S., Kent, J., Miller, W. and Haussler, D. (2006) Identification and Classification of Conserved RNA Secondary Structures in the Human Genome, *PLoS*, 2(4), e33.

Rastetter, R. H., Smith, C. A. and Wilhelm, D. (2015) The role of non-coding RNAs in male sex determination and differentiation, *Reproduction*, 150(3), R93–R107.

Raymond, C. S., Kettlewell, J. R., Hirsch, B., Bardwell, V. J. and Zarkower, D. (1999) Expression of Dmrt1 in the Genital Ridge of Mouse and Chicken Embryos Suggests a Role in Vertebrate Sexual Development, *Dev Biol*, 215, 208–220.

Reed, K. J. and Sinclair, A. H. (2002) FET-1: a novel W-linked, female specific gene up-regulated in the embryonic chicken ovary, *Mechanisms of Development*, 3, S87–S90.

Rodemer-lenz, E. (1989) On cell contribution to gonadal soma formation in quail-chick chimeras during the indifferent stage of gonadal development, *Anat Embryol*, 179, 237–242.

Rodriguez-Leon, J. Rodriguez, E.C. Marti, M. Santiago-Josefat, B. Dubova, I. Rubiralta, X. Izpisua Belmonte, J.C. (2008) Pitx2 regulates gonad morphogenesis, *PNAS*, 105(32), 11242–11247.

Roeszler, K. N., Itman, C., Sinclair, A. H. and Smith, C. A. (2012) The long non-coding RNA, MHM, plays a role in chicken embryonic development, including gonadogenesis, *Developmental Biology*, 366(2), 317–326.

Samman, S., Piu, F., Carter, L. M., Foster, M. J., Ahmad, Z. I., Phuyal, J. L. and Petocz, P. (2009) Fatty acid composition of certified organic , conventional and omega-3 eggs, *Food Chemistry*, 116(4), 911–914.

Sato, Y. (2013) Dorsal aorta formation: Separate origins, lateral-to-medial migration, and remodeling, *Develop. Growth Differ.*, 55, 113–129.

Schmid, M., Smith, J., Burt, D. W., Aken, B. L., Antin, P. B., Archibald, A. L., Ashwell, C., Blackshear, P. J., Boschiero, C., Brown, C. T., Burgess, S. C.,

Damas, J., Davis, R. V. N., Mary, D. D. K., Thomas, E. D., Takele, D., Dunn, I. C., Dunn, M., Ellegren, H., *et al.* (2015) Third Report on Chicken Genes and Chromosomes 2015, *Cytogenet Genome Res*, 145, 78–179.

Scholz, B., Kultima, K., Mattsson, A., Axelsson, J., Brunström, B., Halldin, K., Stigson, M. and Dencker, L. (2006) Sex-dependent gene expression in early brain development of chicken embryos, *BMC Neuroscience*, 7, 1–17.

Smith, C. A., McClive, P. J., Western, P. S., Reed, K. J. and Sinclair, A. H. (1999) Conservation of a sex-determining gene, *Nature*, 402, 601–602.

Smith, C. A., Clifford, V., Western, P. S., Wilcox, S. A., S, B. K. and Sinclair, A. H. (2000) Cloning and expression of a DAX1 homologue in the chicken embryo, *ournal of Molecular Endocrinology*, 24, 23–32.

Smith, C. A., Shoemaker, C. M., Roeszler, K. N., Queen, J., Crews, D. and Sinclair, A. H. (2008) Cloning and expression of R-Spondin1 in different vertebrates suggests a conserved role in ovarian development, *BMC Developmental Biology*, 8, 1–16.

Smith, C. A., Roeszler, K. N., Ohnesorg, T., Cummins, D. M., Farlie, P. G., Doran, T. J. and Sinclair, A. H. (2009) The avian Z-linked gene DMRT1 is required for male sex determination in the chicken, *Nature*, 461(7261), 267–271.

Smith, C. A., Andrews, J. E. and Sinclair, A. H. (1997) Gonadal sex differentiation in chicken embryos: Expression of estrogen receptor and aromatase genes, *The Journal of Steroid Biochemistry and Molecular Biology*, 60(5), 295–302.

Smith, C. A., Katz, M. and Sinclair, A. H. (2003) DMRT1 Is Upregulated in the Gonads During Female-to-Male Sex Reversal in ZW Chicken Embryos, *Biology of Reproduction*, 68, 560–570.

Smith, C. A., Roeszler, K. N. and Sinclair, A. H. (2009) Genetic evidence against a role for W-linked histidine triad nucleotide binding protein (HINTW) in avian sex determination, *International Journal of Developmental Biology*, 53(1), 59–67.

Smith, C. A. and Sinclair, A. H. (2004) Sex determination: insights from the chicken, *BioEssays*, 26(2), 120–132.

Smith, C. A., Smith, M. J. and Sinclair, A. H. (1999) Gene expression during gonadogenesis in the chicken embryo, *Gene*, 234(2), 395–402.

Spencer, W. (1927) A Gynandromorph in Drosophila funebris, *The American Naturalist*, 61(672), 89–91.

Stein, D., Foster, E., Huang, S. B., Weller, D. and Summerton, J. (1997) A specificity comparison of four antisense types: morpholino, 2'-O-methyl RNA, DNA, and phosphorothioate DNA., *Antisense and Nucleic Acid Drug Development*, 7(3), 151–157.

Straub, D. and Wenkel, S. (2017) Cross-Species Genome-Wide Identification of Evolutionary Conserved MicroProteins, *Genome Biol Evol*, 9(3), 777–789.

Su, M., Ling, Y., Yu, J., Wu, J., Xiao, J., Wang, X. and United, H. (2013) Small proteins: untapped area of potential biological importance, *Frontiers in Genetics*, 4(286), 1–9.

Summerton, J. (1999) Morpholino antisense oligomers: the case for an RNase H-independent structural type, *Biochimica et Biophysica Acta*, 1489(1), 141–158.

Teranishi, M., Shimada, Y., Hori, T., Nakabayashi, O., Kikuchi, T., Macleod, T., Pym, R., Sheldon, B., Solovei, I., Macgregor, H. and Mizuno, S. (2001) Transcripts of the MHM region on the chicken Z chromosome accumulate as non-coding RNA in the nucleus of female cells adjacent to the DMRT1 locus, *Chromosome Research*, 9(2), 147–165.

Thome, M. H., Nicholas, F. W., Moran, C. and Sheldon, B. L. (1997) Genetic Analysis of Triploidy in a Selected Line of Chickens, *J Heredity*, 88, 495–498.

Wang, Q., Mank, J. E., Li, J., Yang, N. and Qu, L. (2017) Allele-Specific Expression Analysis Does Not Support Sex, *Genome Biol Evol*, 9, 619–626.

Waterhouse, A. M., Procter, J. B., Martin, D. M. A., Clamp, M. and Barton, G. J. (2009) Jalview Version 2 — a multiple sequence alignment editor and analysis workbench, *Bioinformatics*, 25(9), 1189–1191.

Williams, R.M. Senanayake, U. Artibani, M. Taylor, G. Wells, D. Ahmed, A.A. Sauka-Spengler, T. (2018). Genome and epigenome engineering CRISPR toolkit for in vivo modulation of cis-regulatory interactions and gene expression in the chicken embryo. *Development*, 145(4), dev160333.

Yamamoto, I., Tsukada, A., Saito, N. and Shimada, K. (2003) Profiles of mRNA expression of genes related to sex differentiation of the gonads in the chicken

embryo, *Poultry Science*, 82(9), 1462–1467.

Yang, X., Tschaplinski, T. J., Hurst, G. B., Jawdy, S., Abraham, P. E., Lankford, P. K., Adams, R. M., Shah, M. B., Hettich, R. L., Lindquist, E., Kalluri, U. C., Gunter, L. E., Pennacchio, C. and Tuskan, G. A. (2011) Discovery and annotation of small proteins using genomics, proteomics, and computational approaches, *Genome Res*, 21, 634–641.

Yang, X., Deng, J., Zheng, J., Xia, L., Yang, Z., Qu, L., Chen, S., Xu, G., Jiang, H., Clinton, M. and Yang, N. (2016) A window of MHM demethylation correlates with key events in gonadal differentiation in the chicken, *Sexual Development*, 10(3), 152–158.

Zhang, L., Lu, H., Xin, D., Cheng, H. and Zhou, R. (2010) A novel ncRNA gene from mouse chromosome 5 trans-splices with Dmrt1 on chromosome 19, *Biochem Biophys Res Commun*, 400(4), 696–700.

Zhang, S. O., Mathur, S., Hattem, G., Tassy, O. and Pourquié, O. (2010) Sex-dimorphic gene expression and ineffective dosage compensation of Z-linked genes in gastrulating chicken embryos, *BMC Genomics*, 11, 1–13.

Zhao, D., Mcbride, D., Nandi, S., Mcqueen, H. A., Mcgrew, M. J., Hocking, P. M., Lewis, P. D., Sang, H. M. and Clinton, M. (2010) Somatic sex identity is cell autonomous in the chicken, *Nature*, 464(7286), 237–242.

Zheng, X. Y. J., Chen, L. Q. S. and Xu, J. L. G. (2011) Methylation Status of cMHM and Expression of Sex-Specific Genes in Adult Sex-Reversed Female Chickens, *Sexual Development*, 5, 147–154.

Zuker, M. (2003) Mfold web server for nucleic acid folding and hybridization prediction, *Nucleic Acids Research*, 31(13), 3406–3415.

Appendix 1: Methods

A1.1. Gel electrophoresis

Gel electrophoresis was performed as described below unless otherwise stated. 1% agarose gels were prepared by dissolving 0.5 g SeaKem LE Agarose (Lonza) in 50 mL 1X TAE (40 mM Tris-Base, 20 mM Acetic acid and 1 mM EDTA). 5 µL of the GeneRuler 1 Kb DNA ladder (Thermo) was used and each sample loaded comprised of 10 µL sample and 1 µL GR green loading dye. Gels were visualized under UV light using the GelDoc XR Imager (BioRad).

A1.2. Colony PCR

8-10 positive colonies were isolated from each transformation reaction and were grown overnight (at 37 °C, 118 rpm) in 6 mL liquid culture (pH 7.4), supplemented with 100 µg/mL ampicillin. Colony PCR was performed to confirm the presence of an insert. 200 µL of each liquid culture was transferred to a 1.5 mL micro-centrifuge tube and centrifuged at 10000g for 1 min to pellet the cells. Each PCR reaction comprised of 12.5 µL Taq DNA Polymerase 2x Master Mix (Ampliqon), 1.5 µL Forward primer, 1.5 µL Reverse primer and 9.5 µL dH_2O. Using a pipette tip, some of the pelleted colony was scraped and placed into the PCR reaction. A no template control (NTC) was also set up and contained the same components, except that no colony was added.

A1.3. Gel extraction

The gel extraction was carried out as per the Zymoclean Gel DNA Recovery Kit (Zymo Research) protocol. The kit uses an optimized agarose dissolving buffer and *Fast-Spin* column technology to bind DNA. The elution buffer was heated to 60 °C before adding it to the column. After the elution buffer was added to the column, the column was incubated for 10 min at room temperature before centrifugation. Both these steps were performed to improve the DNA yield. The DNA was eluted in 6 µL. 1 µL was used to assess the purity and concentration of the eluted DNA using the NanoDrop ND-1000 Spectrophotometer (ISOGEN).

A1.4. *In ovo* electroporation of neural tube

Fertilized White Leghorn chicken (*Gallus gallus*) eggs were incubated at 37.4 °C at 60-70% humidity, in a humidified incubator (Pleysier Incubators) to HH10-11. Embryos were placed horizontally, with their long axis oriented horizontally and the top marked to know where the embryo would be situated. Embryos were windowed as described in **Chapter 2.6.2**, however, the vitelline membrane was left intact.

Microinjection and electroporation were carried out according to the protocol outlined by Itasaki *et al.*, 1999 (Itasaki *et al.*, 1999). The capillary needle (containing the construct) was inserted through the vitelline membrane into the neural tube. The construct was delivered to the neural tube by blowing through the mouth piece of the mouth pipette as described in **Chapter 2.6.3** and the electrodes were placed on opposite sides of the embryo. The ECM 830 Electro Square Porator (BTX) was used to deliver the voltage with the following parameters: 5 pulses, of 18 V with a 50 ms width, with 100 ms between pulses. 0.5 mL of Ringer's solution (0.12 M NaCl, 4.96 mM KCl, 1.53 mM $CaCl_2 \cdot H_2O$, pH 7.3-7.5) was added to the embryo and the opening was sealed tightly with cellotape. Embryos were incubated for 24 hr at 37.4 °C at 60-70% humidity, in a humidified incubator (Pleysier Incubators). Embryos were collected and processed as described in **Chapter 2.6.4** and **2.6.5**. Embryos were electroporated with either pCI-RFP (250 ng), the control MO (0.5 mM) or a combination of both the control MO (0.5 mM) and pCI-RFP (250 ng).

Appendix 2: Recipes

Below depicts the recipes for the reagents used, organized alphabetically.

Ampicillin (5 mg/mL)

For 3 mL:

15 mg of Ampicillin powder was dissolved in 3 mL of Ringer's Solution. The solution was filtered using 0.2 µm filter and 2 mL of Ampicillin was added to 50 mL of Ringer's Solution.

Ampicillin (100 mg/mL)

1 g of Ampicillin was dissolved in 10 mL of autoclaved dH_2O and filtered using 0.2 µm filter. Ampicillin was stored -20 °C

Crude DNA lysis solution

For 20 mL:

Component	Stock concentration (M)	Final concentration (mM)	Volume added (µL)
Tris-HCl	1	10	200
EDTA	0.5	2	80
NaCl	1	200	800

18.92 mL dH_2O was added and sterilized by autoclaving.

Eosin

Stock solution was prepared by dissolving 2 g of Eosin Y in 40 mL of dH_2O. 160 mL of 95% ethanol was then added and the solution was mixed well.

The working solution was prepared by adding 200 mL of eosin Y stock solution to 600 mL of 80% ethanol. 2-3 drops of glacial acetic acid was added and the solution was mixed well.

India Ink (24X dilution)

For 5 mL:

200 µL of Indian Ink (Talens) was added to 4800 µL of sterilized Ringer's solution. The mixture was heated in a sealed container at 115 °C until mixture boiled. This heating step was repeated three times and the mixture was aliquoted into 2 mL tubes and stored at 4 °C.

LB Agar plates (supplemented with Ampicillin)

For 1 L:

10 g Tryptone, 5 g yeast extract and 5 g NaCl was added to 900 mL dH_2O and the pH was adjusted to 7.4. The final volume was adjusted to 1 L with dH_2O. 15 g of Agar was then added and the solution was autoclaved. The solution was left to cool to 50 °C and then 1 mL of Ampicillin (100 mg/mL) was added. Plates were poured and left to solidify overnight at room temperature.

LB Liquid broth (supplemented with Ampicillin)

For 1 L:

10 g Tryptone, 5 g yeast extract and 5 g NaCl was added to 900 mL dH_2O and the pH was adjusted to 7.4. The final volume was adjusted to 1 L with dH_2O and then autoclaved.

6X Loading dye

For 200 mL:

0.5 g Bromophenol blue was added to 170 mL dH_2O. 0.5 g xylene cyanol was added to this mixture. 30 mL of glycerol was then added. The solution was mixed well, aliquoted and stored at -20 °C.

Mayer's Haematoxylin

1 g of Hematoxylin, 50 g of potassium/aluminium alum, 0.2 g sodium iodate was added to 1000 mL autoclaved dH_2O and left to stand overnight at room temperature. 50 g chloral hydrate and 1 g citric acid was added and the mixture was boiled for 5 min. The solution was left to cool and then filtered with filter paper. The chloral hydrate acted as a preservative and the citric acid sharpened nuclear the stain.

10X PBS

For 1 L:

- 90 g NaCl

- 11.375 g Na_2HPO_4

- 2.4 g NaH_2PO_4

The abovementioned reagents were dissolved in 900 mL dH_2O and the pH was adjusted to 7.4. The solution was brought to a final volume of 1 L using dH_2O and autoclaved.

1X PBS

For 900 mL:

90 mL 10X PBS was added to 900 mL dH_2O and autoclaved.

4% PFA

For 1 L:

- 600 mL dH_2O was heated to 60-65 °C in a fume hood.

- 40 g Paraformaldehyde was added

- The solution was stirred and 100% HCl was added dropwise until the solution cleared.

- 100 mL 10X PBS was added

- The volume was adjusted to 950 mL by adding dH_2O (at 4 °C)

- The solution was left to cool to reach room temperature and then the pH was adjusted to 7.4.

- The solution was dispensed into 50 mL aliquots and stored at 4 °C.

Ringer's Solution

For 1 L:

- 7.2 g NaCl

- 0.37 g KCl

- 0.335 g $CaCl_2 \cdot 6H_2O$

The abovementioned reagents were dissolved in 900 mL dH_2O and the pH was adjusted to 7.3-7.4. The final volume was adjusted to 1 L using dH_2O and autoclaved. The autoclaved solution was filter sterilized using 0.2 µm filter and was dispensed into 50 mL aliquots. The aliquots were stored at 4 °C.

Sodium Citrate buffer

For 1 L:

2.94 g trisodium citrate was added to 900 mL autoclaved dH_2O and the pH was adjusted to 6. 0.5 mL Tween 20 was added and the solution was mixed well.

50X TAE

For 1L:

242 g of Tris base and 18.61 g of EDTA was dissolved in 800 mL dH_2O. 57.1 mL of glacial acetic acid was added and the final volume was adjusted to 1 L with dH_2O.

1X TAE

18 mL of 50X TAE was added to 882 mL dH_2O and sterilized by autoclaving

1X TBS

For 1 L:

- 8.0 g NaCl
- 0.2 g KCl
- 3 g Tris Base

The abovementioned reagents were dissolved in 800 mL dH_2O and the pH was adjusted to 7.4. The solution was brought to a final volume of 1 L with dH_2O and autoclaved.

TBST

For 500 mL:

0.25 mL Tween 20 was added to 500 mL TBS and mixed well.

Appendix 3: Dilutions of construct for electroporation

Below are the dilutions of each construct used for electroporation.

Table A3.1. Preparation and calculation of MO electroporation mix to a final concentration of 1 mM.

Component	Stock concentration	Final concentration	Volume added (µL)
pCI-RFP plasmid	1.27 µg/µL	0.74 µg/µL [**]	7.82
MO	3 mM	1 mM	2.96
Tracking dye *	N/A	N/A	1.05

[*] A 8X dilution of tracking dye was used to visualize successful delivery of the construct and does not harm embryos.
[**] Since approximately 0.5 µL was delivered to each embryo, the final concentration is obtained by multiplying by 0.5.

Table A3.2. Preparation and calculation of MO electroporation mix to a final concentration of 2 mM.

Component	Stock concentration	Final concentration	Volume added (µL)
pCI-RFP plasmid	1.27 µg/µL	0.64 µg/µL	7.79
MO	3 mM	2 mM	5.91
Tracking dye	N/A	N/A	1.08

Table A3.3. Preparation and calculation of *FAF* MO combo electroporation mix to a final concentration of 1 mM.

Component	Stock concentration	Final concentration	Volume added (µL)
pCI-RFP plasmid	1.27 µg/µL	0.74 µg/µL	7.82
FAF MO	3 mM	1 mM*	2.96 (1.48 per MO)

Tracking dye	N/A	N/A	1.05

[*] Each *FAF* MO was delivered at a final concentration of 0.5 mM

Table A3.4. Preparation and calculation of pCI-*FAF*-RFP electroporation mix to a final concentration of 1.01 µg/µL.

Component	Stock concentration	Final concentration	Volume added (µL)
pCI-*FAF*-RFP	1.17 µg/µL	1.01 µg/µL	9.5
dH_2O	N/A	N/A	0.5
Tracking dye	N/A	N/A	1

Table A3.5. Preparation and calculation of pCI-RFP electroporation mix to a final concentration of 1 µg/µL.

Component	Stock concentration	Final concentration	Volume added (µL)
pCI-RFP	1.27 µg/µL	1 µg/µL	8.66
dH_2O	N/A	N/A	1.34
Tracking dye	N/A	N/A	1

Appendix 4: Preparation of pulled glass capillary needles.

Glass capillary needles (Lasec) with an outer diameter of 1.40 mm and an inner diameter of 1.0 mm were pulled using a micropipette puller (Narishige) with the following parameters: heater: 80 °C, magnet: 50 and main magnet: 50. The tip of the pulled end was broken off and the pulled needles produced had an external bore size of approximately 70 µm.

Appendix 5: *FAF* MO design and off-target screening

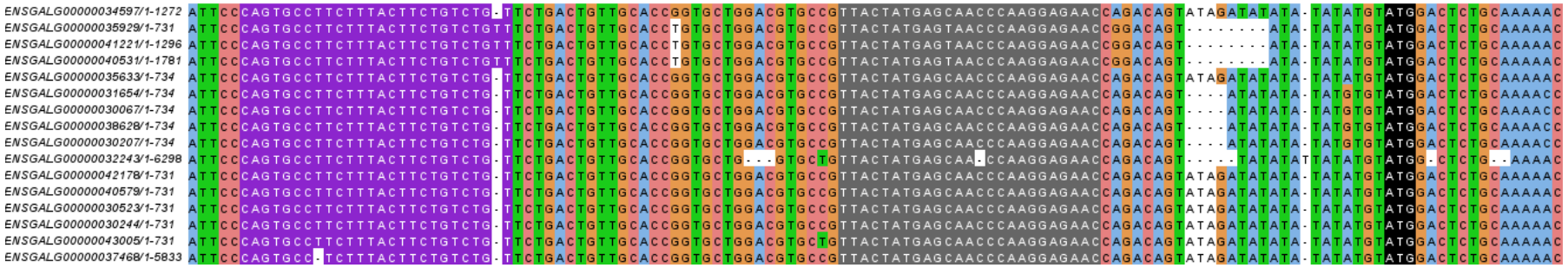

Figure A5.1. *Multiple sequence alignment of the 16 FAF transcripts and where the MO bind to them. FAF* MO1 is highlighted in purple. *FAF* MO2 is highlighted in grey. The start codon is highlighted in black.

The subsequent tables below depict the off-targets identified from the Blast search for *FAF* MO 1, *FAF* MO 2 and the control MO.

FAF MO 1

FAF MO 1: 5’ ACAGACAGAAGTAAAGAAGGCACTG 3’ (25 bases)

Target sequence: 5’-CAGTGCCTTCTTTACTTCTGTCTGT-3’

Table A5.1. BLAST results of *FAF* MO1 potential off-targets.

Faf targets	**Off-targets**							
	Gene name	Bind to 5’ UTR?	Bind to first 25 bases of coding sequence?	Bind to intron/exon boundary?	Homology, no. of mismatches	Location	Expression pattern (expressed in gonads?)	Temporal expression & Function
All 16	PREDICTED: Gallus gallus family with sequence similarity 172 member A (FAM172A), mRNA	No	No	No	Bases 8-23 of MO. 16 consecutive bases	Z chromosome	Yes (Testis + Ovary) – Expression Atlas Also expressed in kidney, liver, heart	- E10 + (no data prior) Contributes to siRNA binding, mRNA splicing, neural crest development
	PREDICTED: Gallus gallus uncharacterized LOC107051642 (LOC107051642), ncRNA	No	No	No	Bases 6-21 of MO. 16 consecutive bases	Chromosome 2	Automatic predicted non-coding RNA (lncRNA) that was found using bioinformatics pipeline/algorithm found on Chr2. No more data available.	

	PREDICTED: Gallus gallus mutL homolog 1 (MLH1), transcript, mRNA	No	No	No	Bases 4-23 of MO. 12 consecutive bases, gap and then 7 consecutive bases	Chromosome 2	Yes (Testis + Ovary) – Expression Atlas Also expressed in kidney, liver, heart	- E10 + (no data prior) - DNA repair/mismatch repair
	PREDICTED: Gallus gallus hook microtubule tethering protein 3 (HOOK3), mRNA	No	No	No	Bases 11-25 of MO. 15 consecutive bases	Z chromosome	Yes (Testis + Ovary) – Expression Atlas Also expressed in kidney, liver, heart	- E10 + (no data prior) - Aids in attachment to microtubules to mediate binding to organelles
	PREDICTED: Gallus gallus acyl-CoA synthetase short-chain family member 3 (ACSS3), mRNA	No	No	No	Bases 4-18 of MO. 15 consecutive bases	Chromosome 1	Yes (Testis + Ovary) – Expression Atlas Also expressed in kidney, liver, heart	- E10 + (no data prior) - Plays a role in lipogenesis by synthesizing acetyl-CoA from acetate. - Catalyzes the synthesis of acetyl-CoA from short-chain fatty acids.
	PREDICTED: Gallus gallus uroporphyrinogen decarboxylase (UROD), mRNA	No	No	No	Bases 2-15 of MO. 14 consecutive bases	Chromosome 8	Yes (Testis + Ovary) – Expression Atlas Also expressed in kidney, liver, heart	- E10 + (no data prior) - Involved in heme biosynthesis
	PREDICTED: Gallus gallus bone morphogenetic protein receptor	No	No	No	Bases 11-24 of MO. 14 consecutive bases	Chromosome 7	Yes (Testis + Ovary) – Expression Atlas Also expressed in kidney, liver, heart	- E10 + (no data prior) - Essential morphogenetic

	type 2 (BMPR2), mRNA							signals for limb bone patterning - Retina development? - Involved in dorsal aorta formation
	PREDICTED: Gallus gallus phospholipase C epsilon 1 (PLCE1), mRNA	No	No	No	Bases 7-24 of MO. 10 consecutive bases, gap, 7 consecutive bases.	Chromosome 6	Yes (Testis + Ovary) – Expression Atlas Also expressed in kidney, liver, heart	- E10 + (no data prior) - catalyzes the hydrolysis of phosphatidylinositol-4,5-bisphosphate to generate two second messengers: inositol 1,4,5-triphosphate (IP3) and diacylglycerol (DAG). These second messengers subsequently regulate various processes affecting cell growth, differentiation, and gene expression.

FAF MO 2

FAF MO 2: 5'-GTTCTCCTTGGGTTGCTCATAGTAA-3' (25 bases)

Target sequence: 5'-TTACTATGAGCAACCCAAGGAGAAC-3'

Table A5.2. BLAST results of *FAF* MO2 potential off-targets.

Faf targets	**Off-targets**							
	Gene name	Bind to 5' UTR?	Bind to first 25 bases of coding sequence?	Bind to intron/exon boundary?	Homology, no. of mismatches	Location	Expression pattern (expressed in gonads?)	Temporal expression & Function
All 16	PREDICTED: Gallus gallus solute carrier family 7 member 2 (SLC7A2), mRNA	No	No	No	Bases 4-18 of MO. 15 consecutive bases	Chromosome 4: 63,027,358-63,067,114 reverse strand. GRCg6a:CM000096.5	Yes (Testis + Ovary) – Expression Atlas Also expressed in kidney, liver, skeletal muscle	E10 + (no data prior). Involved in uptake of sugars, minerals, amino acids.
	PREDICTED: Gallus gallus kinesin family member 27 (KIF27), mRNA	No	No	No	Bases 11-24 of MO. 14 consecutive bases	Chromosome Z: 40,053,080-40,077,364 reverse strand. GRCg6a:CM000122.5	Yes (Testis + Ovary) – Expression Atlas Also expressed in brain, kidney, liver, skeletal muscle	E10 + (no data prior). Essential to Hedgehog signalling pathway
	PREDICTED: Gallus gallus uncharacterized LOC107053990 (LOC107053990), ncRNA	No	No	No	Bases 10-23 of MO. 14 consecutive bases	Chromosome 8	Not studied	Not studied
	PREDICTED: Gallus gallus PHD finger protein 20 (PHF20), mRNA	No	No	No	Bases 8-25 of MO. 6 consecutive bases, gap	Chromosome 20: 905,966-962,906 reverse strand. GRCg6a:CM000112.5	Yes (Testis + Ovary) – Expression Atlas	E10 + (no data prior). Involved in transcriptional regulation

					then 11 consecutive bases.		Also expressed in brain, kidney, liver, heart, skeletal muscle	
	PREDICTED: Gallus gallus uncharacterized LOC107054832 (LOC107054832), ncRNA	No	No	No	Bases 1-14 of MO. 14 consecutive bases	Chromosome 20	Not studied	Not studied
	PREDICTED: Gallus gallus ubiquitin specific peptidase 9, X-linked (USP9X), mRNA	No	No	No	Bases 1-14 of MO. 14 consecutive bases	Chromosome 1: 113,385,291-113,456,709 reverse strand. GRCg6a:CM000093.5	Yes (Testis + Ovary) – Expression Atlas Also expressed in brain, kidney, liver, heart, skeletal muscle	E10 + (no data prior). Acts like ubiquitin-specific proteases, cleaving ubiquitin molecule from ubiquitin-fused precursors and ubiquitinylated proteins
	PREDICTED: Gallus gallus uncharacterized LOC107053451 (LOC107053451), ncRNA	No	No	No	Bases 3-15 of MO. 13 consecutive bases	Chromosome 5	Not studied	Not studied
	PREDICTED: Gallus gallus SprT-like N-terminal domain (SPRTN), mRNA	No	No	No	Bases 12-24 of MO. 13 consecutive bases	Chromosome 3: 39,844,405-39,848,234 reverse strand. GRCg6a:CM000095.5	Yes (Testis + Ovary) – Expression Atlas Also expressed in brain, kidney, liver, heart, skeletal muscle	E10 + (no data prior). Involved in DNA repair

Control MO

Control MO: 5'-CCTCTTACCTCAGTTACAATTTATA-3' (25 bases)

Target sequence: 5'-TATAAATTGTAACTGAGGTAAGAGG-3'

Table A5.3. BLAST results of control MO potential off-targets.

Off-targets							
Gene name	Bind to 5' UTR?	Bind to first 25 bases of coding sequence?	Bind to intron/exon boundary?	Homology, no. of mismatches	Location	Expression pattern (expressed in gonads?)	Temporal expression & Function
PREDICTED: Gallus gallus APC, WNT signaling pathway regulator (APC), mRNA	No	No	No	Bases 7-21 of MO. 15 consecutive bases.	Chromosome Z	Yes (Testis + Ovary) – Expression Atlas Also expressed in brain, kidney, liver, heart	APC protein acts as tumour repressor by interacting with β-catenin (E10+)
PREDICTED: Gallus gallus probable G-protein coupled receptor 83-like (LOC100859173), mRNA	No	No	No	Bases 1-15 of MO. 15 consecutive bases.	Chromosome 4	No - Brain and skeletal muscle (Expression Atlas)	Involved in cell signalling across cell membrane (E10+)
PREDICTED: Gallus gallus SUMO1/sentrin specific peptidase	No	No	No	Bases 4-18 of MO.	Chromosome 3	Yes (Testis + Ovary) – Expression Atlas	Binds to other proteins aiding in things such as nuclear pore

6 (SENP6), mRNA				15 consecutive bases.		Also expressed in brain, kidney, liver, heart	binding, stabilisation. (E10+)
PREDICTED: Gallus gallus uncharacterized LOC107052000 (LOC107052000), ncRNA	No	No	No	Bases 8-22 of MO. 15 consecutive bases	Chromosome 2	Not studied	Not studied
PREDICTED: Gallus gallus myomesin 3 (MYOM3), mRNA	No	No	No	Bases 11-24 of MO. 14 consecutive bases	Chromosome 23	Yes (Testis + Ovary) – Expression Atlas Also expressed in skeletal muscle, heart	Helps stabilize other proteins during muscle formation
PREDICTED: Gallus gallus uncharacterized LOC107053659 (LOC107053659), ncRNA	No	No	No	Bases 12-25 of MO. 14 consecutive bases	Chromosome 1	Not studied	Not studied
PREDICTED: Gallus gallus gamma-aminobutyric acid type A receptor gamma1 subunit (GABRG1), mRNA	No	No	No	Bases 1-14 of MO. 14 consecutive bases	Chromosome 4	No, expressed in kidney and brain (Expression Atlas)	Transmembrane protein involved in inhibiting neurotransmission

Appendix 6: 5'-RACE alignment of off-targets

SPARC

Score	Expect	Identities	Gaps	Strand
2002 bits(1084)	0.0	1114/1128(99%)	7/1128(0%)	Plus/Plus

```
Query  1     AGACTCCTCCAGTCCTTCCCAGCGCCTGGAGTTCCCTCAGCCCTGCTCGGGACTACGAGG  60
             ||||||||||||||||||||||||||||||||||||||||||||||||||||||||||||
Sbjct  1     AGACTCCTCCAGTCCTTCCCAGCGCCTGGAGTTCCCTCAGCCCTGCTCGGGACTACGAGG  60

Query  61    GTTTGCTAAAAGATGAGAACCTGGATTTTCTTCTTCCTCTGCCTGGCAGGCAAAGCCCTG  120
             ||||||||||||||||||||||||||||||||||||||||||||||||||||||||||||
Sbjct  61    GTTTGCTAAAAGATGAGAACCTGGATTTTCTTCTTCCTCTGCCTGGCAGGCAAAGCCCTG  120

Query  121   GCAGCTCCGCAAGAGGCTCTGCCTGATGAGACGGAGGTGATTGAAGATCTCACCACAGAG  180
             ||||||||||||||||||||||||||||||||||||||||||||||||||||||||||||
Sbjct  121   GCAGCTCCGCAAGAGGCTCTGCCTGATGAGACGGAGGTGATTGAAGATCTCACCACAGAG  180

Query  181   GGGCCTGTGGGGGCCAACCCTGTCCAGGTGGAGGTGGGAGAGTTTGAGGAACCTACAGAA  240
             ||||||||||||||||||||||||||||||||||||||||||||||||||||||||||||
Sbjct  181   GGGCCTGTGGGGGCCAACCCTGTCCAGGTGGAGGTGGGAGAGTTTGAGGAACCTACAGAA  240

Query  241   GATGTASAGGAGATCKTCGCAGAGAATCCCTGCCAGAACCATCACTGCAAGCATGGCAAG  300
             |||||| |||||||| ||||||||||||||||||||||||||||||||||||||||||||
Sbjct  241   GATGTAGAGGAGATCGTCGCAGAGAATCCCTGCCAGAACCATCACTGCAAGCATGGCAAG  300

Query  301   GTGTGTGAGGTGGATGACAACAACTCACCCATGTGCGTGTGCCAGGACCCCTCCAGCTGC  360
             ||||| ||||||||||||||||||||||||||||||||||||||||||||||||||||||
Sbjct  301   GTGTGCGAGGTGGATGACAACAACTCACCCATGTGCGTGTGCCAGGACCCCTCCAGCTGC  360

Query  361   CCAGCCACCTCCGGCGTCTTTGAGAAGGTCTGTGGCACTGACAACAAGACCTATGACTCC  420
             || |||||||||||| ||||||||||||||||||||||||||||||||||||||||||||
Sbjct  361   CCGGCCACCTCCGGCATCTTTGAGAAGGTCTGTGGCACTGACAACAAGACCTATGACTCC  420

Query  421   TCCTGCCAC-TCTTTGCCACCAAGTGCACCTTGGAGGG-ACCAAGAAGGGACACAAGCTG  478
             ||||||||| |||||||||||||||||||||||||||| |||||||||||||||||||||
Sbjct  421   TCCTGCCACTTCTTTGCCACCAAGTGCACCTTGGAGGGAACCAAGAAGGGACACAAGCTG  480

Query  479   CACCTGGATTACATCGGGCCTTGCAAAATTCATCCCTGCCTGCCTGGACACTGAGCTGAC  538
             ||||||||||||||||||||||| |||||||||||||||||||||||||||||||||||
Sbjct  481   CACCTGGATTACATCGGGCCTTGC-AAATTCATCCCTGCCTGCCTGGACACTGAGCTGAC  539

Query  539   AGAGTTCCCCCTGCGCATGCGGGACTGGCTGAAGAATGTGCTGATCACCCTGTATGAGCG  598
             ||||||||||||||||||||||||||||||||||||||||||||||||||||||||||||
Sbjct  540   AGAGTTCCCCCTGCGCATGCGGGACTGGCTGAAGAATGTGCTGATCACCCTGTATGAGCG  599

Query  599   CGATGAGGACAACAACCTGCTGACCGAGAAGCAGAAGCTCAAGGTGAAGAAGATCCACGA  658
             ||||||||||||||||||||||||||||||||||||||||||||||||||||||||||||
Sbjct  600   CGATGAGGACAACAACCTGCTGACCGAGAAGCAGAAGCTCAAGGTGAAGAAGATCCACGA  659

Query  659   GAATGAGAAGCGCCTGGAGGCCGGCGACCACACCGTGGAGCTGCTGGCCCGCGACTTTGA  718
             ||||||||||||||||||||||||||||||||||||||||||||||||||||||||||||
Sbjct  660   GAATGAGAAGCGCCTGGAGGCCGGCGACCACACCGTGGAGCTGCTGGCCCGCGACTTTGA  719

Query  719   GAAGAACTACAACATGTACATCTTCCCCGTGCACTGGCAGTTCGGGCAGCTGGACCAGCA  778
             |||||||||||||||||||||||||||||||||||||||||| ||||||||||||||||||
Sbjct  720   GAAGAACTACAACATGTACATCTTCCCCGTGCACTGGCAGTTTGGGCAGCTGGACCAGCA  779

Query  779   CCCCATTGATGGGTACCTGTCCCACACCGAGCTGGCCCCGCTCCGTGCCCCACTCATCCC  838
             ||||||||||||||||||||||||||||||||||||||||||||||||||||||||||||
Sbjct  780   CCCCATTGATGGGTACCTGTCCCACACCGAGCTGGCCCCGCTCCGTGCCCCACTCATCCC  839

Query  839   CATGGAGCACTGCACCACTCGCTTCTTTGAGGCCTG-GACTTAGACAACGACAAGTACAT  897
             |||||||||||||||||||||||||||||||||||| |||||||||||||||||||||||
Sbjct  840   CATGGAGCACTGCACCACTCGCTTCTTTGAGGCCTGCGACTTAGACAACGACAAGTACAT  899

Query  898   CGCCCTGGAGGAATGGGCCAGCTGCTTTGGCATTAAGGAGCAGGACATAGACAAGGATCT  957
             ||||||||||||||||||||||||||||||||||||||||||||||||||||||||||||
Sbjct  900   CGCCCTGGAGGAATGGGCCAGCTGCTTTGGCATTAAGGAGCAGGACATAGACAAGGATCT  959

Query  958   GGTGATCTAAAGCCTCAGCTTCCTCCTCTGCTGCCAACTTTGTCTTGTTTTAACCTTCCC  1017
             ||||||||||||||||||||||||||||||||||||||||||||||||||||||||||||
Sbjct  960   GGTGATCTAAAGCCTCAGCTTCCTCCTCTGCTGCCAACTTTGTCTTGTTTTAACCTTCCC  1019

Query  1018  ACTTCCTTCGGTTTTCAAACCGCTTTTGTTTTGTTTTCCCTGGGAACAAGGTGCTAATAT  1077
             |||||||||||||||| ||||||||||||||||||||||||||||||||||||||||||||
Sbjct  1020  ACTTCCTTCGGTTTTCGAACCGCTTTTGTTTTGTTTTCCCTGGGAACAAGGTGCTAATAT  1079

Query  1078  AGGTCTAAACGTATGTAGTATCGGTGCTAAGAGAAA-AA-AG-CCTTC  1122
             |||||||||||||||||||||||||||||||||||| || || |||||
Sbjct  1080  AGGTCTAAACGTATGTAGTATCGGTGCTAAGAGAAATAACAGTCCTTC  1127
```

Figure A6.1. *Pairwise alignment of SPARC*. The clone obtained from RACE (Query) shows a 99% match to the *SPARC* mRNA sequence deposited in NCBI (Subject). The red box shows the bases that are the same as the *FAF* reverse primer used in 5'-RACE.

VIM

Score	Expect	Identities	Gaps	Strand
1234 bits(668)	0.0	670/672(99%)	0/672(0%)	Plus/Plus

```
Query  1    CTTCTTCGCCCGCCGCGCTCCGAGCCCCGCTCCGCTCCCGGATTACAAAGCCGCTCCGTT  60
            ||||||||||||||||||||||||||||||||||||||||||||||||||||||||||||
Sbjct  4    CTTCTTCGCCCGCCGCGCTCCGAGCCCCGCTCCGCTCCCGGATTACAAAGCCGCTCCGTT  63

Query  61   CCTCGCCGCCATGAGCTTCACCAGCAGCAAGAACTCCTCGTACCGCCGCATGTTCGGCGG  120
            ||||||||||||||||||||||||||||||||||||||||||||||||||||||||||||
Sbjct  64   CCTCGCCGCCATGAGCTTCACCAGCAGCAAGAACTCCTCGTACCGCCGCATGTTCGGCGG  123

Query  121  GGGCAGCCGGCCCAGCAGCGGCACCCGCTACATCACGTCCAGCACCCGCTATTCCCTGGG  180
            ||||||||||||||||||||||||||||||||||||||||||||||||||||||||||||
Sbjct  124  GGGCAGCCGGCCCAGCAGCGGCACCCGCTACATCACGTCCAGCACCCGCTATTCCCTGGG  183

Query  181  CAGCGCCCTGCGGCCCAGCAGCGCCCGCTACGTGTCCGCCTCGCCCGGCGGCGTGTACGC  240
            ||||||||||||||||||||||||||||||||||||||||||||||||||||||||||||
Sbjct  184  CAGCGCCCTGCGGCCCAGCAGCGCCCGCTACGTGTCCGCCTCGCCCGGCGGCGTGTACGC  243

Query  241  CACCWAGGCGACGTCGGTGCGGCTGCGGAGCAGCATGCCGCCCATGCGGATGCACGACGC  300
            |||| ||||||||||||||||||||||||||||||||||||||||||||||||||||||||
Sbjct  244  CACCAAGGCGACGTCGGTGCGGCTGCGGAGCAGCATGCCGCCCATGCGGATGCACGACGC  303

Query  301  CGTGGACTTCACCCTGGCGGACGCCATCAACACGGAGTTCAAGGCGAACCGCACCAACGA  360
            ||||||||||||||||||||||||||||||||||||||||||||||||||||||||||||
Sbjct  304  CGTGGACTTCACCCTGGCGGACGCCATCAACACGGAGTTCAAGGCGAACCGCACCAACGA  363

Query  361  GAAGGTAGAGCTGCAGGAGCTCAACGACCGCTTCGCCAACTACATCGACAAGGTGCGCTT  420
            ||||||||||||||||||||||||||||||||||||||||||||||||||||||||||||
Sbjct  364  GAAGGTAGAGCTGCAGGAGCTCAACGACCGCTTCGCCAACTACATCGACAAGGTGCGCTT  423

Query  421  CCTGGAGCAGCAGAACAAGATCCTGCTGGCCGAGCTGGAGCAGCTCAAGGGCAAAGGCAC  480
            ||||||||||||||||||||||||||||||||||||||||||||||||||||||||||||
Sbjct  424  CCTGGAGCAGCAGAACAAGATCCTGCTGGCCGAGCTGGAGCAGCTCAAGGGCAAAGGCAC  483

Query  481  GTCCCGCTTGGGCGACCTGTACGAGGAGGAGATGCGGGAGCTGCGGCGGCAGGTGGACCA  540
            ||||||||||||||||||||||||||||||||||||||||||||||||||||||||||||
Sbjct  484  GTCCCGCTTGGGCGACCTGTACGAGGAGGAGATGCGGGAGCTGCGGCGGCAGGTGGACCA  543

Query  541  GCTGACCAACGACAAGGCCCGCGTCGAGGTGGAGCGCGACAACCTGGCCGACGACATCAT  600
            ||||||||||||||||||||||||||||||||||||||||||||||||||||||||||||
Sbjct  544  GCTGACCAACGACAAGGCCCGCGTCGAGGTGGAGCGCGACAACCTGGCCGACGACATCAT  603

Query  601  GCGCCTGCGGGAGAAGTTGCAGGAGGAGATGYTGCAGCGGGAGGAGGCCGAGAGCACCCT  660
            |||||||||||||||||||||||||||||| ||||||||||||||||||||||||||||
Sbjct  604  GCGCCTGCGGGAGAAGTTGCAGGAGGAGATGCTGCAGCGGGAGGAGGCCGAGAGCACCCT  663

Query  661  GCAGTCCTTCCG  672
            ||||||||||||
Sbjct  664  GCAGTCCTTCCG  675
```

Figure A6.2. *Pairwise alignment of VIM*. The clone obtained from RACE (Query) shows a 99% match to the *VIM* mRNA sequence deposited in NCBI (Subject). The red box shows the bases that are the same as the *FAF* reverse primer used in 5'-RACE.

PPIA

Score	Expect	Identities	Gaps	Strand
1144 bits(619)	0.0	628/632(99%)	1/632(0%)	Plus/Plus

```
Query  1    ccgctgcgccgcgctctccgagctgtccgccgccatcgccgctctccgtcgcccgcgccg  60
            ||||||||||||||||||||||||||||||||||||||||||||||||||||||||||||
Sbjct  1    CCGCTGCGCCGCGCTCTCCGAGCTGTCCGCCGCCATCGCCGCTCTCCGTCGCCCGCGCCG  60

Query  61   ccATGGCCAACCCCGTTGTGTTCTTCGACATCGCCGCCAACGGCGAGCCCCTGGGCCGCG  120
            ||||||||||||||| ||||||||||||||||||||||||||||||||||||||||||||
Sbjct  61   CCATGGCCAACCCCGTCGTGTTCTTCGACATCGCCGCCAACGGCGAGCCCCTGGGCCGCG  120

Query  121  TCACCTTCGAGCTCTTCGCTGACAAGGTGCCCATAACAGCAGAGAACTTCCGTGCTTTGA  180
            ||||||||||||||||||||||||||||||||||||||||||||||||||||||||||||
Sbjct  121  TCACCTTCGAGCTCTTCGCTGACAAGGTGCCCATAACAGCAGAGAACTTCCGTGCTTTGA  180

Query  181  GCACCGGCGAGAAGGGATTTGGCTACAAGGGCTCCTGCTTCCACCGGATCATCCCCGGCT  240
            ||||||||||||||||||||||||||||||||||||||||||||||||||||||||||||
Sbjct  181  GCACCGGCGAGAAGGGATTTGGCTACAAGGGCTCCTGCTTCCACCGGATCATCCCCGGCT  240

Query  241  TCATGTGTCAGGGTGGTGACTTTACGCGCCACAACGGCACTGGTGGCAAATCCATTTATG  300
            |||||||||||||||||||||||||||||||||||||||||||||||||||||||||| |
Sbjct  241  TCATGTGTCAGGGTGGTGACTTTACGCGCCACAACGGCACTGGTGGCAAATCCATTTACG  300

Query  301  GGGAGAAGTTTGCCGACGAGAACTTCATCCTGAAGCACACAGGGCCCGGCATCCTGTCCA  360
            |||||||||||||||||||||||||||||||||||| ||||||||||||||||||||||
Sbjct  301  GGGAGAAGTTTGCCGACGAGAACTTCATCCTGAAGCACACGGGGCCCGGCATCCTGTCCA  360

Query  361  TGGCCAACGCCGGCCCCAACACGAACGGCTCCCAGTTCTTCATCTGCACTGCCAAGACCG  420
            ||||||||||||||||||||||||||||||||||||||||||||||||||||||||||||
Sbjct  361  TGGCCAACGCCGGCCCCAACACGAACGGCTCCCAGTTCTTCATCTGCACTGCCAAGACCG  420

Query  421  AGTGGTTGGACGGCAAGCACGTCGTCTTCGGCCGCGTCAAGGAGGGGATGAACGTGGTGG  480
            ||||||||||||||||||||||||||||||||||||||||||||||||||||||||||||
Sbjct  421  AGTGGTTGGACGGCAAGCACGTCGTCTTCGGCCGCGTCAAGGAGGGGATGAACGTGGTGG  480

Query  481  AGGCCATGGAGCGCTGCGGCTCCAAAGACGGCAAGACGAGCAAGCAGATCACCATTTCCA  540
            ||||||||||||||||||||||||||||||||||||||||||||||||||||||||||||
Sbjct  481  AGGCCATGGAGCGCTGCGGCTCCAAAGACGGCAAGACGAGCAAGCAGATCACCATTTCCA  540

Query  541  ACTGCGGGCAGCTCTCGTAAACCCTGCGTCTTAACGCCTGACATTCCGCCTGCGGCCCGG  600
            ||||||||||||||||||||||||||||||||||||||||||||||||||||||||||||
Sbjct  541  ACTGCGGGCAGCTCTCGTAAACCCTGCGTCTTAACGCCTGACATTCCGCCTGCGGCCCGG  600

Query  601  GCAGCTCGCCTGGCGCAGcccccccTCCTTCC  632
            |||||||||||||||||||||||| ||||||
Sbjct  601  GCAGCTCGCCTGGCGCAGCCCCCCC-CCTTCC  631
```

Figure A6.3. *Pairwise alignment of PPIA.* The clone obtained from RACE (Query) shows a 99% match to the *PPIA* mRNA sequence deposited in NCBI (Subject). The red box shows the bases that are the same as the *FAF* reverse primer used in 5'-RACE.

Appendix 7: Electroporation of genital ridge (merged image)

Figure A7. *Electroporation of the genital ridge (HH18-20) using the control morpholino (green) and pCI-RFP (red).* The merged channel confirms that both constructs localize to the same cells (noted by the yellow colour) within the left genital ridge (indicated by the dotted line).

Appendix 8: Sexing PCR (*FAF* MO)

Sexing PCR was conducted on tissue collected from electroporated embryos as described in Chapter 2.3.3. The gels below depict the genotypic sex of these electroporated embryos.

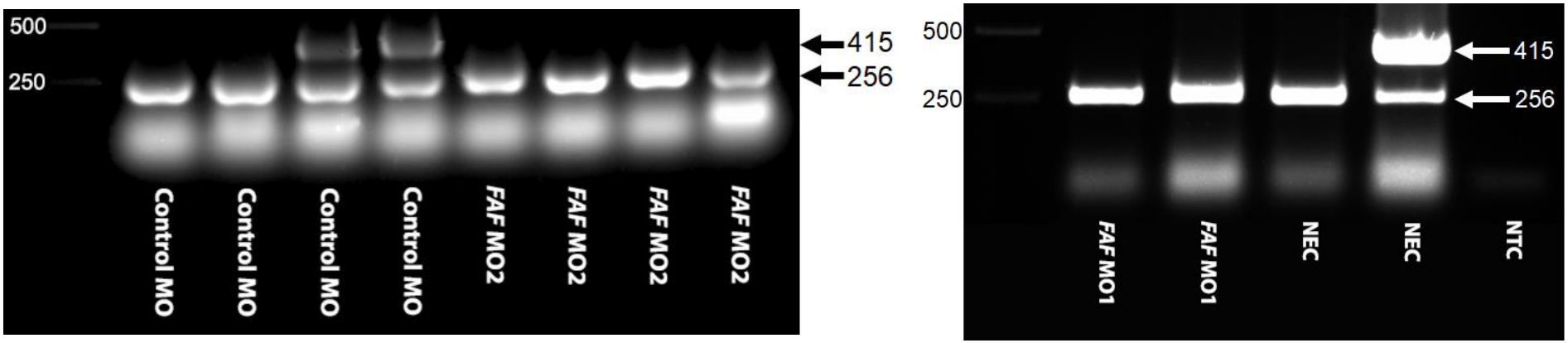

Figure A.8. *Genotype analysis by sexing PCR of embryos electroporated with MO.* 1% agarose gel electrophoresis of DNA extracted from electroporated embryos. Females are identified by the presence of two prominent bands (415 bp and 256 bp) and males are identified by one prominent band (256 bp). Two males and two females successfully electroporated with the control MO is shown. Only males were successfully electroporated with *FAF* MO1 and *FAF* MO 2. A male and female no electroporation control (NEC) is shown. The no template control (NTC) shows no DNA contamination occurred during PCR setup.

Appendix 9: Restriction enzyme digestion to create pCI-*FAF*-RFP

The resulting restriction digest after using *Xba*I and *Sma*I is shown below. Both digested and undigested samples are shown below. While a size difference will not be noticed on a gel between the digested and undigested FAF CDS samples, a clear size difference was observed between the digested and undigested pCI-RFP samples. Two distinct bands (6403 bp and 197 bp) were observed after pCI-RFP was digested, consistent with what was expected.

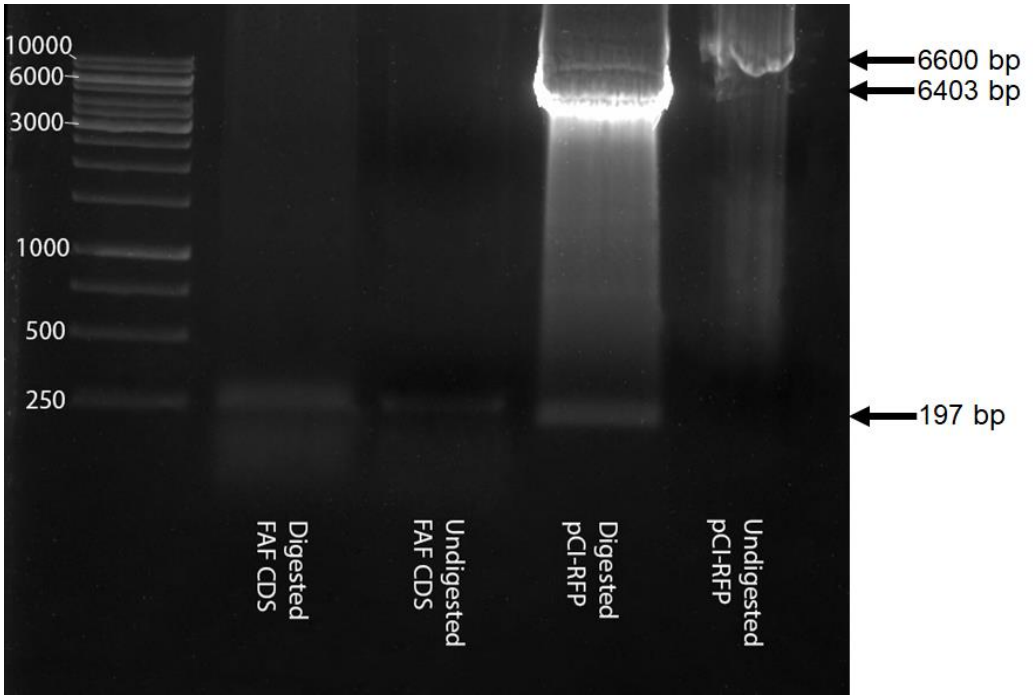

Figure A9. *Restriction digest of FAF CDS and pCI-RFP.* 1% agarose gel electrophoresis of digested and undigested *FAF* CDS and pCI-RFP samples. The *FAF* CDS and pCI-RFP were digested with *Sma*I and *Xba*I. No noticeable size difference was expected between the digested and undigested *FAF* CDS samples. Successful digestion was observed based on a noticeable size difference between the digested and undigested pCI-RFP samples. Only two distinct bands are seen (6403 bp and 197 bp) as expected.

Appendix 10: Sexing PCR (pCI-*FAF*-RFP)

Sexing PCR was conducted on tissue collected from electroporated embryos as described in Chapter 2.3.3. The gel below depicts the genotypic sex of these electroporated embryos.

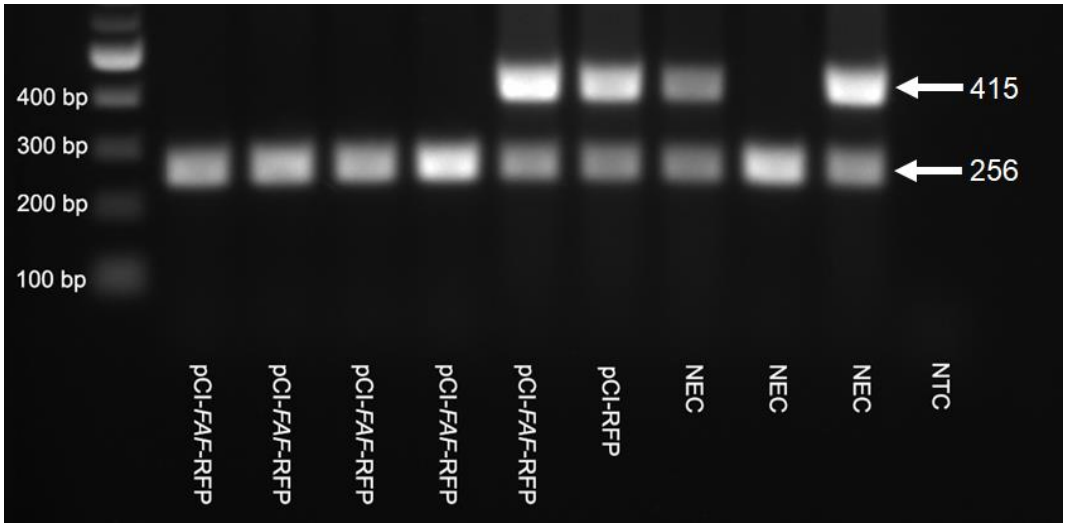

Figure A10. *Genotype analysis by sexing PCR of embryos electroporated with pCI-FAF-RFP.* 1% agarose gel electrophoresis of DNA extracted from electroporated embryos. Females are identified by the presence of two prominent bands (415 bp and 256 bp) and males are identified by one prominent band (256 bp). Four males and one female successfully electroporated with pCI-*FAF*-RFP is shown. A single female was successfully electroporated with pCI-RFP. A male and two female no electroporation control (NEC) is shown. The no template control (NTC) shows no DNA contamination occurred during PCR setup.

Appendix 11: Left and right gonad histological comparison (pCI-*FAF*-RFP)

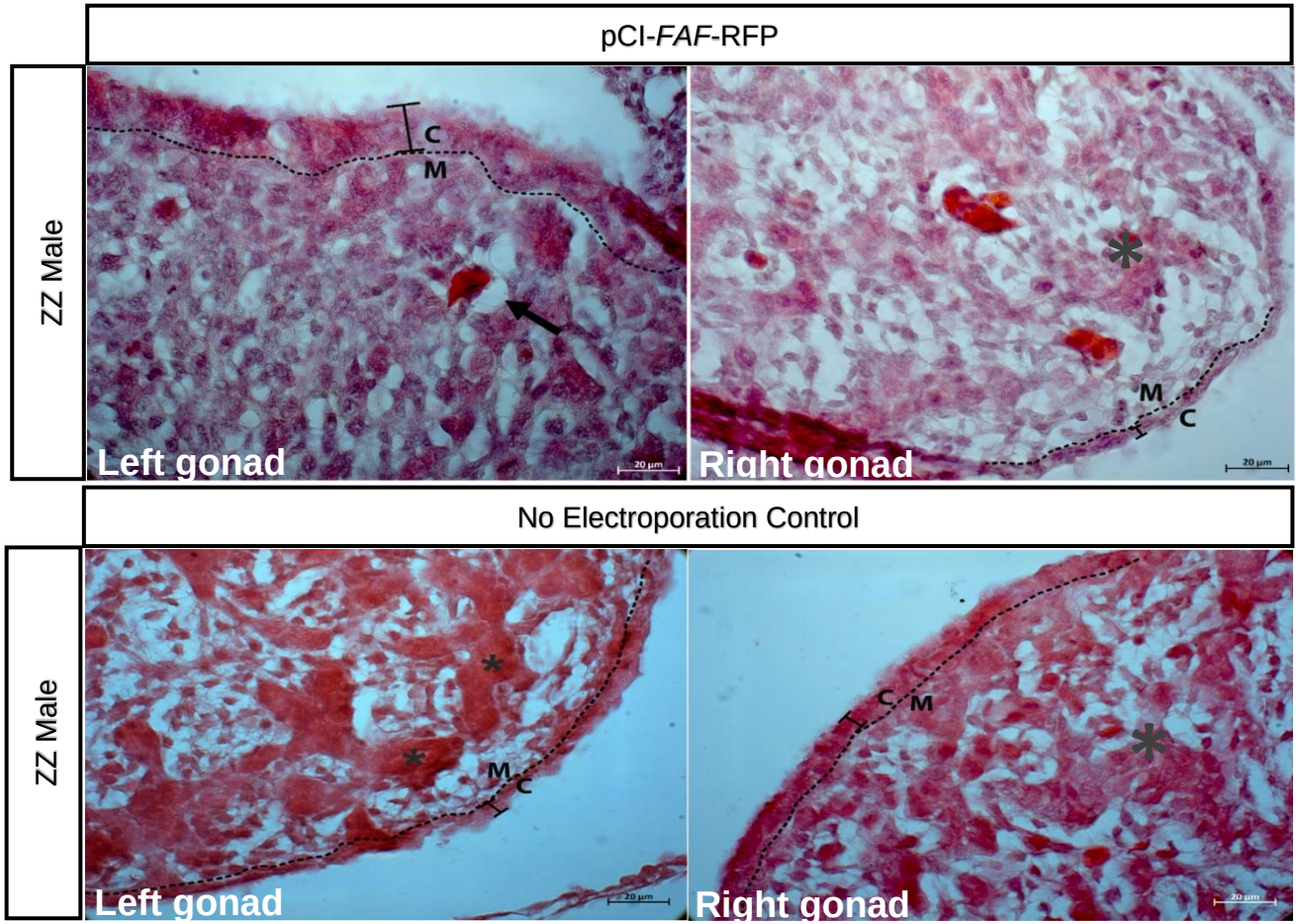

Figure A11.1. *Histological analysis of left and right gonad.* The left and right gonad of the unelectroporated ZZ male is very similar in morphology, characterized by a thin cortex (C) and an organized medulla (M) where seminiferous tubes can be seen (asterisks). The left gonad of the electroporated ZZ male is distinctly different from the right gonad. The cortex of the electroporated ZZ male has thickened and no seminiferous tubes are seen in the medulla. The right gonad of the electroporated ZZ male however, shows morphology similar to the NEC.

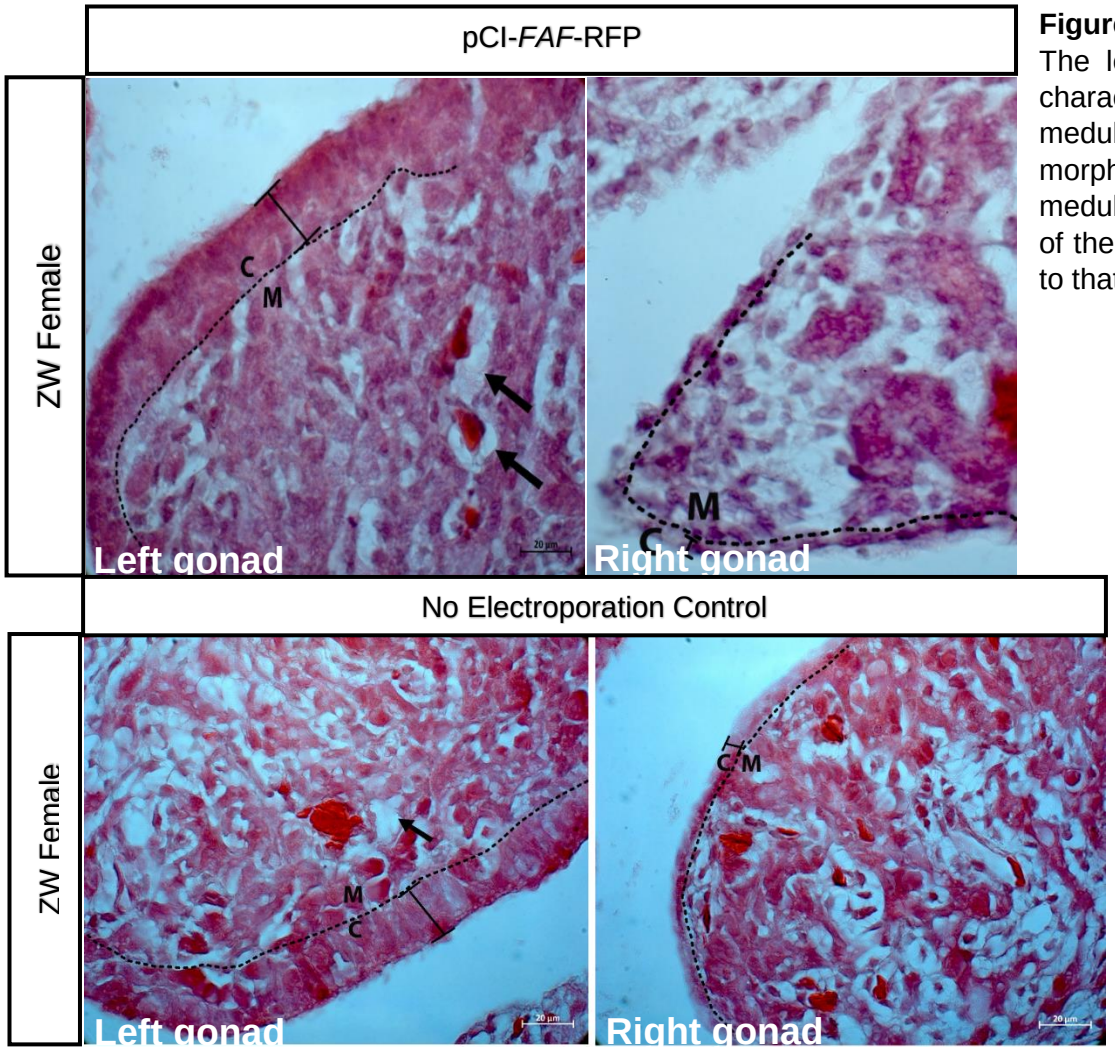

Figure A11.2. *Histological analysis of left and right gonad.* The left gonad of the unelectroporated ZW female is characterized by a thick cortex (C) and a disorganized medulla (M) whereas the right gonad shows a male-like morphology, consisting of a thin cortex and organized medulla. The morphology of both the left and right gonad of the pCI-*FAF*-RFP electroporated ZW female is similar to that of the unelectroporated ZW female.

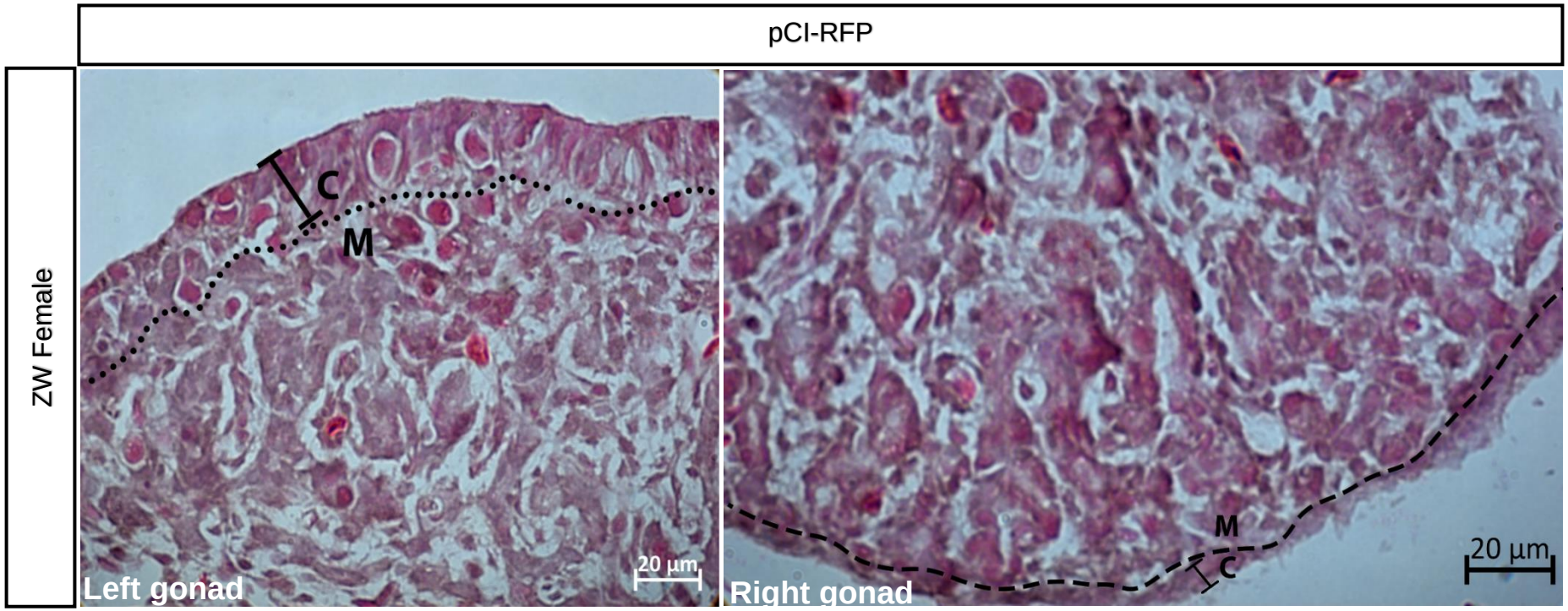

Figure A11.3. *Histological analysis of left and right gonad.* The left gonad of the unelectroporated ZW female is characterized by a thick cortex (C) and a disorganized medulla (M) whereas the right gonad shows a male-like morphology, consisting of a thin cortex and organized medulla. The morphology of both the left and right gonad of the pCI-RFP electroporated ZW female is similar to that of the unelectroporated ZW female.

Appendix 12: Animal Ethics Clearance Certificate

STRICTLY CONFIDENTIAL

ANIMAL ETHICS SCREENING COMMITTEE (AESC)

CLEARANCE CERTIFICATE NO. 2017/01/01/0

APPLICANT: Dr N Nikitina

SCHOOL: School of Molecular and Cell Biology
DEPARTMENT:
LOCATION:

PROJECT TITLE: What is the W-linked female sex determinant in chicken?

Number and Species

4500 fertilized eggs of domestic chicken Gallus gallus over a period of 3 years

Approval was given for the use of animals for the project described above at an AESC meeting held on 2017/01/31. This approval remains valid until 2019/02/12.
Unreported changes to the application may invalidate the clearance given by the AESC
An annual progress report must be provided

The use of these animals is subject to AESC guidelines for the use and care of animals, is limited to the procedures described in the application form and is subject to any additional conditions listed below:

None

Signed: _____ (Chairperson, AESC) Date: 15 February 2017

I am satisfied that the persons listed in this application are competent to perform the procedures therein, in terms of Section 23 (1) (c) of the Veterinary and Para-Veterinary Professions Act (19 of 1982)

Signed: _____ (Registered Veterinarian) Date: 16/02/2017.

cc: Supervisor: N/A
Director: CAS

Works 2000/lain0015/AESCCert.wps

AREC 2017 M&E

Please note that only typewritten applications will be accepted.

UNIVERSITY OF THE WITWATERSRAND

ANIMAL RESEARCH ETHICS COMMITTEE
MODIFICATIONS AND EXTENSIONS TO EXPERIMENTS

a. Name: **Natalya Nikitina**

b. School and email address: **School of Molecular and Cell Biology**

natalya.nikitina@wits.ac.za

c. Experiment to be modified / extended

	AREC/AESC NO		
Original AESC number	**2017**	**01/01**	**O**
Other M&Es :			No

d. Project Title: **What is the W-linked female sex determinant in chicken?**

		No.	Species
e.	Number and species of animals originally approved:	4500	*Fertilized eggs of domestic chicken*
f.	Number of additional animals previously allocated on M&Es:	0	
g.	Total number of animals allocated to the experiment to date:	4500	
h.	Number of animals used to date:	1380	

i. Specific modification / extension requested:

The permit for this project has just expired. We have not managed to use up all of the allocated eggs, and the project is still ongoing. We are asking for an extension for this permit for another year, until 02/2020 to enable us to complete experiments.

j. Motivation for modification / extension:

The ethics approval was granted for 2 years, while the duration of the project and the funding is 3 years. We really need this extension in order to be able to complete the proposed experiments. We still have 3120 eggs remaining on the original permit that have not yet been used up.

Date: 19/03/2019 Signature:

RECOMMENDATIONS

Extension of time until 02/2021

Date: 19/03/2019 Signature:

Chairman, AREC pp.